What evolutionary secrets lie buried in Baltic Sea sediments?

The evolutionary responses of resurrected Baltic Sea cyanobacteria in a warming world

Michael Oseremen Edetanlen

Hamburg 2026

The evolutionary responses of resurrected Baltic Sea cyanobacteria in a warming world

Michael Oseremen Edetanlen

Dissertation for the award of the doctoral degree in Natural Sciences

Faculty of Mathematics, Informatics and Natural Sciences

Department of Biology at the University of Hamburg

Institute of Marine Ecosystem and Fisheries Science

Hamburg 2026

Michael Oseremen Edetanlen

MONOGRAPH

The evolutionary responses of resurrected Baltic Sea cyanobacteria in a warming world

Dissertation

submitted to the Faculty of Mathematics, Informatics and Natural Sciences

Department of Biology

University of Hamburg

Hamburg, 2026

Supervisor: Prof. Dr. C.-Elisa Schaum

Preface

This dissertation is submitted as a MONOGRAPH pursuant to §8 Abs. 2 lit. a of the promotionsordnung MIN-Fakultät 2018 – a single coherent scientific narrative.

Chapters 2.1 – 2.3 represent sequential, interdependent research phases forming one unified evolutionary story of Baltic Sea *Nodularia spumigena*:

- Chapter 2.1: Hot is the new cool: historical Baltic Sea cyanobacteria show trade-offs in thermal performance, carbon metabolism, and biotic interactions
- Chapter 2.2: Divergent evolutionary trajectories under experimental warming in pre-industrial and contemporary Baltic Sea *Nodularia spumigena*
- Chapter 2.3: Global DNA methylation correlates with thermal selection in Baltic Sea *Nodularia spumigena*

These chapters are NOT independent publications but integrated components building toward the synthesis in Chapter 3. All chapters are intended for submission to peer review, but none are currently in review.

All conception, experimental work, data analysis, visualization, and writing represent my independent contributions under supervision of Prof. C.-Elisa Schaum.

Michael Oseremen Edetanlen

Hamburg, 20 March 2026

Commission:

Prof. Dr. Charlotte-Elisa Luise Schaum (supervisor), University of Hamburg

Prof. Dr. Björn Christian Rost (evaluator), Alfred-Wegener-Institut, Bremerhaven

Prof: Dr. Kai Jensen, University of Hamburg

Prof. Dr. Flemming Dahlke, University of Hamburg

Disputation

4th June 2026

I dedicate this work to my children,

Matthew Ehiremen Edetanlen, Mikayla Osetale Eseose Edetanlen, Mirka-Magdalene Ofure Edetanlen, Michael Oseremen Edetanlen II, Mateo Oselumese Edetanlen

Acknowledgements

This dissertation would not exist without the unwavering support of people who believed in it, and in me, long before I did.

First and foremost, I am deeply grateful to my supervisor, Elisa Schaum, who gave me the opportunity to fulfil this dream. I will never forget my interview session, there she was, rocking baby Ylva in her arms, nodding me along through every question asked of me with the kind of calm encouragement that told me everything would be alright. Even when my pace resembled that of an organism I once studied, the snail, she never gave up on me. Her support has been unmatched, and I could not have asked for a better scientific home. I am equally grateful to Inga Hense and Anke Kremp, the two other principal investigators who, together with Elisa Schaum, conceived the intellectual framework that made this dissertation possible. They remain an important part of this story.

I owe a special debt of gratitude to Cynthia Medwed of the Leibniz Institute for Baltic Sea Research Warnemünde, who resurrected my companions (the cyanobacterial isolates) of the last four and a half years, without whom none of this work would have been possible. Thank you for bringing them back to life. And to everyone at the Institute of Marine Ecosystem and Fisheries Science (IMF), and particularly the members of AG Schaum with whom I have shared the last several years, thank you for making the office and laboratory a place worth coming to. A special mention must go to the two guardians of our group: Stefanie Schnell and Luisa Listmann. Lady Stefanie, your kind words were a constant source of strength, and your persistent belief that this day would come was the multivitamin that kept me going when the work felt endless. Thank you, Stefie. And to you too, Luisa, your relentless encouragement pushed me forward more than you know. I am grateful to you both.

I am grateful to StarSEQ GmbH for conducting the whole-genome sequencing of my samples and the initial bioinformatic processing to generate the SNP dataset, as well as for their consistently responsive and supportive communication.

Laura Schmidt, though with us for only a short while, we all benefitted from your professional touch and warmth.

Without the support in the laboratory from Moritz Aehle, Tabea Schneider, Nina Müller, Lydia Schramm, Janice C. de Mata, such beautiful data would have been difficult to put together. I am grateful!

To Herr. Dr. Barton, your return mid-journey was nothing short of a gift. Your suggestions, insights, and inputs were priceless, and this dissertation is richer for your involvement.

I am also grateful to Björn Rost, Kai Jensen, Flemming Dahlke, who not only agreed to constitute my examination committee but resolved the date of my disputation with remarkable grace and efficiency. I am honoured by your willingness to engage with this work.

To my friends Efe-Philip Osazee-Obazee and Patrick Chimeudeonwo, you were forever present throughout this journey, through every doubt and every small victory. The gold medals are yours, and you have earned them.

Finally, and most profoundly, to my family – my mom and brothers, your support meant everything to me. To Timothy Ehi Edetanlen, my five-star General with a heart of gold: thank you. This one is for you.

In the preparation of this dissertation, ChatGPT (OpenAI, GPT-4) was used for language editing and grammar improvement, and NotebookLM (Google) was used to assist in generating schematic illustrations in Chapter One. Both tools were operated in a mode where user inputs were not used for model training, and all outputs were reviewed and validated by the author and supervisor.

And to those still on the journey, let this energise you to the finish line. Rock on!

Universität Hamburg
DER FORSCHUNG | DER LEHRE | DER BILDUNG

FACULTY
OF MATHEMATICS, INFORMATICS
AND NATURAL SCIENCES

Declaration about personal contribution to manuscripts/publications in a

cumulative thesis (please submit one form per manuscript/publication)

Candidate's name: Michael Oseremen Edetanlen

Manuscript (including all authors, title, and if applicable journal, year; mark all first authors with asterisk):

"Chapter 2.1" - "Hot is the new cool: historical Baltic Sea cyanobacteria show trade-offs in thermal performance, carbon metabolism, and biotic interactions", in submission to Limnology& Oceanography as a report. Authors: Michael Edetanlen (ME) *, Amelie Kofler (AK), Samuel Barton, C.-Elisa Schaum(ES) "

Link to publication (if published):

Detailed description of own contribution to this manuscript

Conceptualization and planning of project:

ES (obtained funding), ME (helped to design the experiments)

Method development:

ES (conceptually) and ME (in the laboratory)

Data generation and analyses (including contribution to specific figures) :

ME (data generation), ESand ME (analyses, discussion of appropriate statistics, and visual representationof the data). AK contributed to generating the pilot data for 2.1.

Writing and editing of manuscript:

ME wrote all first drafts of all manuscripts. ES commented in detail on the first draft, and all other authors contributed to subsequent versions. SB in particular was involved in editing the manuscript.

I confirm that the above information is accurate

Candidate		**Supervisor name:** Elisa Schaum	
Hamburg, 20.03.2026		Hamburg, 20.03.2026	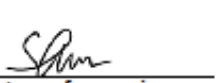
Place, date	Signature of candidate	Place, date	Signature of supervisor

Universität Hamburg
DER FORSCHUNG | DER LEHRE | DER BILDUNG

FACULTY
OF MATHEMATICS, INFORMATICS
AND NATURAL SCIENCES

Declaration about personal contribution to manuscripts/publications in a

cumulative thesis (please submit one form per manuscript/publication)

Candidate's name: Michael Oseremen Edetanlen

Manuscript (including all authors, title, and if applicable journal, year; mark all first authors with asterisk):
Chapter 2.2 " Divergent evolutionary trajectories under experimental warming in pre-industrial and contemporary Baltic Sea Nodularia spumigena", in submission to Science Advances, Authors "Michael Edetanlen *, Samuel Barton, C.-Elisa Schaum"

Link to publication (if published):

Detailed description of own contribution to this manuscript

Conceptualization and planning of project:
ES (obtained funding), ME (helped to design the experiments)

Method development:
ES (conceptually) and ME (in the laboratory)

Data generation and analyses (including contribution to specific figures) :
ME (data generation), ES and ME (analyses, discussion of appropriate statistics, and visual representation of the data).

Writing and editing of manuscript:
ME wrote all first drafts of all manuscripts. ES commented in detail on the first draft, and all other authors contributed to subsequent versions. SB in particular was involved in editing the manuscript.

I confirm that the above information is accurate

Candidate		**Supervisor name:** Elisa Schaum	
Hamburg, 20.03.2026		Hamburg, 20.03.2026	
Place, date	**Signature of candidate**	**Place, date**	**Signature of supervisor**

Universität Hamburg
DER FORSCHUNG | DER LEHRE | DER BILDUNG

FACULTY
OF MATHEMATICS, INFORMATICS
AND NATURAL SCIENCES

Declaration about personal contribution to manuscripts/publications in a

cumulative thesis (please submit one form per manuscript/publication)

Candidate's name: Michael Oseremen Edetanlen

Manuscript (including all authors, title, and if applicable journal, year; mark all first authors with asterisk):
Chapter 2.3 "Global DNA methylation correlates with thermal selection in Baltic Sea Nodularia spumigena" Authors "Michael Edetanlen *, C.-Elisa Schaum" under preparation - potentially for submission to Evolutionary Applications

Link to publication (if published):

Detailed description of own contribution to this manuscript

Conceptualization and planning of project:
ES (obtained funding), ME (helped to design the experiments)

Method development:
ES (conceptually) and ME (in the laboratory)

Data generation and analyses (including contribution to specific figures) :
ME (data generation), ES and ME (analyses, discussion of appropriate statistics, and visual representation of the data). A mini project student (Molly Showers) helped in generating part of the methylation assay data and is acknowledged in the acknowledgments.

Writing and editing of manuscript:
ME wrote all first drafts of all manuscripts. ES commented in detail on the first draft, and all contributed to subsequent versions

---

I confirm that the above information is accurate

Candidate

Hamburg, 20.03.2026 
Place, date Signature of candidate

Supervisor name: Elisa Schaum

Hamburg, 20.03.2026 
Place, date Signature of supervisor

Main Abstract

What makes cyanobacteria such formidable winners of climate change? In many aquatic systems, cyanobacteria often outperform their eukaryotic counterparts because they tolerate environmental conditions that constrain growth in other phytoplankton groups. Owing at least in part to their important roles in the nitrogen and carbon cycle, cyanobacteria and their physiological responses to environmental drivers are fairly well studied. However, short-term responses cannot always directly predict long-term responses, but we need to know the latter in order to say with more certainty whether and why cyanobacteria are indeed going to be the winners of a warming planet.

This dissertation investigates the eco-evolutionary responses of re-germinated bloom-forming cyanobacteria from different sediment layers (each layer representing different times, from pre-industrial times to the late 1990s) in response to increasing temperature using molecular (whole genome sequencing, methylation assays) and trait-based approaches (thermal performance curves, carbon use efficiency, organic carbon utilisation, biotic interaction assays). The comparative whole genome analysis of historic and recent lineages of *Nodularia spumigena* tests to what extent cyanobacteria have already evolved in an environment that has seen, among other changes, 2°C of warming over the past 170 years. We find that past evolution in *Nodularia spumigena* does not follow the "hotter is broader and better" prediction: pre-industrial (1824) lineages had the highest thermal optima but the lowest growth rates at prevailing summer temperatures, while contemporary (1996) lineages had lower thermal optima but higher growth rates at prevailing Baltic Sea summer temperatures, reduced allelopathic capacity, and broader organic carbon substrate use. These patterns are consistent with adaptation to increased thermal variability rather than directional warming alone. Carbon use efficiency was broadly conserved across sediment ages and temperatures, though the contemporary lineage showed the greatest capacity for CUE improvement under experimental warming. Experimental evolution over ~100 generations revealed that all cohorts can reach a similar post-selection T_{opt}, though the magnitude of shift required differs substantially across sediment ages, while the capacity for metabolic efficiency evolution is historically contingent and restricted to lineages with more recent evolutionary histories. Global DNA methylation is historically structured and co-varies with evolutionary shifts in thermal performance, establishing epigenetic state as a dynamically regulated molecular layer accompanying thermal adaptation. Together, these results indicate that *N. spumigena* has undergone substantial multi-trait evolutionary reorganisation over the past two centuries, and retains rapid adaptive potential under continued warming, but that the specific traits through which evolution is expressed depend on prior evolutionary history.

Zusammenfassung

Was macht Cyanobakterien zu so erfolgreichen Gewinnern des Klimawandels? In vielen aquatischen Systemen übertreffen Cyanobakterien häufig ihre eukaryotischen Gegenstücke, da sie Umweltbedingungen tolerieren, die das Wachstum anderer Phytoplanktongruppen einschränken. Aufgrund ihrer wichtigen Rolle im Stickstoff- und Kohlenstoffkreislauf sind Cyanobakterien und ihre physiologischen Reaktionen auf Umweltfaktoren vergleichsweise gut untersucht. Kurzfristige Reaktionen lassen jedoch nicht immer direkte Rückschlüsse auf langfristige Entwicklungen zu. Gerade Letztere sind jedoch entscheidend, um mit größerer Sicherheit beurteilen zu können, ob und warum Cyanobakterien tatsächlich zu den Gewinnern einer sich erwärmenden Welt zählen werden.

Diese Dissertation untersucht die öko-evolutionären Reaktionen von reaktivierten, blütenbildenden Cyanobakterien aus verschiedenen Sedimentschichten (wobei jede Schicht unterschiedliche Zeiträume repräsentiert, von vorindustriellen Zeiten bis in die späten 1990er Jahre) auf steigende Temperaturen. Hierfür werden sowohl molekulare Ansätze (Gesamtgenomsequenzierung, Methylierungsanalysen) als auch merkmalsbasierte Ansätze (thermische Leistungskurven, Kohlenstoffnutzungseffizienz, Nutzung organischer Kohlenstoffquellen, Tests biotischer Interaktionen) kombiniert. Die vergleichende Analyse ganzer Genome historischer und rezenter Linien von *Nodularia spumigena* untersucht, in welchem Ausmaß sich Cyanobakterien bereits an eine Umwelt angepasst haben, die unter anderem in den letzten 170 Jahren eine Erwärmung von etwa 2 °C erfahren hat.

Unsere Ergebnisse zeigen, dass die vergangene Evolution von *Nodularia spumigena* nicht der Vorhersage „hotter is broader and better“ folgt: Vorindustrielle (1824) Linien weisen die höchsten thermischen Optima auf, jedoch die niedrigsten Wachstumsraten bei vorherrschenden Sommertemperaturen, während rezente (1996) Linien niedrigere thermische Optima, aber höhere Wachstumsraten bei den gegenwärtigen Sommertemperaturen der Ostsee, eine reduzierte allelopathische Kapazität sowie eine breitere Nutzung organischer Kohlenstoffsubstrate aufweisen. Diese Muster sprechen eher für eine Anpassung an zunehmende thermische Variabilität als an eine rein gerichtete Erwärmung.

Die Kohlenstoffnutzungseffizienz war über Sedimentalter und Temperaturen hinweg weitgehend konserviert, wobei die rezente Linie die größte Fähigkeit zur Verbesserung der CUE unter experimenteller Erwärmung zeigte. Experimentelle Evolution über etwa 100 Generationen zeigte, dass alle Kohorten ein ähnliches thermisches Optimum nach Selektion erreichen können, wobei das Ausmaß der erforderlichen Verschiebung je nach Sedimentalter deutlich variiert. Die Fähigkeit zur Evolution metabolischer Effizienz ist hingegen historisch kontingent und auf Linien mit jüngerer Evolutionsgeschichte beschränkt. Die globale DNA-Methylierung ist historisch strukturiert und kovariiert mit evolutionären Veränderungen in

der thermischen Leistungsfähigkeit, was darauf hindeutet, dass epigenetische Zustände eine dynamisch regulierte molekulare Ebene darstellen, die thermische Anpassung begleitet.

Zusammenfassend zeigen diese Ergebnisse, dass *N. spumigena* in den letzten zwei Jahrhunderten eine umfassende evolutionäre Reorganisation über mehrere Merkmale hinweg durchlaufen hat und weiterhin ein hohes Anpassungspotenzial unter fortschreitender Erwärmung besitzt. Gleichzeitig hängt jedoch die spezifische Ausprägung evolutionärer Veränderungen von der jeweiligen evolutionären Vorgeschichte ab.

Table of contents

Glossary

Adaptation and Evolution: Evolution refers to a process by which organisms adjust and become better suited to their environment through mechanisms such as mutation, selection, genetic drift, and gene flow. When evolutionary change leads to increased fitness of an organism or population, it is referred to as adaptation.

Ancestor: Selected lineages used as the starting population at the commencement of evolution experiment regardless of age or origin.

De-novo mutation: A non-inherited spontaneous change in the DNA genetic sequence, observed for the first time.

Evolutionary potential: The capacity of an organism or population to evolve and/or adapt to changing environmental conditions, determined by factors such as standing genetic variation, mutation rates, selection pressure, and population sizes.

Fitness landscape: Represents a conceptual relationship between phenotypic or genotypic variation and fitness, where trait combinations correspond to diverse fitness values. Across environments, this can change in time space, influencing the rate, direction, and predictability of evolutionary responses.

Functional group: This refers to a set of organisms with similar ecological roles or functional traits, respond comparatively to environmental drivers, and contribute in the same way to the ecosystem irrespectively of taxonomic relatedness.

Natural selection: The process by which better-suited alleles or genes become more prevalent in a population.

Phenotypic plasticity: Refers to the capacity of a genotype to produce different phenotypes in response to environmental changes without any heritable genetic change. It can lead to increased or reduced fitness of an organism and can occur within one generation or across generations.

Phytoplankton thermal tolerance: The measured response of one or more fitness traits to temperature typically represented as a unimodal curve.

Reaction norm: The expected range of phenotypes expressed by a genotype as a function of the environmental drivers e.g. temperature. This can be linear or non-linear for the same trait, depending on the range of environments chosen.

Single nucleotide polymorphism (SNPs) **or single nucleotide variant (SNV)**: A variation at a single nucleotide location in the DNA sequence, among individuals of a population often occurring at a frequency greater than one percent.

Standing genetic variation: The allelic variation at one or more loci within a population at a given time.

Trait: A characteristic feature or attribute of an organism. This could be morphological, physiological, a life-history or behavioural attribute.

Chapter One: Main introduction

Mighty microbes in a warming world: concepts, mechanisms, and challenges

Earth's temperature is rising at an unprecedented rate, and organisms across ecosystems respond to environmental changes through a combination of phenotypic plasticity and evolutionary adaptation, range shifts, or extinction (Gienapp et al., 2008), complicating predictions of biological thermal responses. While plastic responses reflect rapid physiological adjustments within a few generations, evolutionary responses arise from genetic changes across several generations that determine long-term persistence. Marine organisms are no exception. As with all ectotherms, temperature modulates physiological responses. However, due to their short generation times, many microorganisms experience rapid climate change as a gradual shift across generations, facilitating the unfolding of genetic responses on ecologically relevant timescales (Barton et al., 2020; Padfield et al., 2016; Schaum, Buckling, et al., 2018). Understanding these responses is not only vital for modelling species distribution and ecosystem function, but also for predicting the degree to which biota have the potential to influence biogeochemical cycles as oceans warm.

Nearly every aspect of an organism's performance is influenced by temperature because biochemical reactions noticeably accelerate with warming up to an upper limit imposed by enzyme stability and cellular homeostasis. The Metabolic Theory of Ecology (MTE) underscores this by linking temperature to metabolic rates, resource allocation, and growth through activation energy kinetics (Brown et al., 2004). Even though MTE provides such elegant framework, recent empirical studies have shown that living-organisms often deviate from predictions because they possess mechanisms that modulate metabolic constraints. In phytoplankton, rapid evolution and regulatory changes in metabolic traits can drive thermal adaptation (Padfield et al., 2016), and environmental fluctuations can accelerate molecular evolution of thermal tolerance (Schaum, Buckling, et al., 2018). Particularly for phytoplankton, these deviations frequently arise because organisms adjust intracellular resource use, membrane composition, or protein turnover as temperature fluctuate – reactions that boost performance in the short term, but can mask underlying evolutionary limits (Padfield et al., 2016; Schaum, Buckling, et al., 2018; Schaum et al., 2022).

Researchers often turn to thermal performance curves (TPCs) and thermal reaction norms (TRNs), in order to understand how organisms, respond to warming. TPCs describe how fitness or fitness proxies such as growth rate change as a function of temperature, while TRN is often used to describe the way in which traits other than growth change across temperatures. Together, these frameworks capture key traits such as growth rate, photosynthetic capacity, respiration, cell size, or nitrogen fixation as they change across temperature gradients. Although TPCs/TRNs are valuable tools, they have fundamental limitations especially when used to infer long-term responses because if used at a single point in time, they primarily

elucidate plasticity and not adaptive evolutionary potential. Therefore, predicting long-term persistence or adaptation from short-term assays alone may be misleading, as fluctuating-environment selection experiments in marine diatoms demonstrate strong lineage- and context-dependence (Schaum, Buckling, et al., 2018), and theoretical work suggests that plastic responses are not always reliable predictors of evolutionary change (Draghi & Whitlock, 2012; Ghalambor et al., 2007). In addition, natural systems impose thermal fluctuations and unpredictable heat events, adding a layer of complexity as organisms evolve plasticity and generalist strategies that trade-off thermal breadth against performance optimum (Padfield et al., 2016; Schaum, Buckling, et al., 2018; Schaum et al., 2022).

Predictions are further complicated by genetic and lineage-level variability (Burga & Lehner, 2012; Mäkelä et al., 2017). Cyanobacteria such as *Nodularia spumigena* harbour genetically diverse lineages displaying variable thermal responses (Medwed et al., 2024). It is important to integrate multiple methodologies in order to capture both plastic and evolutionary responses because extrapolating information from single-lineage data alone exposes the inherent risk of distorting species-wide adaptive capacities.

This dissertation, through a multi-pronged approach combines resurrection ecology – reviving historical *Nodularia spumigena* lineages from dated Baltic Sea sediments, with experimental evolution under sustained warming, and genome-wide molecular analysis including DNA methylation profiling. Resurrection ecology uniquely captures direct temporal thermal-trait comparisons elucidating evolutionary shifts across decades; experimental evolution directly reveals rates and constraints of adaptation as it occurs; molecular data annotates the genetic and epigenetic mechanisms underlying these phenotypic variations.

The theoretical, ecological, and methodological foundations for this approach are highlighted in the sections below:

1.1 Organisms in a warming world: ecological and theoretical foundations

Temperature drives organismal biological performance because it affects all enzymatic reactions. Reaction rates accelerate as temperature rises, until biochemical limits are reached (Hobbs et al., 2013). At extremely high temperatures, enzyme denaturation and membrane integrity loss sets in, together with constraints imposed by imbalances between photosynthesis and respiration (Raven & Geider, 1988). These fundamental biochemical sensitivities generate predictable thermal dependences across taxa and underscore the MTE framework (Brown et al., 2004).

For aquatic microorganisms, thermal response is particularly pronounced. Their metabolic networks – photosynthesis, respiration, nitrogen fixation, and carbon-concentrating mechanisms are all strongly temperature-dependent. Because these networks are tightly connected, warming can shift the balance between energy costs and gains. For example, respiration often increases more steeply with temperature

than photosynthesis, leading to lower carbon use efficiency (CUE, the amount of carbon potentially available for growth, structural, and other processes after respiration has been accounted for) at higher temperatures (Barton et al., 2020; Hobbs et al., 2013). These metabolic imbalances can cascade into altered nutrient cycling, shifts in community composition, and changes in bloom dynamics (Listmann et al., 2021).

Organisms exhibit physiological plasticity in response to temperature fluctuations, or gradual changes in temperature. In diverse thermal conditions, phytoplankton can quickly adjust cellular resource distribution, enzyme expression, membrane fluidity, and pigment concentration, facilitating short-time persistence (Padfield et al., 2016). However, while plasticity can often predict short-term fitness outcomes, under certain conditions it can also be a good predictor for evolution (Botero et al., 2015; Schaum & Collins, 2014). Plasticity may temporarily enhance performance and at the same time mask underlying evolutionary constraints, trade-offs, or limits to long-term adaptive response that only emerge over generations (Schaum, Buckling, et al., 2018). Relying on plastic responses can consequentially obscure how phenotypes evolve, and which specific traits contribute to long-term ecological and evolutionary outcomes.

As environments warm, they often also become more thermally variable, exposing organisms to more fluctuations around mean conditions. This variability can modulate how organisms respond to temperature change and how fast evolutionary adaptation occurs. Selection often favours narrow thermal niches and characterised by high performance near a thermal optimum in a relatively stable temperature condition (Angilletta, 2009; R. B. Huey & Kingsolver, 1989). On the other hand, high thermal variability tend to select for generalist strategies that broaden thermal tolerance to the detriment of optimal performance (Padfield et al., 2016; Schaum et al., 2022). These eco-evolutionary interactions imply that understanding thermal responses requires attention to the shape of TPCs/TRNs and the timescales over which they are measured.

1.2 Limits of thermal performance curves (TPCs) and thermal reaction norms (TRNs)

TPCs demonstrate how a performance-related trait, commonly growth rate, responds to temperature. They are generally unimodal if measured across a sufficiently broad range of temperatures: performance increasing with warming until an optimum (T_{opt}) is reached, beyond which it declines sharply due to accumulated damage and stress at high temperatures (Angilletta, 2009; Baker et al., 2016; R. B. Huey & Kingsolver, 1989; Kingsolver, 2009).

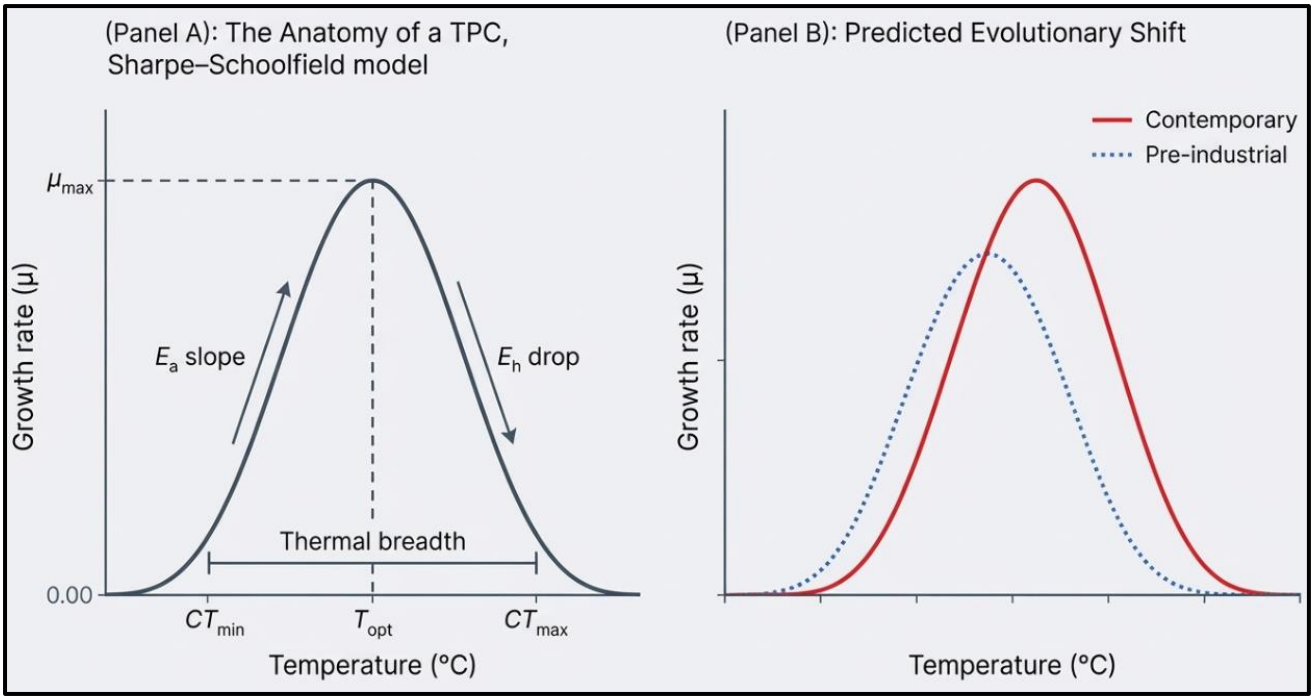

Fig. 1. Anatomy of a thermal performance curve (TPC) and comparison of predicted versus observed thermal evolution in *Nodularia spumigena*. **(A)** Key parameters of the Sharpe-Schoolfield model used throughout this dissertation: the thermal optimum (T_{opt}), maximum growth rate (μ_{max}), activation energy (E_a) representing thermal sensitivity below the optimum, high-temperature deactivation energy (E_h), and thermal breadth (CT_{min}–CT_{max}). **(B)** The classical "hotter is better and broader" prediction, under which adaptation to warming should yield higher T_{opt}, elevated μ_{max}, and expanded thermal breadth in contemporary relative to pre-industrial lineages. Schematic prepared by the author.

TPCs are a specific form of thermal reaction norms (TRNs), which capture the temperature response of any trait. For example, TRNs can describe the variation in cell size, toxin production, photo-physiological traits, respiration rates, nitrogen fixation, or even nutrient uptake. These non-fitness traits often have different thermal sensitivities than growth. While photosynthesis may plateau or decline earlier, respiration tend to increase steeply with warming such that their combined response can result in mismatches in carbon balance on physiological timescales (Bernhardt et al., 2018).

Despite their widespread application, TPCs and TRNs have notable limitations. First, TPCs/TRNs typically capture phenotypic plasticity, not evolutionary adaptation if measured at a single point in time or space (Angilletta Jr., 2009; R. B. Huey & Kingsolver, 1989; Kingsolver, 2009). Second, they tend to ignore environmental variability associated with natural systems – thermal fluxes, heatwaves, and diurnal patterns, as most assays are conducted under constant temperatures (Baker et al., 2016; Striebel et al., 2016). Because thermal performance assumes nonlinearity, mean performance under fluctuating temperatures differs from that under constant temperatures (Bernhardt et al., 2018). Third, phytoplankton species, including cyanobacteria harbour genetically diverse lineages with distinct thermal traits so that extrapolating purely from single-lineage data alone risks the misrepresentation of the species' true thermal niche underscoring the substantial lineage-level variation (Bernhardt et al., 2018; Striebel et al., 2016). Finally, TPCs/TRNs

omit sub-lethal processes such as oxidative stress, protein chaperone use, membrane damage, or cumulative metabolic costs which are not often visible in short-term assays but tend to determine long-term viability. These limitations motivate the integration of long-term approaches – resurrection ecology and experimental evolution, to investigate the evolutionary potential of thermal traits. The anatomy of a TPC and the departure of our findings from classical predictions are illustrated in Fig. 1.

1.3 When short-term responses fail to predict long-term outcomes

In some cases, short-term physiological or fitness responses can provide valuable insights into long-term outcomes, particularly under stable or single, well-defined environmental drivers. However, under broad-acting environmental drivers such as temperature, which simultaneously affects enzyme kinetics, membrane integrity, metabolic rates, and growth, their predictive power often breaks down. Knowledge on phytoplankton thermal responses remains dominated by short-term experiments that track performance over hours to days. Although these assays are high throughput and repeatable, their reliance on immediate responses imply they primarily reflect plasticity, which can predict evolution for drivers of less broad effect than temperature (Ghalambor et al., 2007), but can also either mask or exaggerate temperature-dependent fitness constraints over longer timescales (Collins et al., 2014; Padfield et al., 2016; Schaum, Buckling, et al., 2018).

Studies comparing short-term responses and long-term adaptation under warming often reveal marked discrepancies (Barton et al., 2020; Schaum et al., 2017). For example, populations may in the short-term exhibit strong thermal tolerance owing to rapid physiological acclimation, yet this short term performance does not necessarily reflect long-term evolutionary outcomes as warming persists across several generations (Padfield et al., 2016). Populations often initially exhibit reduced performance under warming but can subsequently adapt, in some cases rapidly. Although the strength of evolutionary responses can often be predicted, the direction of trait change as well as the specific traits under selection are considerable less so (Collins & Schaum, 2021; Hinners et al., 2017; Padfield et al., 2016; Schaum, Buckling, et al., 2018).

Given natural systems rarely experience constant temperatures, with heatwaves, rapid fluctuations, and shifts in temperature regimes possibly producing negative outcomes that can be masked in constant-condition assays, predictions based solely on short-term TPCs risk missing actual population trajectories (Baker et al., 2016; Gill et al., 2022). These complex dynamics simply imply that while short-term responses only provide snapshots of organismal performance, long-term ecological success depends on their capacity to evolve amid persistent warming, hence the need for approaches integrating plasticity and evolution.

1.4 Evolutionary potential under warming: timescales, mechanisms, and constraints

Due to the short generation times associated with microorganisms, they have the potential to evolve in step with environmental changes. In principle, evolutionary adaptation could buffer or mitigate the negative effects of warming. The central question therefore is not whether evolution occurs, but how fast evolutionary processes proceed, in which direction traits shift together with the predictability of these responses. Outcomes depend on a number of factors such as: standing genetic variation, mutation rates, effective population sizes, and the shape of the fitness landscape itself (Collins et al., 2014; Padfield et al., 2016; Schaum, Buckling, et al., 2018).

Because organismal traits typically evolve at different rates, traits underlain by many genes with small effects (polygenic traits) tend to shift gradually under selection, whereas traits governed by a few key loci may exhibit rapid evolution if beneficial mutations prevail (Collins & Schaum, 2021). Phytoplankton studies have shown that evolution can affect growth rates, thermal optima, cell sizes, and metabolic rates across as few as dozens or as many as hundreds of generations (Barton et al., 2020; Padfield et al., 2016; Schlüter et al., 2016). These timescales are within the limits of seasonal or annual climate fluxes, an indication that evolution is essential for microbial responses to warming (Hinners et al., 2017; Padfield et al., 2016; Schaum, Buckling, et al., 2018).

The speed and direction of evolutionary responses remain difficult to predict despite evolution being synonymous with persistence and reproduction. In certain scenarios, constraints such as trade-offs between growth and stress tolerance may limit thermal adaptation (Buckley & Kingsolver, 2021; Raymond B. Huey & Kingsolver, 1993; Pörtner et al., 2006). For example, populations with high thermal adaptation may suffer reduced performance at lower temperatures, thereby narrowing their thermal breadths. In other studies, physiological limits such as enzyme stability or resource allocation trade-offs have limited upward shifts in T_{opt} notwithstanding strong selection for warmer conditions (Collins et al., 2014; Hinners et al., 2017; Schaum, Buckling, et al., 2018; Schaum & Collins, 2014).

Adaptational – evolutionary change leading to higher fitness, also depends on an environment's predictability (Rescan et al., 2022; Schaum et al., 2016). In systems with strong environmental abiotic fluctuations, populations may evolve generalist strategies that reduce performance trade-offs across temperatures but also limit specialization at the warmest extremes. Albeit remaining vulnerable to extreme heat events, such generalists may persist across a wide range of temperatures (Baker et al., 2016; Gill et al., 2022).

Importantly, evolutionary responses interact with ecological dynamics. As populations evolve and, perchance, adapt, they may alter nutrient uptake rates, competitive interactions, or even trophic dynamics. These eco-evolutionary feedbacks complicate predictions and underscore the necessity for approaches

that integrate both ecological and evolutionary processes when investigating organismal response to warming (Bernhardt et al., 2018; Padfield et al., 2016; Schaum, Buckling, et al., 2018).

1.5 Long-term responses: approaches and insights

Understanding long-term evolutionary responses to changes in the environment remains a central challenge in ecology and evolutionary biology. Although short-term experiments provide valuable insights on physiological limits and plastic responses, several complementary strategies to short-term assay including space-for-time, resurrection ecology, and experimental evolution, have been developed to help address the challenge of investigating responses over ecological and evolutionary timescales.

Space-for-time substitution is a common method used to compare populations across geographic-temperate-gradients, assuming that spatial variation can serve as a proxy for temporal change. Under this framework, thermal adaptation can be deduced from scenarios where warm-region populations outperform cooler-region populations at high temperatures. Although useful, interpretations can be confounded by spatial differences in salinity, nutrients, grazing pressure, and light regimes (Angilletta, 2009; Baker et al., 2016). This makes attributing causality to warming alone difficult because many environmental factors co-vary with temperature across space, apart from rare studies leveraging strong environmental gradients across short distances (Schaum, Ffrench-Constant, et al., 2018). Within a single population, space-for-time comparisons also do not capture historical changes, making it very difficult to disentangle local adaptation from colonization by warm-adapted lineages.

Resurrection ecology offers a backward-in-time approach as a powerful alternative to study organisms as they existed decades to centuries ago. Because many phytoplankton functional groups e.g. cyanobacteria, diatoms, dinoflagellates, and chlorophytes form resting stages that sink into sediments (Ellegaard & Ribeiro, 2018; Hallegraeff & Bolch, 1992; McQUOID et al., 2002), remaining viable for long periods, it becomes possible to revive these historical lineages from dated sediment archives, and comparing same directly with contemporary ones under controlled conditions. This approach has been applied with success to dinoflagellates and other protists from the Baltic Sea, revealing historical shifts in life-cycle traits, growth rates, and thermal responses. Findings from these studies demonstrate that evolution and demographic changes that affect bloom phenology and population resilience have occurred over the last century (Hinners et al., 2017). Importantly, resurrection studies provide access to both trait-based and genomic information from historical populations, enabling the study of evolutionary mechanisms across time. These three complementary methodological frameworks are compared schematically in Fig. 2.

For cyanobacteria however, resurrection ecology is comparatively unexplored. Despite cyanobacteria producing resting stages such as akinetes, their long-term viability in sediments, frequency of deposition,

and their response to long-term burial remain less well understood than in dinoflagellates. This makes cyanobacteria a good candidate for testing the generality of resurrection-based evolutionary inferences.

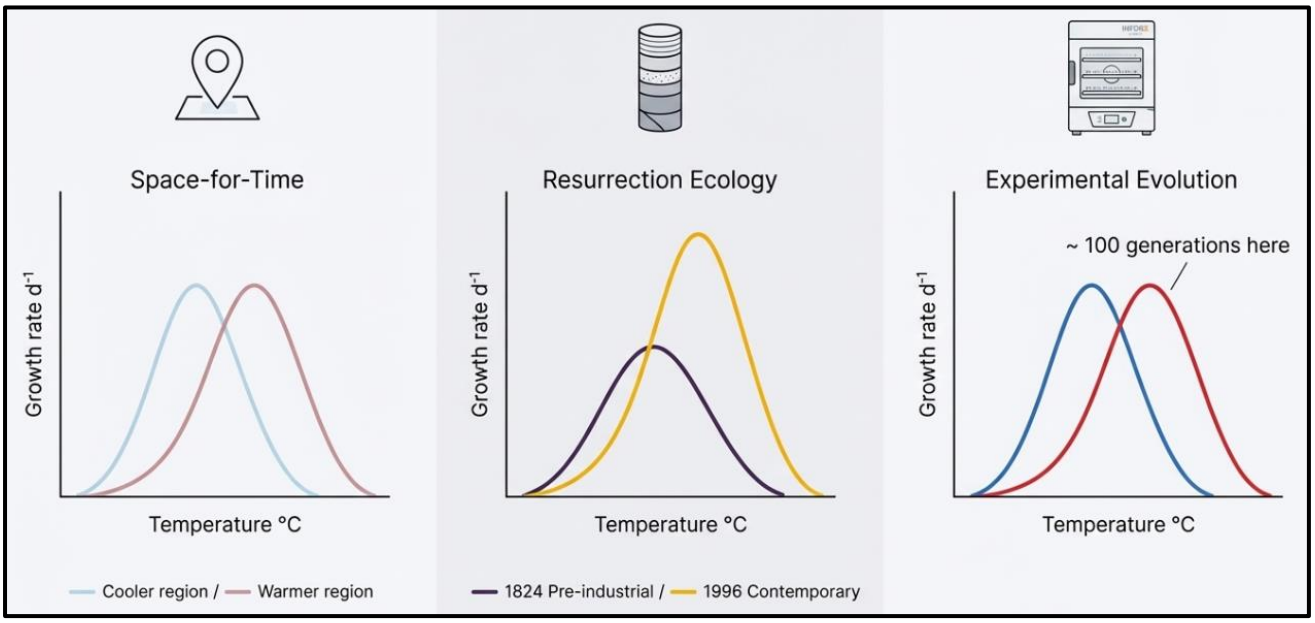

Fig. 2. Three complementary methodological approaches that can be used to decouple phenotypic plasticity from evolutionary adaptation in cyanobacteria under warming. All panels show specific growth rates (d^{-1}) as a function of temperature (°C), with unimodal curves fitted using the Sharpe-Schoolfield model. **(A)** Space-for-time substitution uses populations from cooler and warmer regions (pale blue and pale red, respectively) to infer local adaptation from spatial thermal gradients, though interpretations are susceptible to confounding by co-varying environmental factors. **(B)** Resurrection ecology provides a direct temporal comparison of lineages resurrected from Sea sediment archives e.g. spanning nearly two centuries (1824–1996; dark purple, and golden yellow respectively), enabling evolutionary inference under common-garden conditions. Contemporary lineages (1996) show higher T_{opt} and higher growth rates at prevailing summer temperatures than pre-industrial lineages (1824). **(C)** Experimental evolution tracks real-time adaptation over above 100 generations of sustained thermal selection, comparing ancestral (light blue) and evolved (dark red) populations. Schematic prepared by the author.

Experimental evolution offers a forward-in-time approach, which complements the backward-in-time approach (resurrection ecology) by observing adaptation in real time. In such studies, microbial populations are exposed to novel or altered environmental pressures, and trait or genomic variability are measured over hundreds and possibly thousands of generations. When applied to warming, experimental evolution can reveal how quickly thermal traits evolve, whether adaptation is constrained, which life-history traits or metabolic pathways are most affected, and how different genetic backgrounds respond to identical selection pressures (Gill et al., 2022; Padfield et al., 2016; Schaum, Buckling, et al., 2018).

Experimental evolution is particularly powerful because it elucidates causality and can in combination with molecular studies and trait monitoring, track evolutionary responses in real time. Additionally, if populations evolve higher thermal tolerance under warming, confounding factors can be excluded, attributing this directly to temperature. This approach also allows for high replication, a key advantage over historical comparisons.

Trait data and molecular data comparison, provide insight into organismal performance and ecological function by measuring trait-based parameters e.g. growth, photosynthesis, respiration, and nitrogen fixation, while also revealing mechanisms – sequence variation across historical and modern lineages, structural variants, potential regulatory loci, and DNA methylation patterns that may affect epigenetic responses.

Even without a genome-wide association study on the population level, whole-genome comparisons can detect selection signatures, divergence among lineages, or changes in gene content that accompany phenotypic shifts. A combination of trait and molecular data provides a complete picture of evolutionary change – traits revealing what has changed while molecular information provides clues as to why and how.

1.6 Unravelling evolutionary secrets in a natural laboratory – the Baltic Sea

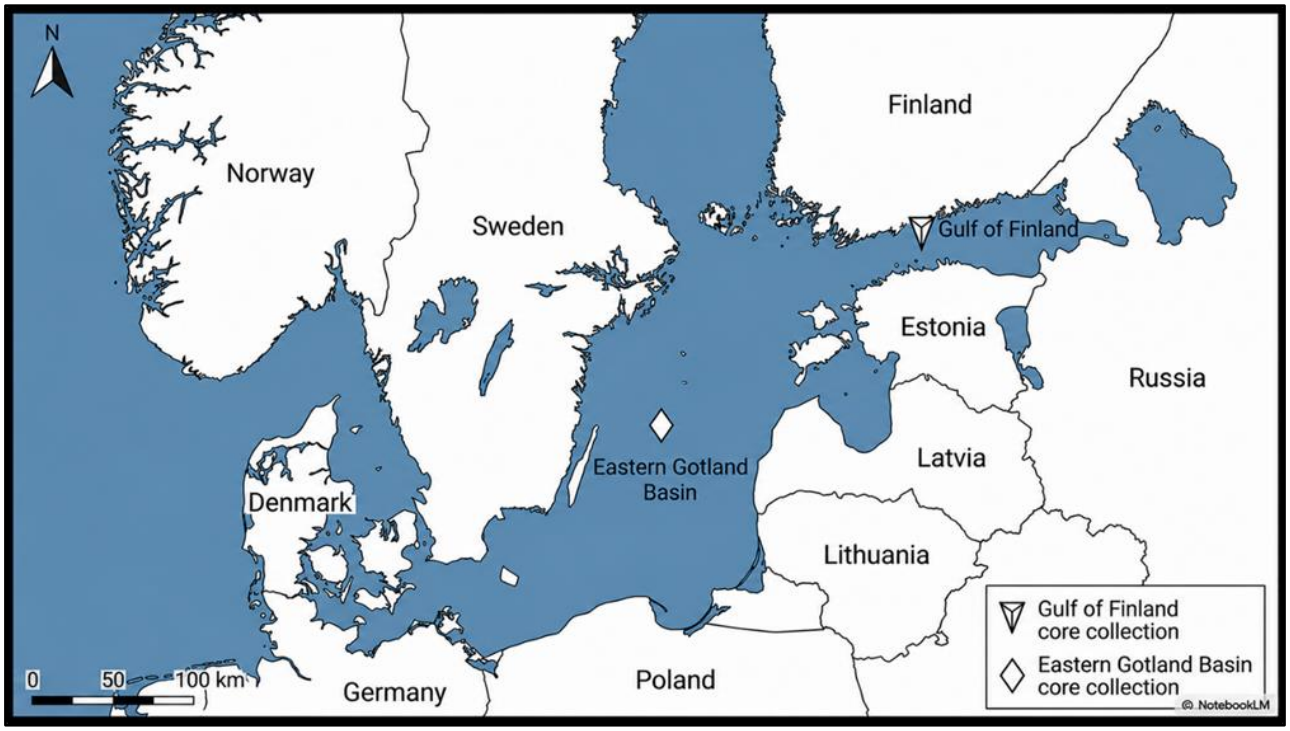

Fig. 3. Map of the Baltic Sea showing the two sediment core sampling sites used in this dissertation. *Nodularia spumigena* resting stages (akinetes) were re-germinated from dated sediment layers originating from the **Eastern Gotland Basin** the **Gulf of Finland**, representing two environmentally distinct sub-basins with different warming histories and sedimentation conditions. Map prepared by the author.

The Baltic Sea is an important brackish water reservoir harbouring diverse and sometimes endemic life forms. Its vast expanse of briny water, second in size only to the Black Sea is characterised by pronounced environmental gradients, limited water exchange, and strong sensitivity to climatic variation. Over the past century, the Baltic Sea has experienced substantial warming, especially during summer months where surface temperatures in some basins regularly exceed 20°C (Kniebusch et al., 2019; Meier et al., 2022). These warming trends coincide with changes in salinity, stratification, nutrient inputs, and plankton

community structure, making the Baltic Sea an ideal natural laboratory for investigating ecological and evolutionary responses to long-term ecosystem modification. The two sediment core sites used in this study are shown in Fig. 3.

1.6.1 Environmental history and warming trends

Palaeoecological reconstructions and long-term monitoring suggest that the Baltic Sea has warmed significantly since the beginning of the 20th century, particularly with accelerated warming since the 1980s (Lehmann et al., 2011; MacKenzie & Schiedek, 2007). These changes have altered circulation patterns, strengthened stratification, and prolonged periods of calm, stable surface water conditions favourable for cyanobacteria growth (Elken et al., 2015; Hense et al., 2013; Neumann et al., 2012). Concurrently, eutrophication from agricultural runoff and altered nutrient ratios have boosted the persistence of summer blooms. (Savage et al., 2010; Stigebrandt & Andersson, 2020; Vahtera et al., 2007).

Field-based approaches to decouple these trends and patterns have been particularly challenging because warming trends have unfolded alongside shifting nutrient dynamics, making it difficult to distinguish physiological and evolutionary responses to warming from those driven by eutrophication. This challenge therefore highlights the need for laboratory-based approaches such as resurrection ecology and experimental evolution to underpin temperature effects in controlled conditions (Hinners et al., 2017).

1.6.2 The unique value of sediment archives

The relatively slow sedimentation facilitated by the semi-enclosed nature of the Baltic Sea produces well-preserved stratified sediment layers. The sediments harbour resting stages of numerous phytoplankton groups including dinoflagellate cysts and cyanobacteria akinetes, providing a chronological record of past communities. (Hinners et al. (2017) studied dinoflagellates revived from approximately 100-year-old Baltic Sea sediments, and revealed historical changes in thermal tolerance and life-history, demonstrating the validity of resurrection ecology as backward-in-time approach for linking past environmental conditions to biological responses.

Cyanobacteria however remain underrepresented in resurrection-based studies. *Nodularia spumigena,* a key Baltic Sea bloom-forming species, form akinetes that settle into sediments particularly at the end of the bloom season. The viability, abundance, spatial distribution, and long-term integrity of these akinetes vary across basins and are influenced by local conditions such as oxygen availability close to the sediment-water surface. Nevertheless, akinetes have been successfully revived from layers several decades old, an indication that Baltic Sea sediments can preserve cyanobacterial akinetes sufficiently long enough for evolutionary comparisons across time.

1.6.3 The relevance of *Nodularia spumigena*

Nodularia spumigena, a filamentous diazotroph – nitrogen-fixing cyanobacterium, plays a central role in Baltic Sea biogeochemistry. By fixing atmospheric nitrogen during summer blooms, it contributes substantially to the internal nutrient loading of the system, sustaining productivity even when external nitrogen inputs are limited. *Nodularia spumigena* bloom events can extend over large areas with pronounced ecological impacts including surface-water shading, reduced oxygen concentrations at depth, and toxin (hepatotoxin nodularin) production, which poses risks to wildlife and human health.

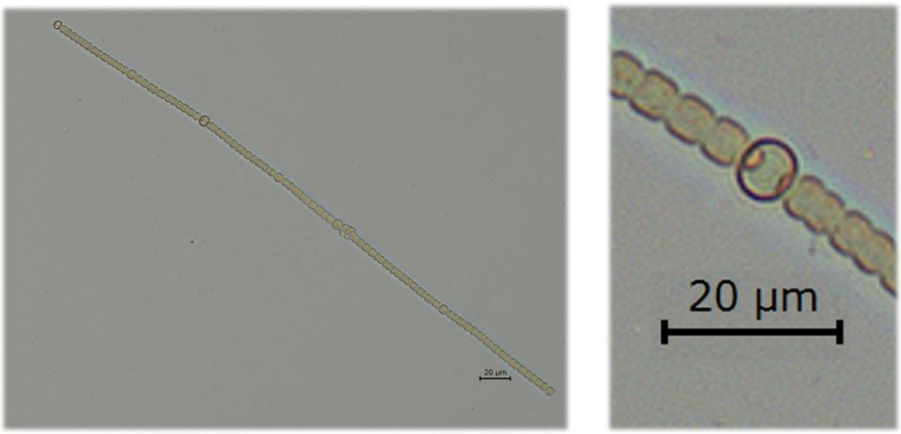

Fig. 4. Light microscope image of the filamentous diazotrophic cyanobacterium *Nodularia spumigena*. The left image shows a filament (trichome) consisting of a chain of vegetative cells interspersed with specialised nitrogen-fixing heterocysts, visible as larger thick-walled cells occurring at regular intervals along the trichome. The right image shows a magnified section highlighting the heterocyst morphology. Heterocysts provide a micro-oxic environment required for nitrogen fixation, enabling growth in nitrogen-limited conditions. Scale bar: 20 µm.

Nodularia spumigena serves as an ideal candidate for investigating thermal adaptation through time due to its summer surface-water dominance, strong temperature dependence, and capacity to form long-lived akinetes. Understanding its physiological and evolutionary responses to warming is both relevant to bloom ecology and for predicting how biogeochemical cycling in the Baltic Sea will shift under ongoing climate change.

1.7 Cyanobacteria and resurrection ecology: opportunities and challenges

Our knowledge of temporal ecological and evolutionary processes have been revolutionised by resurrection ecology providing the framework allowing for direct comparisons of pre-industrial and contemporary populations (Kerfoot & Weider, 2004; Medwed et al., 2024). While this approach has been applied to other phytoplankton taxa and even freshwater zooplankton, its application to cyanobacteria remains limited. Notwithstanding, cyanobacteria remains a promising candidate for resurrection studies.

1.7.1 Cyanobacteria resting stages

Many bloom-forming cyanobacteria – including *Nodularia spp., Aphanizomenon spp.,* and *Dolichospermum spp.,* produce akinetes with thick cell wall, reduced metabolic activity, and high resistance to environmental stress. These resting stages facilitate overwintering and dispersal across basins. In the Baltic Sea, akinetes can accumulate in sediments, potentially preserving genetic material, and phenotypic information from pre-industrial populations (Medwed et al., 2024; Śliwińska-Wilczewska et al., 2019).

The longevity of cyanobacterial akinetes is less well investigated compared to that of dinoflagellate cysts. However, viable akinetes have been isolated from decades-old sediments, demonstrating that resurrection is possible (Medwed et al., 2024). Despite multi-decadal archives providing valuable temporal windows for investigating evolutionary responses, it remains to be seen whether akinetes can remain viable for centuries.

1.7.2 Potential and limitations

Unlike dinoflagellates with fundamental cyst morphologies facilitating species identification in sediments, cyanobacteria lack these complexes, making quantification of historical population complicated leaving molecular confirmation of revived lineages as the only alternative (Kremp et al., 2018; Monchamp et al., 2016). Additionally, akinete abundance is dependent on, and varies with bloom intensity, sedimentation rates, and bioturbation, potentially limiting spatial and temporal coverage.

In spite of these challenges, resurrection ecology provides valuable insights into cyanobacterial evolution. It enables the comparison of thermal performance between historical and contemporary lineages without confounding environmental variability. Resurrection ecology when combined with molecular analysis can elucidate changes in the genomic content, selection signatures, and shifts in regulatory processes such as DNA methylation.

1.7.3 Integrating resurrection ecology with experimental evolution

The combination of resurrection ecology and experimental evolution represent a powerful methodological approach for evolution studies. While resurrection provides snapshots of past evolutionary states, experimental evolution reveals the dynamics of ongoing adaptation (Gill et al., 2022; Padfield et al., 2016; Schaum, Buckling, et al., 2018). By comparing the adaptive thermal response of historical and modern lineages, researchers can determine if:

- historical or recent lineages have greater potential shifting in T_{opt}, to higher temperatures or otherwise modulating their thermal performance as the environment warms,
- contemporary lineages have already evolved thermal tolerance due to recent warming, or
- evolutionary constraints limit thermal adaptation regardless of historical baseline.

This integrated approach is central to this dissertation and forms the empirical foundation for investigating both short-term physiological plasticity and long-term evolutionary shifts in Baltic Sea *Nodularia spumigena*.

1.8 Knowledge gaps in *Nodularia spumigena* long-term thermal response

As with other phytoplankton groups, extensive research using cyanobacteria have been conducted but major uncertainties persist on how cyanobacteria respond to long-term warming physiologically and in evolutionary terms. Several key knowledge gaps limiting predictions of future bloom dynamics remain because there are only a handful of studies examining multi-decadal or evolutionary processes, with majority of studies focusing on short-term thermal responses.

1.8.1 Absence of historical baselines for cyanobacterial thermal adaptation

It is difficult to determine if current thermal performance reflects recent adaptation derived from inherent species-dependent traits since most available data on *Nodularia spumigena* are from modern isolates. Without historical baselines, interpreting contemporary thermal reaction norms will be speculative. Resurrection ecology has provided these baselines for Baltic Sea dinoflagellates, revealing shifts in growth, life-cycle traits, and thermal responses over the last century (Hinners et al., 2017). However, similar studies using cyanobacteria remain unavailable. Therefore, determining if *Nodularia spumigena* have evolved comparable traits in response to temperature remains a central question to answer.

1.8.2 Insufficient quantification of lineage-level thermal variation

Within a single cyanobacteria bloom alone, *Nodularia spumigena* habour genetically unique lineages that may vary in growth rates, nitrogen fixation, toxin production, and thermal tolerance (Cegłowska et al., 2018; Mazur-Marzec et al., 2016; Voss et al., 2013). However, the extent of intraspecific variability in thermal traits, and how this variation has changed over time remain to be explored. Therefore, examining historical-modern differences is essential because thermal reaction norms explains persistence under warming. **This knowledge gap is addressed in Chapter 2.1., where thermal performance curves of ancestor and descendant lineages are compared.**

1.8.3 Unknown evolutionary potential under sustained warming

Empirical data for evolutionary responses of cyanobacteria to warming are rare although such studies on other phytoplankton taxa reveal evolved higher thermal optima or reorganised metabolic pathways under warming (Barton et al., 2023; Medwed et al., 2024; Padfield et al., 2016). It becomes essential to investigate if *Nodularia spumigena* can do the same. Cyanobacteria incur high energy demands associated with nitrogen fixation, photosynthesis, and stress protection, potentially constraining upward shifts in T_{opt}. It remains unclear if historical and modern lineages differ in evolutionary potential, or whether trajectories show constraints or trade-offs. **Chapter 2.2 investigates this by exposing historical and modern lineages to sustained warming over hundred generations.**

1.8.4 Limited mechanistic understanding: links between traits and molecular understanding

The underlying mechanisms driving detectable physiological changes remain unclear. Cyanobacteria may demonstrate stable regulatory changes through DNA methylation even though they can plastically modulate gene expression. Although methylation-based regulation plays a role in cell cycle control, stress response, and metabolic allocation in bacteria, its role in thermal adaptation remains less well characterized. **Chapter 2.3 aims to elucidate whether warming drives consistent methylation changes across historical and modern lineages, and if these correlate with trait shifts, helping to identify whether mechanistic pathways are involved in thermal responses.**

1.8.5 Missing integration of ecological and evolutionary processes

There is a strong correlation between warm summers and cyanobacterial bloom intensity (M. Kahru et al., 1994). However, long-term monitoring observations alone cannot determine whether such bloom intensity is an indication of physiological plasticity, demographic shifts, or true evolutionary adaptation. Integrating a multi-faceted approach – resurrection ecology, experimental evolution, trait-based measurements, and molecular analysis provides a framework for decoupling these processes and improving predictions of bloom behaviour under projected climate change scenarios.

These gaps motivate this dissertation's comprehensive, multi-timescale investigation of *Nodularia spumigena* temperature-dependent response.

1.9 Aims, objectives, and hypotheses of this dissertation

The overarching aim of this dissertation is to investigate how, and how fast Baltic Sea cyanobacteria – *Nodularia spumigena* in particular evolve in response to warming, and to disentangle past, present, and

laboratory induced evolutionary changes across physiological, genomic, and epigenomic levels. This is achieved through an integrated three-part framework:

Objective one: Past evolution

Chapter 2.1

The main objective of Chapter 2.1 is to test whether *Nodularia spumigena* has undergone evolutionary change over the past two centuries by comparing resurrected historical and contemporary lineages from Baltic Sea sediments across thermal performance, carbon metabolism, ecological interactions, and genome-wide sequence variation.

Hypotheses:

1. Following the "hotter is broader and better" prediction (Knies et al., 2009), we predicted that contemporary lineages would exhibit higher thermal optima (T_{opt}) and higher peak growth rates than pre-industrial lineages, reflecting two centuries of warming in the Baltic Sea
2. Following the same framework, we predicted that contemporary lineages would exhibit broader thermal breadth, and faster growth at T_{opt} than pre-industrial lineages, as adaptation to a warmer and more variable environment is expected to widen the range of temperatures over which growth is sustained.
3. Genomic divergence appeared smaller than phenotypic divergence, suggesting that relatively few genetic changes may underpin substantial shifts in thermal performance.

Objective two: Experimental evolution under warming

Chapter 2.2

The main objective of Chapter 2.2 is to quantify the evolutionary potential of historical and contemporary *Nodularia spumigena* lineages under controlled warming by conducting a long-term experimental evolution study at 22°C, 26°C, and 30°C, and comparing physiological and genomic changes between ancestral (T_{start}) and evolved (T_{end}) populations.

Hypotheses

1. Both historical and modern lineages can evolve higher fitness (approximated as growth rate) than the ancestor at elevated temperature.

2. Among historical and modern lineages, adaptive responses to temperature selection differ and this depends on the degree of mismatch between ancestral thermal optima and ancestral thermal performance strategies and the selection temperature, so that lineages experiencing greater thermal displacement exhibit stronger evolutionary responses.
3. Thermal adaptation is associated with evolutionary trade-offs, such as reduced performance at non-selected temperatures, consistent with specialist-generalist dynamics.

Objective three: Molecular basis for adaptation – The role of global methylation patterns as one aspect of epigenetic change

Chapter 2.3

The main objective of Chapter 2.3 is to examine the genetic and epigenetic correlates associated with thermal selection by analysing global DNA methylation patterns and genome-wide variation between ancestral (T_{start}) and evolved (T_{end}) populations under warming conditions.

Hypotheses

1. Sustained warming is associated with changes in global DNA methylation levels across lineages.
2. Global DNA methylation levels vary among historical and contemporary lineages and across thermal selection scenarios.
3. Variation in global DNA methylation levels co-varies with differences in thermal performance, linking molecular and phenotypic responses without implying causality.

This dissertation leverages the complementary strengths of resurrection ecology, experimental evolution, trait-based physiology, and molecular analysis to investigate how *Nodularia spumigena* responds to warming across ecological and evolutionary timescales. By integrating historical baselines, contemporary variation, real-time adaptation, and mechanistic regulation, this work provides one of the most comprehensive assessment to date of long-term thermal responses in a bloom-forming cyanobacterium.

The results presented in this dissertation have implications for understanding the future of harmful cyanobacterial blooms in the Baltic Sea, predicting shifts in nitrogen cycling under climate warming, and improving theoretical models that link plasticity, evolution, and ecology in microbial systems. Ultimately, this dissertation demonstrates that past, present, and future populations of *Nodularia spumigena* form a continuum of biological responses shaped by environmental change, and that studying these responses across time is essential for anticipating the ecological futures of warming marine ecosystems.

Chapter Two: Studies of this thesis

Chapter 2.1: Hot is the new cool: historical Baltic Sea cyanobacteria show trade-offs in thermal performance, carbon metabolism, and biotic interactions

Michael Edetanlen[1]*, Amelie Kofler[1], Samuel Barton[1], C.-Elisa Schaum[1]

*Corresponding author: michael.edetanlen@uni-hamburg.de

[1]Institute of Marine Ecosystem and Fisheries Science, University of Hamburg, Hamburg, Germany

[2]Leibniz-Institut for Baltic Sea Research Warnemünde, Rostock, Germany

Author ORCID IDs:

Michael Edetanlen: https://orcid.org/0009-0008-1852-006X

Elisa Schaum: https://orcid.org/0000-0001-6949-7367

Publication status and authorship statement

This study contains work prepared for publication in a peer-reviewed scientific journal.

Chapter 2.1, entitled "Hot is the new cool for resurrected Baltic Sea cyanobacteria", is prepared for submission to Limnology and Oceanography.

Michael Edetanlen is the first and corresponding author of the manuscript presented in the chapter. Elisa Schaum, Anke Kremp, and Inga Hense conceived the overarching research framework, and Elisa Schaum supervised the work. Cynthia Medwed contributed to lineage resurrection. Amelie Kofler contributed to conducting the experiment. Elisa Schaum, Amelie Kofler, Samuel Barton contributed to manuscript revisions. All co-authors approved the final version of the manuscript.

Abstract

Understanding how cyanobacteria populations have survived past environmental shifts may help predict future ecosystem trajectories under accelerating climate change. We used resurrection ecology to characterise five *Nodularia spumigena* lineages re-germinated from dated Baltic Sea sediment archives spanning pre-industrial (ca. 1824) to contemporary (ca. 1996) layers. We measured thermal performance curves (TPCs; growth rates across 15-38°C), carbon use efficiency (CUE) at three temperatures, organic carbon uptake, biotic effects on co-occurring *Ostreococcus tauri*, and whole-genome SNP divergence across sediment ages. Pre-industrial (1824) lineages had higher thermal optima and shallower performance curves; contemporary (1996) lineages had lower thermal optima, steeper sub-optimal curves, and higher growth rates at prevailing summer temperatures. This pattern deviates from the "hotter is broader and better" prediction and is instead consistent with adaptation to increased thermal variability in the modern Baltic Sea. CUE remained broadly conserved across temperatures, with a marginal age effect driven by lower baseline CUE in the contemporary 1996 lineage, contemporary lineages often showed less negative responses to organic substrates at elevated temperatures, and pre-industrial lineages showed stronger inhibition of *O. tauri*. Genomic divergence tracked sediment age, with contemporary lineages enriched for stress-response and energy-metabolism genes. Together these results indicate that *N. spumigena* has undergone multi-trait evolutionary reorganisation over two centuries, with the direction of change reflecting adaptation to a more variable, rather than simply warmer environment.

Keywords: resurrection ecology; thermal performance curves; evolutionary ecology; Baltic Sea, *Nodularia spumigena*; carbon use efficiency; allelopathy

Introduction – Chapter 2.1

Many cyanobacteria, including *Nodularia spumigena*, form toxic blooms that are predicted to increase in severity in a warming world with dire consequences for water quality and ecosystem dynamics (Lehtimaki et al., 1997; McGregor et al., 2012; Sivonen et al., 1989). Through carbon dioxide and nitrogen fixation, these cyanobacteria play essential roles in Baltic Sea biogeochemical cycles (Bullerjahn & Post, 2014; Carpenter & Romans, 1991). Due to their relatively high thermal tolerance, cyanobacteria are often described as "winners" of climate change (Teikari, 2018).

Phytoplankton responses to temperature typically follow a unimodal, left skewed thermal performance curve (TPC), and cyanobacteria are no exception, although their TPCs are generally broad, spanning relatively wide temperature ranges and often maintaining measurable growth across both moderate and elevated temperatures (Kontopoulos et al., 2020; Nalley et al., 2018). TPCs allow us to estimate under which temperatures a species can survive (breadth of the curve), where growth rates or similar fitness proxies are highest (T_{opt}), and the ranges of temperature where growth rate increases quickly up to the optimum (e.g. activation energy E_a in the Sharpe-Schoolfield model) (Angilletta, 2006; Schoolfield et al., 1981; Sharpe & DeMichele, 1977). The shapes of these curves are not fixed, but they are malleable on different time-scales, through different processes, from plasticity to swift evolutionary responses (Padfield et al., 2016; Schaum, Buckling, et al., 2018; Schaum & Collins, 2014). In 100 generations or less the shape and elevation of TPCs can change in the laboratory (Barton et al., 2023; Padfield et al., 2016; Schaum, Buckling, et al., 2018) and mesocosms (Schaum et al., 2017) but not always (Michaletz & Garen, 2024).

A prominent framework for predicting evolutionary TPC shifts is the "hotter is broader and better" hypothesis (Knies et al., 2009), although alternative outcomes are also possible in which TPCs broaden without increases in maximum performance ("hotter is broader" without "better"). This hypothesis predicts that populations evolving under elevated temperatures should, over time, develop TPCs with higher thermal optima, higher peak growth rates, and broader thermal breadths, a combination arising because warming selects simultaneously for higher performance and expanded tolerance, and because enzyme stability trade-offs constraining performance at high temperatures are relaxed as populations adapt. In the Baltic Sea, specifically, sea surface temperatures have increased by approximately 0.5-1.5°C since pre-industrial times depending on sub-basin, with warming concentrated in summer months and accelerating since the 1980s (Kniebusch et al., 2019; Lehmann et al., 2011; Meier et al., 2022). Whether *N. spumigena* populations have responded to this warming by following a "hotter is broader and better" trajectory, or by some other evolutionary strategy, is an open question.

Resurrection ecology – the germination of viable organisms from dated sediment archives, provides an opportunity to directly compare pre-industrial and contemporary populations under common garden

conditions (Kerfoot & Weider, 2004; Medwed et al., 2024; Sanyal et al., 2022). For dinoflagellates revived from Baltic Sea sediments, this approach revealed historical shifts in thermal tolerance spanning approximately a century (Hinners et al., 2017). For *N. spumigena* specifically, (Medwed et al., 2024) found an increase in photosynthetic T_{opt} from 15.3 to 21.1°C between lineages dated to 1987 and 2020, consistent with rapid adaptation to rising sea-surface temperatures. Our study extends this temporal window back to ca. 1824, providing a pre-industrial baseline against which contemporary trait divergence can be measured.

Comparing TPCs within and across species from different sediment depths can then give us an idea of the evolutionary potential of an organism – the more temperatures it can tolerate (and the faster it grows relative to other lineages), and the more it can maximise fitness across temperatures, the more likely it is that evolutionary potential is high.

Beyond growth rate, we examined two further dimensions of ecological function: cellular carbon balance and acquisition, and species interactions. Carbon use efficiency (CUE), the fraction of photosynthetically fixed carbon retained for growth rather than lost through respiration, is central to phytoplankton productivity and ecosystem energy flow (Barton et al., 2020; Collins et al., 2014). Organic carbon uptake may supplement inorganic carbon acquisition under thermal stress (Martens et al., 2024). Allelopathic interactions, in which cyanobacteria release compounds inhibiting neighbouring phytoplankton, reshape community composition during bloom events (Śliwińska-Wilczewska et al., 2019; Suikkanen et al., 2005), yet whether these capacities have changed over the past two centuries is unknown.

Here, we use five *N. spumigena* lineages from sediment cores dated 1824 to 1996 to test for evolutionary shifts in thermal performance, carbon metabolism, biotic interactions, and genomic architecture. We hypothesise that, following a "hotter is broader" evolutionary scenario (Knies et al., 2009), contemporary lineages should display broader TPCs with higher thermal optima compared to pre-industrial lineages, and that genomic divergence should be detectable between lineages from the 1970s and 1996 relative to pre-industrial lineages.

Materials and Methods – Chapter 2.1

Lineage origin and culture conditions

Out of 27 cyanobacterial lineages resurrected from Baltic Sea sediment cores and maintained by Cynthia Medwed at the Leibniz Institute for Baltic Sea Research Warnemünde (IOW), five *N. spumigena* lineages were selected based on their ability to grow reliably under laboratory conditions. Lineages originated from two Baltic Sea locations (Eastern Gotland Basin and Gulf of Finland) and from distinct sediment-core strata representing pre-industrial, mid-twentieth century, and contemporary periods (Table 1). One lineage dated to ca. 1824, three to 1970s, and one to ca. 1996. Sediment ages were determined using the published age model for sediment core EMB262/6-28 established using ^{210}Pb and ^{137}Cs radionuclide dating (Schmidt et al., 2024). Pilot studies showed that date, not location drove differences between lineages. Throughout, genetic barcoding and whole-genome sequencing confirmed our lineages as *N. spumigena*, even though their filament morphology continued to closely resemble *Dolichospermum spp*.

Cultures were maintained in nutrient-replete BG-11 medium in 40mL culture flasks (Thermo Scientific) under controlled laboratory conditions at the Institute of Marine Ecosystem and Fisheries Science (Hamburg) beginning in 2022. Flasks were incubated in shaker incubators (INFORS HT Multitron Pro, Switzerland) at 22°C under a 12:12 h light:dark cycle. Light intensity during the light phase was approximately 150 μmol photons m^{-2} s^{-1}, and cultures were continuously shaking at 60 rpm to maintain homogeneity.

Tab. 1. Summary of *N. spumigena* lineages and numbers of replicates used in this study. n values indicate independent biological replicates per lineage per assay (TPC = thermal performance curves; CUE = carbon use efficiency; BI = biotic interaction assay with *O. tauri*; OC = organic carbon uptake; Gen = whole-genome sequencing where sequencing depth is more informative than replication from the same sample).

Lineage ID	Date (approx.)	Basin (location)	Depth (cm)	n TPC	n CUE	n BI	n OC	n Gen	Age Group
6-MUC-46-2.1	1824	EGB	46	3	6	4	6	1	Pre-industrial
6-MUC-17-2	1970	EGB	17	3	6	4	6	1	Historical (1970s)
12-MUC-10-6	1970	GOF	10	3	6	4	6	1	Historical (1970s)
12-MUC-10-5	1970	GOF	10	3	6	4	6	1	Historical (1970s)
12-MUC-5-30	1996	GOF	5	3	6	4	6	1	Contemporary

Spectrophotometric analysis

Growth was tracked via chlorophyll a fluorescence (excitation 432nm, emission 676nm) and phycocyanin fluorescence (632nm, emission 686nm) measured in 200 µL aliquots in 96-well plates using a SpectraMax iD3 microplate reader (Molecular Devices, USA) as proxies for growth. Fluorescence was calibrated against cell counts obtained by FlowCam imaging, and confirmed by microscopy prior to the start of experiments; details are provided in Table S1.

Thermal performance curves

TPCs were characterised across 12 assay temperatures from 15 to 38°C. Cultures were pre-acclimated for eight days (≥3 generations) at each assay temperature before measurement. Growth rates were estimated from daily time-series chlorophyll a fluorescence using the *growthrates* package (Petzoldt, 2016) in R (R Core Team, 2025). Each lineage was grown in three independent biological replicates at every assay temperature, yielding n = 3, 9, and 3 replicates for the 1824, 1970s, and 1996 age groups, respectively (Table S2).

The Sharpe-Schoolfield equation was fitted to replicate-level growth rates using the *rTPC* and *nls.multstart* packages (Padfield et al., 2021):

$$r(T) = r_{ref} exp\left[E_a\left(\frac{1}{kT_{ref}} - \frac{1}{kT}\right)\right] / \left(1 + exp\left(\frac{E_h}{k}\left(\frac{1}{T_h} - \frac{1}{T}\right)\right)\right)$$

where $r(T)$ is the growth rate at temperature T, r_{ref} is the rate at a reference temperature T_{ref}, E_a and E_h are activation and deactivation energies, T_h is the high-temperature inactivation point, and k is the Boltzmann constant ($8.62 * 10^{-5}$ eV K^{-1}). Temperatures were converted to Kelvin prior to model fitting, and rates were normalised to a reference temperature (T_{ref}) of 22°C, which corresponds to the reference temperature parameter (T_c) in the Sharpe-Schoolfield formulation. In this model implementation, the parameter estimated is $\ln(r_{ref})$ representing the natural logarithm of the growth rate at the reference temperature (T_{ref} = 22°C).

Model selection among TPC formulations used the Akaike Information Criterion corrected for small sample size (AICc); the Sharpe-Schoolfield model provided the best fit in all cases and was used throughout. TPC parameters were compared among age groups using linear mixed-effects models with sediment age as a fixed factor and replicate nested within lineage as a random intercept. Model selection details and AICc are provided in Table S3.

Carbon use efficiency (CUE)

Carbon use efficiency (CUE) was quantified at 22, 26, and 30°C by measuring net photosynthesis and dark respiration in 2 mL culture aliquots using a PreSens optical dissolved-oxygen sensor. Rates were normalised to chlorophyll a fluorescence and CUE calculated as:

$$CUE = 1 - \frac{R}{P}$$

where P (gross photosynthesis) and R (respiration), accounts for the fraction of fixed carbon allocated to biomass production rather than lost through respiration. A CUE value of 0.5 indicates that half of the fixed carbon is retained for growth while the remainder is respired. Data were analysed with a linear mixed-effects model (sediment age, temperature, and their interaction as fixed factors; replicate nested within lineage as a random intercept). Each lineage was measured in six independent biological replicates per temperature.

Biotic interaction assays with *Ostreococcus tauri*

Effects of *N. spumigena* on a co-occurring picophytoplankton were assessed using a Baltic Sea *Ostreococcus tauri* isolate (Bornholm Basin; salinity ~2.5 PSU) in two complementary formats at 22, 26, and 30 °C: (i) indirect co-culture in 6-well ThinCert plates (0.4 µm mesh) and (ii) cell-free supernatant spikes filtered through 0.4 µm syringe filters. *O. tauri* was inoculated at 3000 cells mL^{-1} and monitored by flow cytometry

(BD Accuri). Growth rate expressed as fold-change relative to monoculture controls (fold-change = 1: no effect; <1: inhibition) was the response variable. Assays were conducted with n = 4 independent replicates per *N. spumigena* lineage per treatment per temperature. Data were analysed with a linear mixed-effects model (sediment age, assay temperature, treatment type, and their interactions as fixed effects; replicate as a random intercept). Full model comparison details are provided in Table S4.

Organic carbon uptake

Organic carbon uptake was assessed using Biolog EcoPlates (28 substrate groups; D-Xylose, Tween 40, and Tween 80 excluded due to spectral interference). Cultures were inoculated at ≈1000 cells mL^{-1} (confirmed by microscopy), incubated at 22, 26, or 30°C for 24 h, then re-measured. Growth was normalised to paired water-control wells:

$$ratio = \left(\frac{Growth_{treatment}}{Control_{mean}}\right) - 1$$

Data were analysed by linear mixed-effects models with sediment age, temperature, compound class, and their interactions as fixed effects and replicate as a random intercept (*lmerTest*; estimated marginal means via *emmeans* with Tukey correction).

DNA extraction, whole genome sequencing, and bioinformatics

DNA was extracted from harvested pellets using a modified CTAB protocol (Doyle & Doyle, 1987; Singh et al., 2011), with minor modifications – prior freezing at -80°C, and heating of cell matter at 75°C and vortex to break rigid cell walls. Concentration and purity were confirmed with a Qubit 4 Fluorometer (dsDNA HS Assay, Invitrogen, Thermo Fisher Scientific). Illumina paired-end sequencing (≥30× coverage), adapter trimming (*Trimmomatic* v0.39), alignment (*BWA-MEM* v0.7.17), duplicate marking (*Picard MarkDuplicates*), and SNP calling relative to a reference *N. spumigena* genome (*Snippy* v4.6) were performed by StarSEQ GmbH (Mainz, Germany). SNPs were classified as synonymous, missense, or other. Genomic differentiation was visualised by PCoA on Bray-Curtis dissimilarities and tested with PERMANOVA (999 permutations) using the *vegan package* (Oksanen et al., 2001). Sparse partial least-squares discriminant analysis (sPLS-DA) identified gene products contributing to age-associated divergence using *mixOmics* (Rohart et al., 2017). Figures were prepared in *ggplot2* (Wickham, 2016).

Thermal performance curves

Lineages performed differently across temperatures depending on their sediment age. Pre-industrial (1824) lineages had the highest thermal optima, the shallowest sub-optimal performance curves, and the lowest peak growth rates; contemporary (1996) lineages had the lowest thermal optima, the steepest sub-optimal curves, and the highest peak growth rates (Fig. 1; Table 2). Thermal optimum (T_{opt}) declined across sediment ages (likelihood ratio test: likelihood ratio test: $\chi^2 = 5.42$, df = 2, p = 0.066), from 30.1 ± 1.8°C in 1824 lineages to 26.8 ± 1.1°C in the 1970s and 24.2 ± 1.8°C in 1996 lineages (Tukey-adjusted pairwise comparison 1824 vs. 1996: ΔT_{opt} = 5.8 °C, p = 0.046).

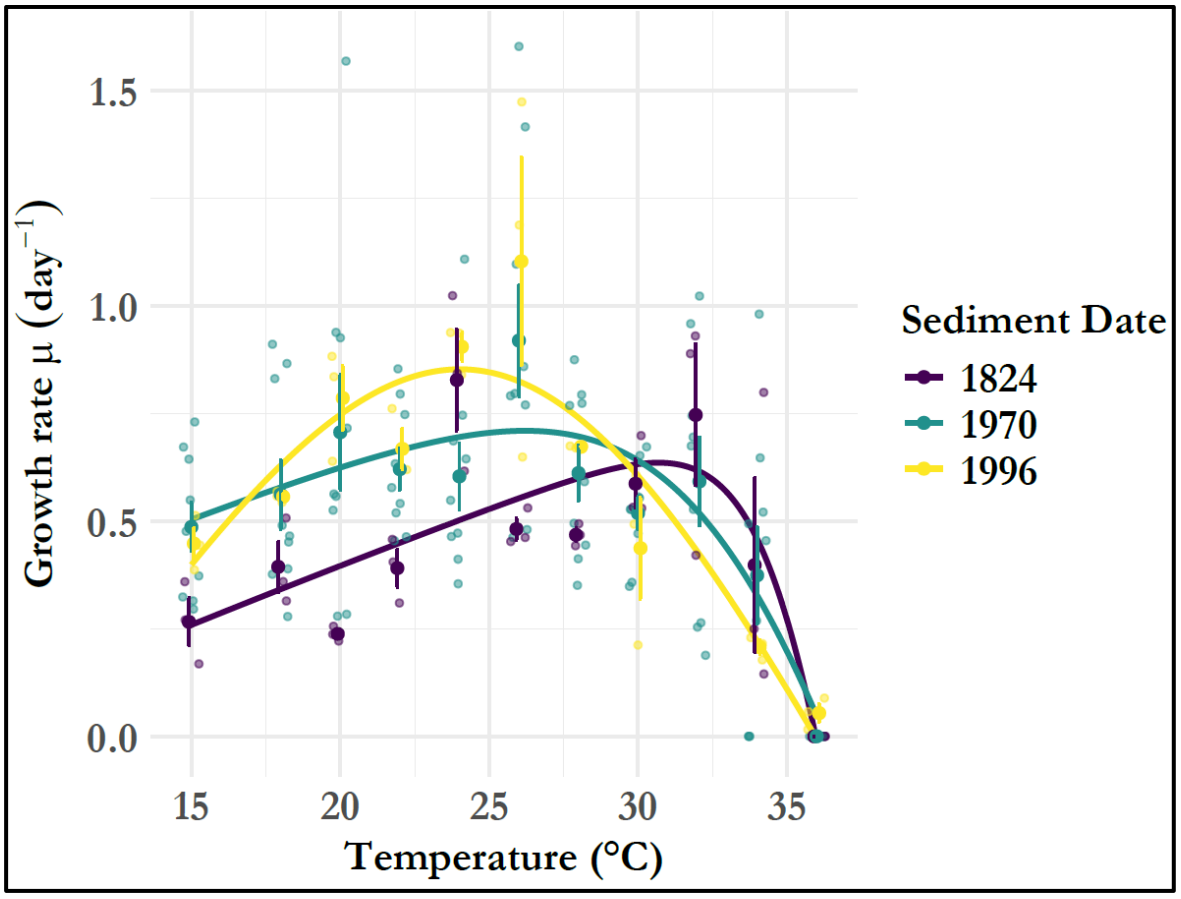

Fig. 1. Thermal performance curves (TPCs) describing temperature-dependent growth rates (μ) for *Nodularia spumigena* lineages resurrected from sediment resting stages dated to 1824, 1970, and 1996. Solid points represent means ± SEM across independent replicates (n = 3, 9, and 3 for 1824, 1970s, and 1996, respectively), with faded points indicate the individual data points. Solid lines denote fitted Sharpe-Schoolfield curves, and colours indicate sediment age (dark purple: 1824, teal: 1970s, yellow: 1996) of the lineages.

Activation energy E_a, describing the steepness of the TPC below T_{opt}, was significantly higher in contemporary than in pre-industrial lineages ($\chi^2 = 7.14$, df = 2, $p = 0.028$): 1824 lineages had the shallowest curves (E_a = 0.25 ± 0.10 eV), followed by the 1970s (0.31 ± 0.06 eV), and 1996 lineages were

steepest (0.66 ± 0.10 eV; 1996 vs. 1824: $p = 0.034$; 1996 vs. 1970s: $p = 0.045$). E_a between 1824 and 1970 lineages was not significantly different ($p = 0.88$).

In contrast, there was no significant difference across sediment ages in the high-temperature deactivation energy (E_h) ($\chi^2 = 2.58$, df = 2, $p = 0.275$), despite a tendency for lower mean E_h values in more recent lineages (Table 2). The natural-log intercept ln(c), representing the natural logarithm of the growth rate at the reference temperature (T_{ref} = 22 °C), increased progressively from pre-industrial to contemporary lineages (Table 2). When incorporated into the fitted Sharpe–Schoolfield model, this resulted in higher predicted maximum growth rates (μT_{opt}) for more recent lineages (1824: 1.61 ± 0.01 d^{-1}; 1996: 2.99 ± 0.17 d^{-1}). These values represent model-derived estimates from the fitted thermal performance curves rather than raw observed growth rates. The crossover occurs near 30°C: below that threshold, contemporary lineages grow faster; above it, pre-industrial lineages, with their higher T_{opt}, outperform contemporary ones, which decline steeply beyond their lower optimum.

Tab. 2. Thermal performance parameters for *Nodularia spumigena* lineages resurrected from dated sediments (1824, 1970s, 1996). Values represent means ± SE derived from Sharpe–Schoolfield model fits describing temperature-dependent growth rates. T_{opt} = optimum growth temperature (°C); μT_{opt} = predicted maximum growth rate at T_{opt} (d^{-1}); E_a = activation energy below T_{opt} (eV); E_h = high-temperature deactivation energy (eV); ln(c) = natural logarithm of the growth rate at the reference temperature (T_{ref} = 22 °C).

Sediment age	T_{opt} (°C)	μT_{opt} (d^{-1})	E_a (eV)	E_h (eV)	ln(c) (mean ± SE)
1824	30.1 ± 1.8	1.61 ± 0.01	0.25 ± 0.10	5.64 ± 2.25	0.47 ± 0.01
1970	26.8 ± 1.1	2.35 ± 0.32	0.31 ± 0.06	3.98 ± 0.89	0.79 ± 0.12
1996	24.2 ± 1.8	2.99 ± 0.17	0.66 ± 0.10	1.87 ± 0.08	1.09 ± 0.06

Carbon Use Efficiency

CUE exceeded 0.5 across all lineages and assay temperatures (22, 26, 30°C; Fig. 2), indicating relatively high carbon-use efficiency compared to typical phytoplankton values reported in the literature (Del Giorgio & Cole, 1998; Manzoni et al., 2018; Worden et al., 2015). Mean CUE ranged from 0.70 ± 0.09 at 22°C to 0.73 ± 0.10 at 26°C and 0.69 ± 0.12 at 30°C, with no significant effect of temperature (mixed model F-test: $F_{2,54} = 0.13$, $p = 0.883$), and post hoc comparisons confirmed the absence of pairwise differences among temperatures (Tukey HSD: all $p > 0.87$). Linear modelling confirmed no directional temperature trend ($\beta 26 = +0.030 \pm 0.026$, $p = 0.254$; $\beta 30 = -0.010 \pm 0.026$, $p = 0.707$).

Variation in CUE among sediment ages was detected. The 1970s lineages exhibited the highest mean CUE (0.72 ± 0.11), followed by the 1824 lineages (0.71 ± 0.11), with the 1996 lineage showing the lowest mean CUE (0.64 ± 0.06). Sediment age had a significant effect on CUE ($F_{2,27} = 3.62$, $p = 0.041$), driven primarily by a significant difference between the 1970s and 1996 lineages (Tukey HSD: $p = 0.032$); pairwise comparisons involving the 1824 lineage did not reach significance (1824 vs. 1970: $p = 0.849$; 1824 vs. 1996: $p = 0.206$). A significant temperature * age interaction was also detected ($F_{4,54} = 3.14$, $p = 0.021$), reflecting particularly low CUE in the 1996 lineage at 26°C relative to other age groups and temperatures. Despite this interaction, all lineages maintained CUE consistently above 0.5 across all assay temperatures, indicating that carbon allocation efficiency remained broadly functional across the full thermal range tested.

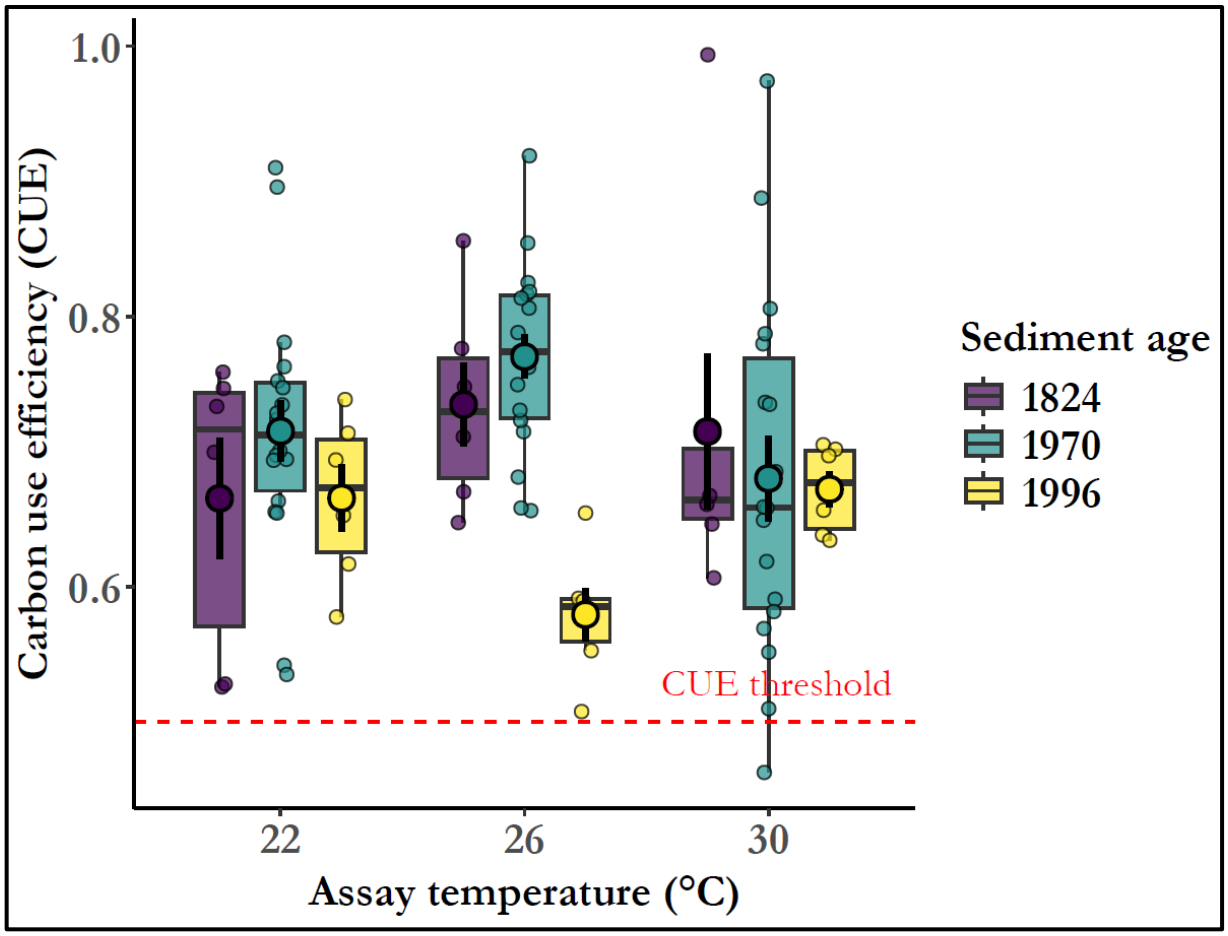

Fig. 2. Carbon use efficiency (CUE) across assay temperatures (22, 26, and 30°C) for *Nodularia spumigena* lineages resurrected from Baltic Sea sediments dated to 1824, 1970s, and 1996. Boxplots summarise CUE values across independent replicates, with individual data points overlaid. Points represent individual biological replicates, coloured by sediment age (dark purple: 1824, teal: 1970s, yellow: 1996). Independent sample sizes were n = 6, 18, and 6 replicates for 1824, 1970s, and 1996, respectively. A significant temperature * sediment age interaction was detected (mixed model: $F_{4,54} = 3.14$, $p = 0.021$), with the 1996 lineage showing notably lower CUE at 26°C relative to other groups. All lineages maintained CUE above 0.5 across all temperatures. The dashed red horizontal line denotes a CUE of 0.5, representing the point at which half of assimilated carbon is retained for biomass production and half is lost through respiration.

Effect of *Nodularia spumigena* growth on *Ostreococcus tauri*

Growth rates of *Ostreococcus tauri*, expressed as fold change relative to monoculture controls, were significantly reduced by exposure to pre-industrial (1824) *N. spumigena* lineages, particularly at 30°C (Fig. 3). Sediment age ($F_{2,59}$ = 13.83, $p < 0.0001$), assay temperature (($F_{2,59}$ = 15.94, $p < 0.0001$), and their interaction ($F_{4,59}$ = 11.11, $p < 0.0001$) were all significant; treatment type (spike vs. ThinCert co-culture) was not (treatment: $F_{1,59}$ = 1.14, p = 0.29).

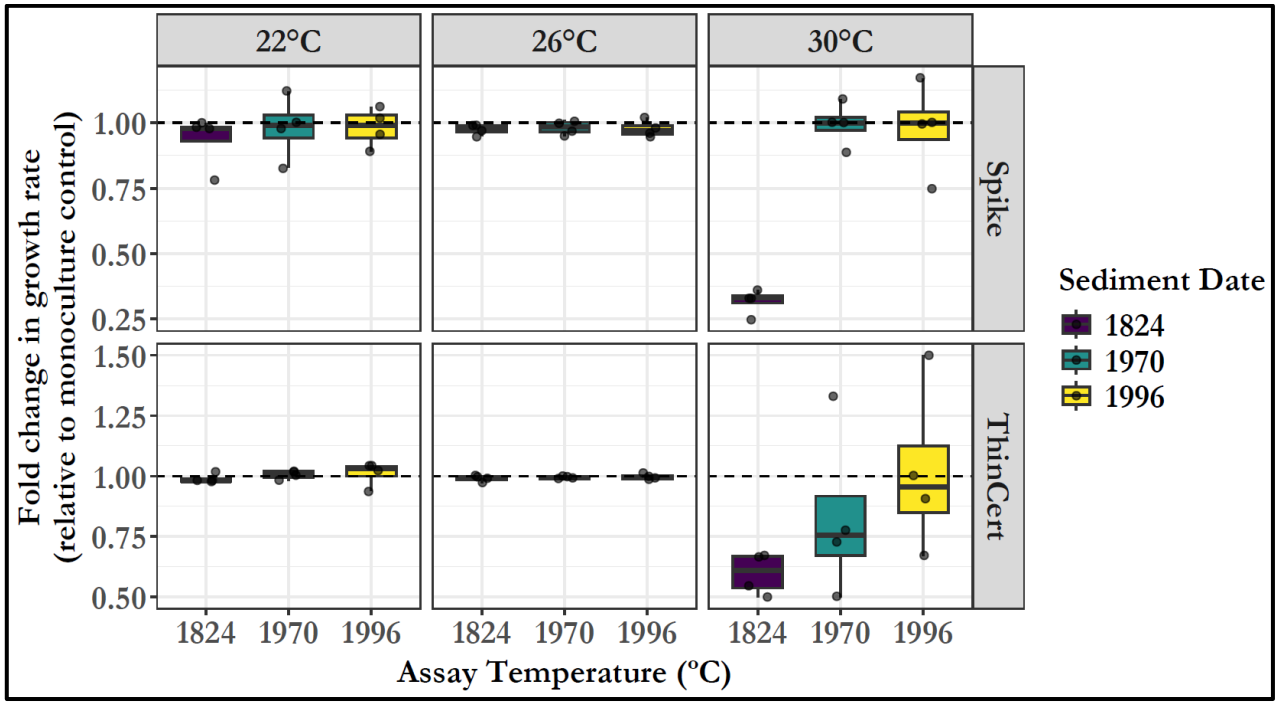

Fig. 3. Fold change in growth rates of *Ostreococcus tauri* relative to monoculture controls following exposure to supernatant spikes of *Nodularia spumigena* ("Spike") or indirect co-culture with the respective *N. spumigena* lineage maintained at carrying capacity ("ThinCert"). Assays were conducted at 22, 26, and 30 °C using *N. spumigena* lineages resurrected from Baltic Sea sediments dated to 1824, the 1970s, and 1996. Boxplots summarise growth responses across independent biological replicates. The dashed horizontal line denotes a fold change of 1, indicating no effect relative to monoculture controls. Colours indicate sediment age (dark purple: 1824; teal: 1970s; yellow: 1996). Sample size was n = 4 biological replicates per treatment * temperature * sediment age combination.

Across assay temperatures, fold changes in *O. tauri* growth rate generally clustered around unity, indicating limited overall effects of exposure to *N. spumigena* relative to control conditions (Fig. 3). However, growth responses differed among sediment ages in a temperature-dependent manner, with larger deviations from control growth observed at elevated temperatures. In particular, reductions in *O. tauri* growth were more pronounced at 30 °C for some lineage-temperature combinations, whereas responses at 22 °C were weak and more variable.

Organic carbon uptake

Organic carbon uptake differed significantly among compound classes (Type III ANOVA: $F_{5,700}$ = 38.59, $p < 2.2 * 10^{-16}$), temperature ($F_{2,700}$ = 17.80, $p = 2.9 * 10^{-8}$), and sediment ages ($F_{2,700}$ = 3.97, p = 0.019),

with significant age * temperature ($F_{4,700}$ = 7.44, p = 7.2 * 10^{-6}) and temperature * compound ($F_{10,700}$ = 2.04, p = 0.028) interactions. Amines supported growth above control at 22 and 26°C; amino acids suppressed growth, particularly at elevated temperatures. At 30°C, contemporary (1996) lineages showed less negative responses to carbohydrates, carboxylic acids, and amino acids than pre-industrial lineages (Fig. 4).

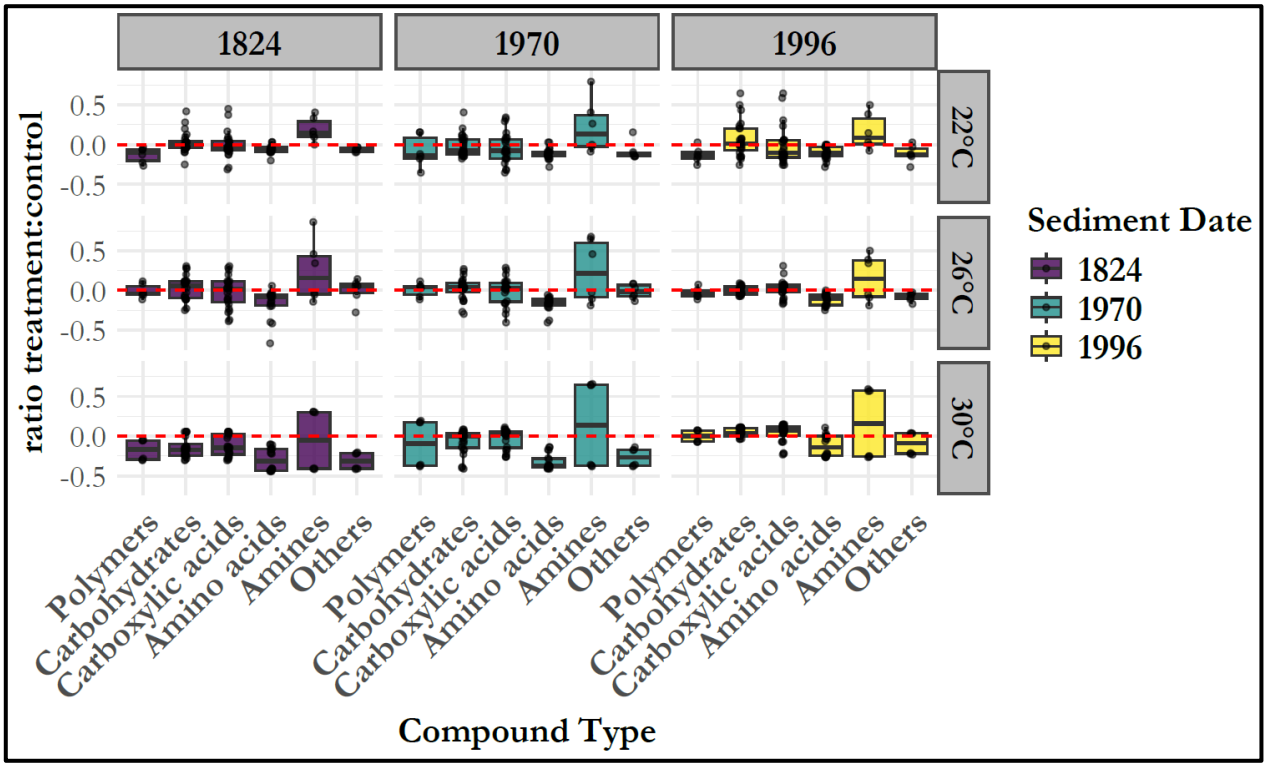

Fig. 4. Organic carbon uptake summarised by compound class for *Nodularia spumigena* lineages resurrected from Baltic Sea sediments dated to 1824, 1970, and 1996. Boxplots show treatment: control growth ratios for five compound classes (polymers, carbohydrates, carboxylic acids, amino acids, amines, others) at 22°C, 26°C, and 30°C. The points represent the individual compounds * replicate combinations (n = 6-24 wells per class, depending on the number compounds and three technical replicates each). Boxplot colours – dark purple = 1824, teal = 1970s, yellow = 1996) indicate the putative time of encystment for the *Nodularia spumigena* lineages. Dashed red line threshold indicate no effect of a compound relative to the control.

Genomic variation among *Nodularia spumigena* lineages

Synonymous variants predominated in all genomes; missense variants formed a smaller but consistent fraction (Fig. 5a). Despite limited statistical power (one genome per age group), PCoA of genome-wide SNP profiles revealed structured age-associated separation (PCoA1: 78.5%; PCoA2: 20.9%; Fig. 5b): the 1996 lineage was most divergent (Bray-Curtis from 1970s: 0.865; from 1824: 0.763), while 1824 and 1970s lineages clustered more closely (0.348). PERMANOVA on the five genomes was not significant (F = 0.53, p = 0.80, R^2 = 0.62), consistent with insufficient power rather than absence of divergence. sPLS-DA identified a subset of genes with relatively high loadings on the first two discriminant axes (Fig. 5c-d). The first discriminant axis was primarily associated with genes involved in core metabolic and translational processes, including ribosomal proteins (e.g. L19 and the ribosome-silencing factor), the photosystem II

reaction center protein Psb28, and hydrogenase subunits (Fig. 5c). The second discriminant axis was characterized by genes linked to stress response, membrane transport, and energy metabolism, such as ATP synthase components, ABC transporters, metalloproteases, and recombinases (Fig. 5d).

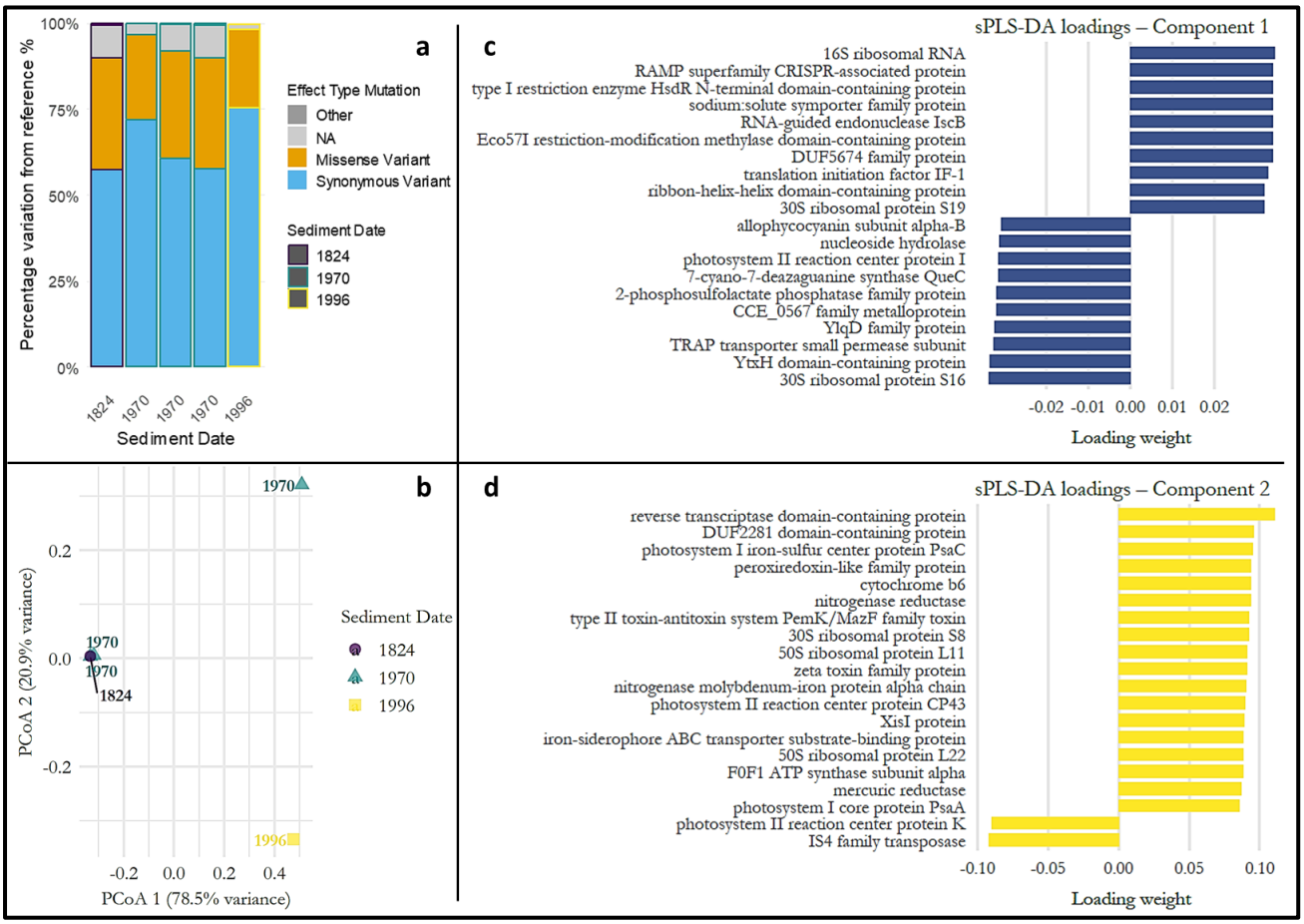

Fig. 5. Genomic variation and multivariate differentiation in *Nodularia spumigena* lineages resurrected from Baltic Sea sediments dated to 1824, 1970, and 1996. (a) Distribution of mutation effect types expressed as the percentage of variants relative to the reference genome. Variants are classified as synonymous, missense, NA (unannotated), or other low-frequency effects aggregated across lineages. (b) Principal coordinates analysis (PCoA) based on genome-wide SNP composition showing separation among lineages according to sediment date (age). The first and second PCoA (PCoA1 and PCoA2) explain 78.5% and 20.9% of the total variance, respectively. Symbols and colours represent sediment dates (lineage ages): dark purple = 1824, teal = 1970s, yellow = 1996. (c-d) Sparse partial least squares discriminant analysis (sPLS-DA) loadings for components 1 and 2, respectively, showing gene products contributing most strongly to multivariate separation among sediment ages. Bars indicate the direction and relative contribution of each gene to the corresponding discriminant axis. Functional annotations reflect discriminant loadings rather than formal functional enrichment. Together, these analyses show structured genomic divergence preserved across temporal lineages in Baltic Sea sediment archives.

Discussion – Chapter 2.1

We compared *N. spumigena* lineages resurrected from Baltic Sea sediments dated 1824 to 1996 under common garden conditions, measuring thermal performance, carbon metabolism, biotic interactions, and genomic architecture. Our central finding is that trait divergence is substantial and spans multiple functional axes (e.g., thermal optima, growth rates, and carbon use efficiency), but does not conform to the "hotter is broader and better" prediction. Instead, the data suggest that two centuries of environmental change in the Baltic Sea have selected for higher performance

at temperatures below the estimated thermal optimum and greater metabolic flexibility, consistent with adaptation to increased thermal variability rather than directional warming alone.

The "hotter is broader and better" framework predicts higher T_{opt}, broader thermal breadth, and higher peak growth rates in population that have evolved under warming (Knies et al., 2009). Our data inverts this prediction: the pre-industrial (1824) lineage has the highest T_{opt} (30.1°C), the shallowest sub-optimal curve, and the lowest peak growth rate; the contemporary (1996) lineage has the lowest T_{opt} (24.2°C), the steepest sub-optimal curve, and the highest peak growth rate.

Critically, the convergence of T_{opt} values at the contemporary time-point is itself evidence of divergent evolutionary trajectories, not of evolutionary stasis. Because the 1824 lineage began with a T_{opt} approximately 6°C above contemporary lineages, the 1970s and 1996 lineages must have undergone the largest downward shifts in T_{opt} to arrive at their present values, while the pre-industrial lineage has remained comparatively stable. This pattern is consistent with the interpretation that the pre-industrial TPC shape, a broad shallow curve that peaked at 30°C, arose under the more thermally stable pre-industrial Baltic Sea, and that subsequent increases in thermal variability have selected against this shape in contemporary lineages (Angilletta Jr., 2009; Feistel et al., 2008). (Medwed et al., 2024) reported an increase in photosynthetic T_{opt} between lineages date to 1987 and 2020, illustrating that not all trait dimensions evolve in parallel: growthrate T_{opt} and photosynthetic T_{opt} can diverge under the same environmental pressure.

The progressive increase in Ea from pre-industrial to contemporary lineages suggests a shift toward steeper thermal sensitivity, with only the more recent lineages approaching canonical activation energy values expected from metabolic theory. A steeper sub-optima curve is not "better" in an absolute sense. It means that growth falls away more sharply below T_{opt}, but delivers higher growth rates across the range of temperatures that currently characterise Baltic Sea summers (roughly 18-26°C; (Kniebusch et al., 2019). Taken together, the shift in E_a and ln(c), elevation of the whole curve rather than a shift in its position may be the more ecologically meaningful signal, as it corresponds to consistently higher growth rates in contemporary lineages at prevailing temperatures, regardless of the location of T_{opt}. Ecologically, the downward shift in T_{opt} in contemporary lineages is itself significant: with T_{opt} values now closer to current Baltic Sea summer temperatures, contemporary *N. spumigena* likely operates near its growth maximum during summer, potentially contributing to the observed intensification and prolongation of cyanobacterial blooms. Pre-industrial lineages, with T_{opt} near 30°C, would only approach peak growth performance during extreme warming events.

Despite pronounced TPC divergence, CUE remained high (>0.5) across all lineages and assay temperatures, indicating that carbon allocation efficiency was broadly maintained across two centuries of evolutionary divergence. A marginal effect of sediment age was detected, driven by lower CUE in the 1996 lineage relative to the 1970s lineages, particularly at 26°C. Rather than undermining the conservation interpretation, this pattern is coherent with the broader findings of this study: the 1996 lineage, which had the steepest sub-optimal TPC and highest peak growth rate, may allocate proportionally more carbon to growth-associated processes at temperatures near its thermal optimum, producing a context-specific reduction in measured CUE. Notably, the 1996 lineage also showed the greatest capacity for CUE evolution under warming in Chapter 2.2 (ΔCUE = +0.21 at 26°C), suggesting it began from a lower baseline with more room to improve. The conservation of CUE across all lineages at 22°C and 30°C, and the absence of any temperature main effect, is consistent with tight cellular regulation of the coupling between photosynthesis and respiration (Barton et al., 2018; García-Carreras et al., 2018), and suggests that the metabolic infrastructure linking carbon fixation to growth remains under stabilising selection across this temporal range.

Pre-industrial lineages showed substantially stronger inhibitory effects on *O. tauri* growth, particularly at 30°C, and spike and ThinCert treatments produced nearly identical results, implicating soluble exudates as the primary mechanism. The reduction in allelopathic potential in contemporary lineages likely reflects an evolutionary trade-off between growth performance and secondary metabolite production, investing less in allelopathy may be advantageous if competitive pressure has shifted or if the metabolic cost of toxin synthesis is reallocated to growth under thermally variable conditions (Fistarol et al., 2005; Leão et al., 2012). A slight increase in *O. tauri* growth relative to monoculture controls was observed for the 1996 lineage at 22 °C in indirect co-culture (Fig. 3). Although modest, this pattern may reflect the release of nitrogen-fixation by-products under nitrogen-limited conditions, consistent with the increasing co-occurrence of *N. spumigena* with small phototrophs in modern Baltic Sea blooms (Munkes et al., 2021).

The complementary organic carbon uptake result, with contemporary lineages showing broader substrate use at elevated temperatures extends this picture. Recent lineages appear to have shifted from competitive exclusion strategies toward greater metabolic opportunism, accessing additional carbon sources at high growth temperatures while reducing allelopathic investment. Whether this shift reflects direct selection for metabolic flexibility or relaxed selection on allelopathic capacity remains to be resolved.

Although PERMANOVA lacked power to reach formal significance with five genomes, the PCoA and sPLS-DA analyses reveal clear age-structured genomic separation, with the contemporary lineage most divergent from pre-industrial lineages. The functional signals in the discriminant loadings are directionally coherent, photosystem II and hydrogenase genes dominated in the pre-industrial lineages (consistent with optimisation of photosynthetic and redox performance under stable conditions), while ATP synthase, recombinase, and stress-response genes dominated in contemporary lineages (consistent with enhanced energy metabolism and genome maintenance under fluctuating stressors). The magnitude of phenotypic divergence, a 5.8°C difference in T_{opt} is large relative to the number of significant SNPs, consistent with polygenic thermal adaptation and raising the possibility that epigenetic or regulatory changes also contribute, a hypothesis explored in Chapter 2.3.

Together, the results indicate that Baltic Sea *N. spumigena* has undergone substantial multi-trait evolutionary reorganisation over the past two centuries: lower T_{opt} but elevated performance at prevailing summer temperatures, conserved metabolic efficiency, greater metabolic breadth, and reduced allelopathic capacity. This combination is consistent with increased bloom success under the warmer, more variable, and nutrient-enriched conditions of the modern Baltic Sea (Medwed et al., 2024; Vahtera et al., 2007). The most important caveat to consider in the context of our findings is the small number of lineages used (one pre-industrial, three from the 1970s, one contemporary), which limits statistical power and means that lineage-specific idiosyncrasies cannot be fully separated from age-cohort patterns, although their presence in the sediment core community alone shows that their strategy allowed them to thrive at the time of encystment. Co-varying changes in nutrient, salinity, and light across the past environments the strains used in this study mean that not all trait-shifts necessarily reflect ancestral temperature-driven selection in isolation (Hinners et al., 2017). Future work should expand the number of resurrected lineages per sediment layer and include multi-stressor designs to disentangle these drivers.

Acknowledgements

We thank our laboratory technician Stefanie Schnell, Luisa Listmann, and the student Moritz Aehle for their assistance during the experiments. We are grateful to Cynthia Medwed and the IOW-Leibniz Institute for Baltic Sea Research (Warnemünde) for resurrecting and providing the sediment core lineages used in this study. This research was supported by the Deutsche Forschungsgemeinschaft (DFG) grant (Project number – 450278268). ChatGPT (OpenAI, GPT-4) was used for language editing and grammar improvement, operated in a mode where user inputs were not used for model training, and all outputs were reviewed and validated by the authors.

Competing Interests

The authors declared no competing interests

Author Contributions

ES conceived the study. CM resurrected the lineages used for the study. ME and ES designed the experiments. ME and AK conducted the experiments. ME produced and analysed the data and produced the figures and wrote the first and final draft of the manuscript. ES contributed to coding and code troubleshooting. ES contributed with analysis input. ES, AK, and SB contributed with manuscript revisions. All authors gave final approval for publication. Funding was acquired by ES.

Data Availability

The data supporting the findings of this study are available in the Supporting Information. R codes and processed data sets used for statistical analysis and figure generation are openly available on GitHub. *Nodularia spumigena* cultures are maintained in the laboratory at the Institute of Marine Ecosystem and Fisheries Science.

Chapter 2.2: Divergent evolutionary trajectories under experimental warming in pre-industrial and contemporary Baltic Sea *Nodularia spumigena*

Michael Edetanlen[1]*, Samuel Barton[1], C.-Elisa Schaum[1]

*Corresponding author: michael.edetanlen@uni-hamburg.de

[1]Institute of Marine Ecosystem and Fisheries Science, University of Hamburg, Hamburg, Germany

[2]Leibniz-Institut for Baltic Sea Research Warnemünde, Rostock, Germany

Author ORCID IDs:

Michael Edetanlen: https://orcid.org/0009-0008-1852-006X

Elisa Schaum: https://orcid.org/0000-0001-6949-7367

Publication status and authorship statement

This study contains work prepared for publication in a peer-reviewed scientific journal.

Chapter 2.2, entitled "Rapid thermal adaptation in historical and modern *Nodularia spumigena* lineages under experimental warming", is prepared for submission to Science Advances.

Michael Edetanlen is the first and corresponding author of the manuscript presented in the chapter. Elisa Schaum, Anke Kremp, and Inga Hense conceived the overarching research framework, and Elisa Schaum supervised the work. Elisa Schaum and Samuel Barton contributed to manuscript revisions. Both co-authors approved the final version of the manuscript.

Abstract

Whether phytoplankton populations with distinct evolutionary histories retain equivalent capacity for rapid thermal adaptation is central to predicting ecosystem responses to climate change. Using experimental evolution, we exposed three *Nodularia spumigena* lineages resurrected from Baltic Sea sediments spanning pre-industrial (1824), historical (1970s), and contemporary (1996) periods to ~100 generations of selection at 22, 26, and 30 °C. Thermal performance curves (TPCs), carbon use efficiency (CUE), and genome-wide SNP variation were quantified before and after selection.

Thermal optima (T_{opt}) converged across sediment-age cohorts following evolution: the pre-industrial lineage, whose ancestral T_{opt} was already ~30 °C, showed little further change, whereas the historical and contemporary lineages shifted upward by ~5–6 °C. Despite differences in ancestral TPC shapes, all lineages displayed comparable capacity for thermal adaptation, indicating that all lineages can achieve similar post-selection T_{opt} though the magnitude of shift required differs across sediment ages. However, metabolic responses differed among cohorts: CUE increased significantly at elevated temperatures in the 1970s and 1996 lineages but not in the pre-industrial lineage.

Genomic analyses revealed strong divergence among sediment-age cohorts (PERMANOVA R^2 = 0.263, p = 0.001) and clear evolutionary responses to thermal selection. Together, these results show that historically distinct *N. spumigena* lineages retain similar adaptive potential under warming, but differ in the metabolic traits and genomic pathways through which this capacity is expressed.

Keywords: experimental evolution; thermal performance curves; cyanobacteria; evolutionary ecology; *Nodularia spumigena*; Baltic Sea; carbon use efficiency; genomics

Introduction – Chapter 2.2

Owing to unprecedented accelerated climate change, surface water temperatures including those of semi-enclosed seas like the Baltic Sea are undergoing rapid warming, testing the resilience of resident phytoplankton communities that are central to aquatic food webs and biogeochemical cycling (Meier et al., 2022). Baltic Sea surface temperatures have increased by approximately 0.5-1.5°C since pre-industrial times depending on sub-basin, with warming concentrated in summer months and accelerating since the 1980s (Kniebusch et al., 2019; Lehmann et al., 2011). Although short-term plastic thermal responses in phytoplankton are well characterised, these acclimatory changes do not necessarily predict long-term evolutionary trajectories (Padfield et al., 2016; Schaum, Buckling, et al., 2018). Understanding whether, and how fast, populations can evolve thermally under sustained warming is therefore crucial for forecasting future bloom dynamics and ecosystem function.

In principle, phytoplankton are well suited for rapid evolution; they can have large population sizes, short generation times, and ample standing genetic variation to facilitate evolutionary responses over relatively short ecologically relevant timescales (Collins et al., 2014). Experimental evolution studies, in which phytoplankton are propagated under controlled thermal selection, have demonstrated that phytoplankton thermal performance curves (TPCs) can shift substantially within tens to hundreds of generations, altering thermal optima, activation energies, and maximum growth rates (Listmann et al., 2016; O'Donnell et al., 2018). However, evolutionary responses are not universal. Some populations exhibit constraints, trade-offs, or context-dependent adaptation, and the factors determining whether a lineage will respond strongly or weakly to thermal selection remain incompletely resolved (Schaum et al., 2022).

One underexplored dimension of evolutionary potential is historical contingency – the idea that a lineage's prior evolutionary history shapes its capacity to respond to new selection pressures. A lineage that has evolved for decades under warm, thermally variable conditions may have already exhausted some of the standing genetic variation relevant to further thermal adaptation, leaving reduced evolutionary headroom, though evidence for this specifically under thermally variable conditions remains limited. Rapid thermal adaptation can deplete genetic diversity (Cheng et al., 2024), but thermal variability may in some cases promote rather than exhaust adaptive potential by selecting for enhanced plasticity and broader thermal tolerance (Schaum et al., 2022; Sjöqvist, 2022). Alternatively, a lineage from cooler, more stable pre-industrial conditions may retain cryptic genetic variation at thermal loci that has not yet been exposed to directional selection, potentially facilitating novel responses to contemporary warming, though we acknowledge the alternative

possibility that historically stable conditions selected for narrower, more specialised thermal strategies (Angilletta, 2009; Schaum et al., 2022). These possibilities make distinct, testable predictions about whether pre-industrial and contemporary lineages should differ in the rate, direction, or magnitude of evolutionary change under identical thermal selection.

In the companion study (Chapter 2.1), we characterised thermal performance, carbon metabolism, biotic interactions, and genomic divergence in *Nodularia spumigena* lineages resurrected from Baltic Sea sediments spanning ca. 1824 to 1996. Our results showed striking divergence in TPC shape: pre-industrial lineages had higher thermal optima (30.1°C) but lower maximum growth rates and shallower sub-optimal curves, whereas contemporary lineages had lower thermal optima (24°C) but steeper sub-optimal curves and higher peak growth rates. This pattern deviated from the "hotter is broader and better" prediction (Knies et al., 2009), suggesting that recent Baltic Sea warming has selected for performance in a variable, sub-optimal thermal environment rather than for directional upward shifts in T_{opt}. These divergent ancestral strategies raise a central question for the present study: do lineages with such distinct thermal backgrounds differ in their capacity for further evolutionary change under sustained experimental warming, and could such differences in evolutionary potential influence future bloom dynamics, timing, or persistence as Baltic Sea temperatures continue to rise?

Here, we directly test this question by exposing the same pre-industrial (1824), historical (1970s), and contemporary (1996) N. spumigena to ~100 generations of experimental evolution at 22, 26, and 30°C, and measuring evolutionary changes in TPCs, CUE, and genome-wide SNP profiles. Building on the ancestral characterisation in Chapter 2.1, we address two primary objectives specific to this experimental study. First, we quantify the magnitude and direction of evolutionary shifts in thermal performance and carbon use efficiency across all sediment-age cohorts, testing whether adaptation to warming occurs and whether it is accompanied by changes in metabolic efficiency (Objective 1). Second, we test whether historical origin modulates the rate or direction of evolutionary change, by comparing cohort-specific responses and assessing trade-offs using a reciprocal transplant design (Objective 2).

We test three main hypotheses. Importantly, whereas Chapter 2.1 integrates two centuries of warming alongside all concurrent environmental changes in the Baltic Sea, Chapter 2.2 isolates temperature as a single, controlled selective pressure, allowing any evolutionary response to be attributed more directly to thermal selection specifically. First, populations selected at elevated temperatures (26 and 30°C) will evolve increased growth rates and upward shifts in T_{opt} relative to their ancestral state, consistent with adaptation to warming (H1; (Barton et al., 2023; Padfield et

al., 2016; Schaum, Buckling, et al., 2018). Second, the magnitude and direction of evolutionary response will depend on the match between ancestral thermal strategy and selection temperature: lineages whose ancestral T_{opt} is furthest from the selection temperature should show the strongest directional evolutionary response, while lineages already near their fitness peak under a given selection temperature should show limited further change (H2). Third, thermal adaptation will be accompanied by evolutionary trade-offs, expressed as reduced performance at non-selection temperatures in reciprocal transplant assays (H3; (Angilletta, 2009; Schaum et al., 2022).

Lineage origin, culture conditions, and ancestral characterisation

All the *Nodularia spumigena* lineages used in this study are the same five lineages characterised in Chapter 2.1 (Table 1 in Chapter 2.1). These include one lineage from ca. 1824 sediment (pre-industrial), three from the 1970s (historical), and one from ca. 1996 (contemporary), originated from the Eastern Gotland Basin and the Gulf of Finland (Table 1). Each lineage was propagated in n = 6 independent biological replicates per selection temperature throughout the experimental evolution. Sediment ages were determined using the published age model for sediment core EMB262/6-28 established using ^{210}Pb and ^{137}Cs radionuclide dating (Schmidt et al., 2024). Throughout, genetic barcoding and whole-genome sequencing confirmed our lineages as *N. spumigena*, even though morphologically they continued to closely resemble *Dolichospermum*.

Tab. 1. Summary of *N. spumigena* lineages used in this study. n values indicate independent biological replicates per lineage per assay (TPC = thermal performance curves; CUE = carbon use efficiency; Gen = whole-genome sequencing).

Lineage ID	Date (approx.)	Basin (location)	Depth (cm)	n TPC	n CUE	n Gen	Age Group
6-MUC-46-2.1	1824	EGB	46	6	6	1	Pre-industrial
6-MUC-17-2	1970	EGB	17	6	6	1	Historical (1970s)
12-MUC-10-6	1970	GOF	10	6	6	1	Historical (1970s)
12-MUC-10-5	1970	GOF	10	6	6	1	Historical (1970s)
12-MUC-5-30	1996	GOF	5	6	6	1	Contemporary

Culture conditions followed Chapter 2.1 throughout: nutrient-replete BG-11 medium, 40 mL sterile culture flasks (Thermo Scientific), 22°C, 12:12 h light:dark, ~150 µmol photons m^{-2} s^{-1}, and continuous shaking at 60 rpm. Stocks were maintained in exponential growth through regular semi-weekly batch transfers prior to and throughout the experiment. Prior to the start of the experimental evolution, all lineages were acclimatised under common-garden conditions (22°C) for at least four weeks to minimise carry-over effects from prior culture history. Ancestral

phenotypic and genomic characterisation was conducted as described in Chapter 2.1; key ancestral TPC parameters are reproduced in Table 1 here for reference.

Experimental evolution design

Experimental evolution was conducted over 31 weeks (~100 generations) using a serial batch transfer protocol. For each of the five lineages, six biological replicate lineages were initiated per temperature treatment, giving 90 evolving populations in total (five lineages * three temperatures * six biological replicates). Each replicate was propagated in a separate 30 mL polypropylene culture bottle under one of three constant temperature regimes: 22°C (sub-optimal for most lineages based on Chapter 2.1 ancestral T_{opt} values), 26°C (close to the mean ancestral T_{opt} of the 1970s lineage and near the population-wide mean), and 30°C (supra-optimal for all lineages except the pre-industrial 1824 lineage). All other culture conditions (light, nutrient medium, shaking) were identical to maintenance conditions.

Every eight days, 2 mL of well mixed culture was transferred into 28 mL of fresh sterile BG-11 medium (1:15 dilution), maintaining a constant dilution factor and preventing nutrient limitation. We chose a fixed volume over a fixed cell count approach (Gomulkiewicz & Holt, 1995; Gross et al., 2020; Travisano et al., 2018) to maximise the speed of adaptive responses and to also be able to take into account selection environments with the potential to lead to extinction — specifically, if a population is in decline at a given selection temperature, fixed-volume transfers progressively bottleneck the population across successive transfers, increasing the probability of stochastic extinction rather than adaptation (though this did not happen in this experiment). An eight-day transfer interval corresponds to approximately 3-4 generations per transfer at typical growth rates, yielding ~13 transfers and ~100 generations over the 31-week experiment.

Growth trajectory monitoring

To monitor evolutionary dynamics throughout the experiment, 200 µL aliquots were sampled from each replicate prior to each transfer and measured spectrophotometrically for chlorophyll a fluorescence (excitation 432 nm, emission 676 nm) using the SpectraMax iD3 microplate reader as described in Chapter 2.1. This generated a time-series dataset on relative growth across the full 31-week experiment. Growth trajectories across all 31 weeks are provided for each selection temperature in Figure S1 of the supporting information.

Specific growth rates (µ) were calculated for each replicate during an early ancestral phase (weeks 4-6, representing near ancestral conditions before selection had time to act) and a late phase (weeks

28-30, after sustained selection). Evolutionary response was quantified as the log-transformed fold change in growth rate:

$$log(FC) = log\left(\frac{\mu_{evolved}}{\mu_{ancestral}}\right)$$

On the log scale, values > 0 indicate evolutionary increases in growth rate, values < 0 indicate decreases, and 0 indicates no evolutionary change.

Reciprocal transplant assays and thermal performance curves

To quantify evolutionary shifts in thermal performance and test for potential trade-offs across temperatures, full reciprocal transplant assays were conducted at both the start (T_{start}) and end (T_{end}) of experimental evolution. At T_{end}, lineages evolved at each of the three selection temperatures (22°C, 26°C, or 30°C) were assayed for growth across all three temperatures, yielding a 3 * 3 selection-by-assay design within each sediment-age cohort, resulting in a total of 270 biological replicates. Prior to measurement, cultures were pre-acclimated to assay temperature for eight days to minimise short-term physiological carry-over effects. To estimate full thermal performance curves (TPCs), growth rates were also measured across the same 12-temperature gradient (15-38 °C) used in Chapter 2.1. TPC parameters were estimated by fitting the Sharpe-Schoolfield model to the multi-temperature growth data as described in Chapter 2.1, extracting optimal temperature (T_{opt}), peak growth rate ($\mu_{max,}$ T_{opt}), activation energy (E_a), high-temperature inactivation energy (E_h), and normalisation constant (ln(c)), representing the natural log of the growth rate at the reference temperature T_{ref} = 16°C.

Carbon use efficiency

CUE measurements were conducted for ancestral and evolved populations using PreSens oxygen optical dissolved-oxygen sensor system, following the protocol described in Chapter 2.1. Assays were conducted at the three selected temperatures (22, 26, 30°C) for all age cohorts, in six biological replicates per lineage per treatment.

Whole-genome resequencing and bioinformatics

Whole-genome resequencing was performed on all five ancestral lineages and 38 evolved populations selected from the experimental evolution lines. Sequencing was originally attempted for 90 evolved populations, but usable genomic data were recovered for 38 due to technical failures during outsourced library preparation. The 1996 lineage evolved at 26°C was missing from genomic analyses for the same reason. Logistics and financial constraints did not allow for

resequencing. In total, 43 population samples (five ancestral and 38 evolved) were included in downstream analyses.

DNA extraction from harvested pellets followed the CTAB protocol described in Chapter 2.1. DNA concentration and purity were assessed using a Qubit 4 Fluorometer (dsDNA HS Assay Kit, Invitrogen). Illumina paired-end whole-genome sequencing (150 bp reads, minimum 30× coverage) was performed by StarSEQ GmbH (Mainz, Germany).

Raw reads were trimmed for adapters and low-quality bases using *Trimmomatic* (v0.39), aligned to the *N. spumigena* reference genome using *BWA-MEM* (v0.7.17), and duplicate reads were marked with *Picard MarkDuplicates*. SNP calling was performed with *Snippy* (v4.6), using per-lineage ancestral genomes as the reference to identify evolved-specific variants. Variant annotation was performed against a *N. spumigena* functional annotation, classifying SNPs as synonymous, missense, or other. For each evolved population, we quantified: (i) total novel SNP count, (ii) novel missense SNP count, (iii) the proportion of novel SNPs that were missense, and (iv) a proxy for dN/dS calculated as (missense + 0.5) / (synonymous + 0.5), following (Tai et al., 2011).

Multivariate genomic divergence was assessed using Bray-Curtis dissimilarities on SNP presence–absence matrices, visualised by principal coordinate analysis (PCoA) using *vegan* (Oksanen et al., 2001). PERMANOVA (999 permutations, marginal tests) was used to partition variance attributable to sediment age and selection temperature among evolved populations. Sparse partial least-squares discriminant analysis (sPLS-DA) was applied using *mixOmics* (Rohart et al., 2017) to identify gene products with disproportionate discriminatory loading for selection temperature. Figures were prepared in *ggplot2* (Wickham, 2016).

Statistical Analyses

All analyses were conducted in R (R Core Team 2025). Linear mixed-effects models were fitted using the *nlme* package, with maximum likelihood (ML) estimation used for model selection via likelihood ration tests between nested models, and restricted maximum likelihood (REML) used for final parameter estimation and inference.

To quantify evolutionary growth responses, log-transformed fold change in growth rate was modelled with sediment age (1824, 1970, 1996), selection temperature (22, 26, 30°C), and their interaction as fixed effects. Replicate nested within lineage was included as a random intercept. Each lineage was propagated in six independent biological replicate lineages per selection temperature. As we had one pre-industrial lineage (1824), three historical (1970s), and one contemporary (1996), this yielded n = 6, n= 18, and n = 6 independent biological replicates per

sediment-age cohort respectively. Replicates were initiated from the same stock culture per lineage and are therefore not fully independent; the nested random-effects structure accounts for this non-independence. When the age * temperature interaction was not statistically supported by likelihood ratio test, reduced additive models were used for inference.

TPC parameters (T_{opt}, μ_{max}, T_{opt}, E_a, E_h, ln(c)) were extracted from Sharpe-Schoolfield fits as described above and analysed using linear mixed-effects models with sediment age, selection temperature (including ancestor level for T_{start} measurements), and their interaction as fixed effects. Unique biological lineages (Age * Replicate) were included as random intercepts to account for non-independence of ancestral and evolved measurements from the same replicate population. Ancestral T_{opt} values reported in Table 1 are reproduced from Chapter 2.1; within Chapter 2.2. Ancestral lineages were included as a separate level of the selection temperature factor to enable mixed-model comparison with evolved populations. The two sets of ancestral estimates differ slightly owing to differences in grouping structure at the fitting stage, not differences in model formulation or parameter bounds. Model selection results for all TPC parameters are summarised in Table S5.

Reciprocal transplant responses were analysed as log-transformed change in growth rate relative to the 22°C selection-assay control within each sediment-age cohort. Sediment age, selection temperature, assay temperature, and their interactions were included as fixed effects, with replicate lineage as a random intercept.

CUE was analysed using mixed-effects models including sediment age, selection temperature, evolutionary state (ancestral vs evolved), and all interactions as fixed effects. Biological replicate was included as a random intercept to account for repeated measures across evolutionary states. Estimated marginal means were computed using the *emmeans* package with Tukey correction for multiple comparisons.

Genomic burden metrics (novel SNP counts, novel missense counts) were log-transformed; missense proportions were logit-transformed; dN/dS proxies were log-transformed. Due to the incomplete factorial structure (missing 1996 lineage * 26°C treatment) and limited replication, genomic burden metrics were analysed using additive models only (no age * temperature interaction). Significance was assessed using Type III Satterthwaite-corrected F-tests (*lmerTest*). Full model outputs are provided in Table S6.

Multivariate genomic divergence was assessed using Bray-Curtis dissimilarities computed on SNP presence-absence matrices and visualised by principal coordinate analysis (PCoA) using *vegan*

(Oksanen et al., 2001). PERMANOVA (999 permutations, marginal tests) was applied to evolved populations to test additive effects of sediment age and selection temperature on genomic composition. Sparse partial least squares discriminant analysis (sPLS-DA) was applied using *mixOmics* (Rohart et al., 2017) to identify gene products contributing disproportionately to temperature-associate divergence among evolved lineages.

Evolutionary growth trajectory responses under thermal selection

Evolutionary response in growth rate differed significantly among selection temperatures ($F_{2,54}$ = 8.59, p = 0.0006), whereas sediment age cohort had no significant main effect (Age: $F_{2,2}$ = 0.10, p = 0.91; Fig 1). Across sediment ages, lineages evolved at 26°C exhibited reduced growth relative to their ancestral state (estimate ± SE = −0.889 ± 0.445, p = 0.051), whereas lineages evolved at 30°C showed increased growth relative to their ancestors (estimate ± SE = 0.678 ± 0.445, p = 0.13). Evolutionary responses at 22°C did not differ significantly from zero. Random-effects estimates indicated substantial among-lineage variation in evolutionary responses (StdDev: Lineages = 0.545), whereas variation among replicate populations within lineages was negligible.

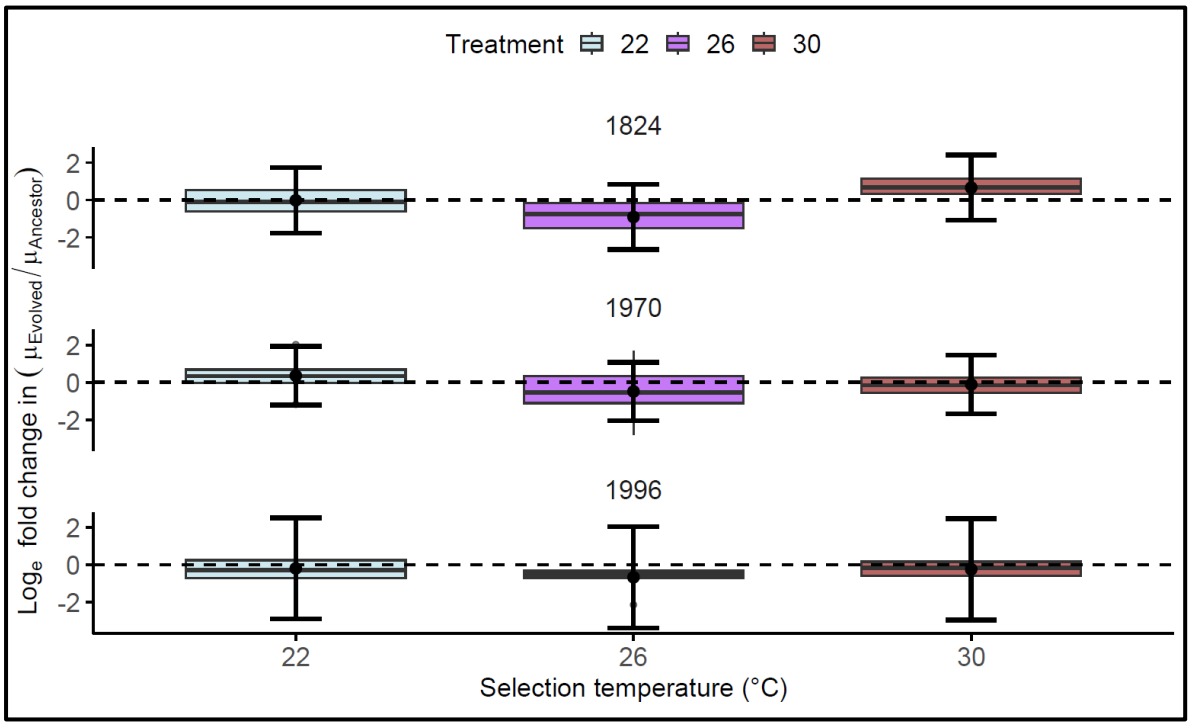

Fig. 1. Evolutionary responses of growth rate under long-term thermal selection. Log-transformed fold-change in growth rate ($\mu_{evolved}$ / $\mu_{ancestral}$) for *Nodularia spumigena* populations evolved at 22, 26, and 30 °C across sediment age cohorts (1824, 1970s, 1996), measured at their respective selection temperatures. Values above zero indicate proportional increases in growth rate relative to ancestral populations in the selection environment, whereas values below zero indicate decreases. Boxplots show the distribution of biological replicate populations within each selection treatment. Black points denote estimated marginal means derived from linear mixed-effects models, with lineage and replicate nested within lineage included as random effects. The dashed horizontal line indicates no evolutionary change (log fold-change = 0). n = 6 replicate populations per lineage from each age at each temperature.

Evolutionary shifts in thermal performance curve parameters

Testing the trajectories of lineages in their evolved environment yields valuable insights about how and how fast fitness or other traits have changed in the selection environment. However, it cannot tell us whether there might have been conditionally neutral changes that have negligible effects in the selection environment but can affect the shape of the thermal performance curve. Thermal performance curves differed among sediment age cohorts and selection regimes (Fig. 2a). Activation energy (E_a) varied significantly among sediment age cohorts across selection temperatures (Age * Selection temperature: $F_{6,36} = 5.9$, $p = 0.0002$; Fig. 2b). Although sediment age alone did not exert a significant main effect ($F_{2,15} = 1.0$, $p = 0.381$), selection temperature significantly influenced E_a ($F_{3,36} = 6.3$, $p = 0.0015$), with the magnitude and direction of responses differing among historical cohorts.

Thermal optimum (T_{opt}) likewise exhibited a significant Age * Selection temperature interaction ($F_{6,36} = 3.0$, $p = 0.0098$; Fig. 2c). Both sediment age ($F_{2,15} = 5.0$, $p = 0.0179$) and selection temperature ($F_{3,36} = 3.0$, $p = 0.0461$) contributed to variation in T_{opt}; however, shifts in thermal optima were contingent on historical origin, indicating cohort-specific evolutionary trajectories. Specifically, the pre-industrial (1824) lineage showed minimal change in T_{opt} across all selection treatments (ancestral: 30.1 ± 1.8°C; evolved range: 29.1–32.3°C), consistent with its already-elevated ancestral optimum. In contrast, the historical (1970s) and contemporary (1996) lineages shifted upward substantially (1970s: from 26.8 ± 1.1°C to 29.1–30.4°C; 1996: from 24.2 ± 1.8°C to 30.7–31.5°C across treatments), resulting in convergence of T_{opt} values across sediment-age cohorts following selection (Table 2).

Tab. 2. Summary of mean thermal optimum (T_{opt},°C) for each sediment-age cohort at the ancestral state (from Chapter 2.1) and following evolution at 22, 26, 30°C. Values represent means ± SE across biological replicate lineages within each cohort. Ancestral T_{opt} values are reproduced from Chapter 2.1 (Table 1); within Chapter 2.2, ancestral lineages were fitted as a separate selection-temperature level within the mixed-effects model, producing slightly different estimates due to differences in grouping structure (see methods). † Large SE reflects high variance among biological replicates for this combination; interpret with caution.

Sediment age	Ancestral T_{opt} (°C)	Evolved 22°C T_{opt} (°C)	Evolved 26°C T_{opt} (°C)	Evolved 30°C T_{opt} (°C)
Pre-industrial (1824)	30.1 ± 1.8	29.1 ± 1.3	29.8 ± 1.0	32.3 ± 0.3
Historical (1970)	26.8 ± 1.1	30.4 ± 0.8	29.1 ± 0.6	30.4 ± 1.0
Contemporary (1996)	24.2 ± 1.8	31.5 ± 0.7	35.8 ± 4.3†	30.7 ± 1.1

This convergence pattern means that the more recently derived lineages, which began furthest from the post-selection T_{opt} values, underwent the largest upward shifts, while the pre-industrial lineage required little further change.

In contrast, peak growth rate (μ_{max}, T_{opt}) did not show a significant interaction between Age and Selection temperature (ML comparison: $p = 0.117$). Peak performance differed significantly among sediment age cohorts ($F_{2,15} = 12.0$, $p = 0.0008$) and across selection temperatures ($F_{3,42} = 5.0$, $p = 0.0048$; Fig. 2d), indicating consistent but parallel evolutionary responses across historical lineages.

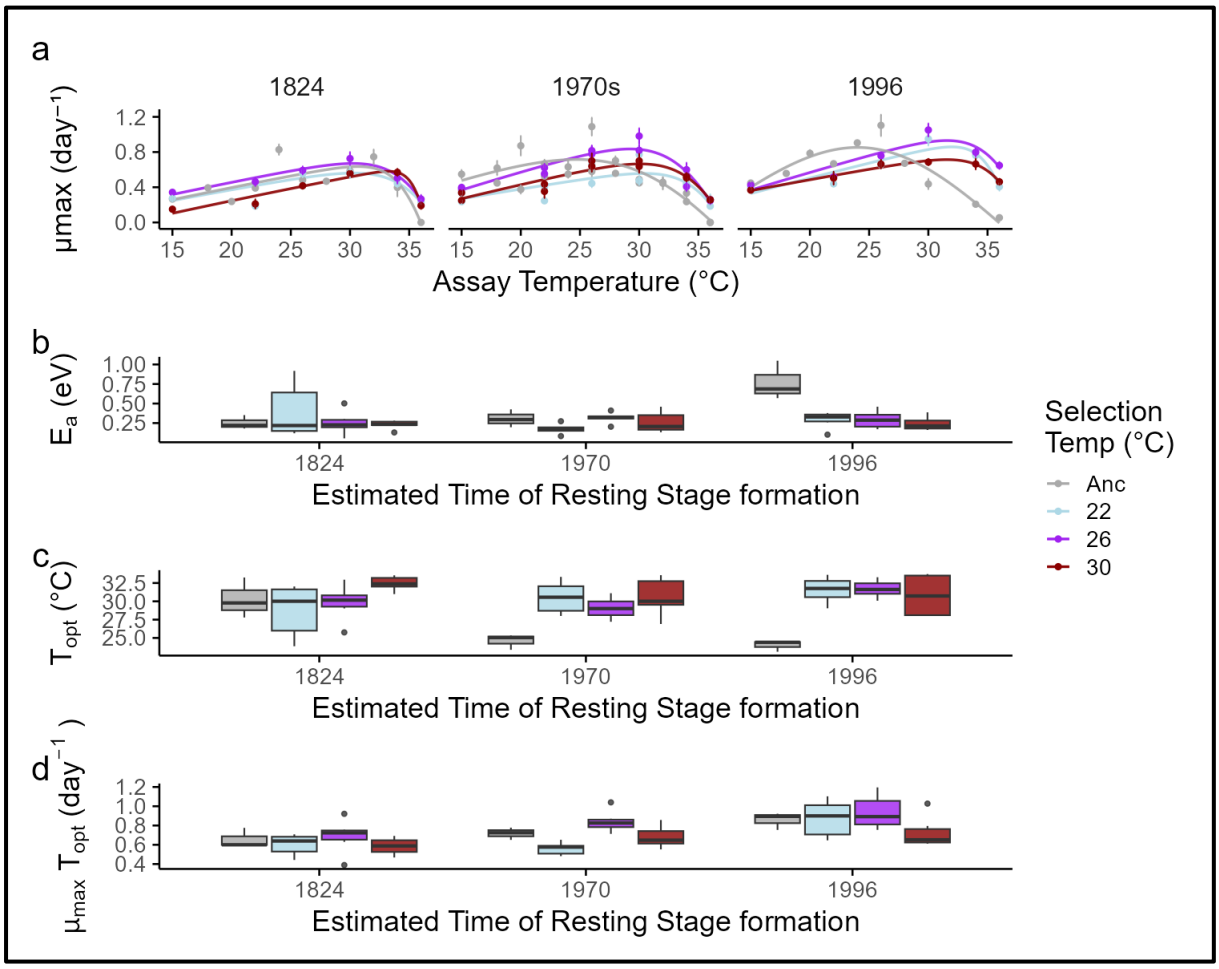

Fig. 2. Evolutionary responses of thermal performance parameters across sediment ages and selection temperatures. Top panel: Temperature-dependent growth rates (μmax, day⁻¹) across assay temperatures for *Nodularia spumigena* populations originating from sediments dated to 1824, 1970s, and 1996, following experimental evolution under ancestral conditions (Anc) or at 22 °C, 26 °C, and 30 °C. Points represent replicate-specific growth rate estimates, and solid lines denote fitted Sharpe-Schoolfield thermal performance curves for each selection treatment within a sediment age. Lower panels: Derived thermal performance parameters from Sharpe-Schoolfield model fits, including activation energy below the optimum temperature (E_a, eV), optimum temperature for growth (T_{opt}, °C), and maximum growth rate at the optimum temperature ($\mu(T_{opt})$, day⁻¹). Boxplots summarise the distribution of replicate-level parameter estimates within each sediment * selection temperature combination, with colours indicating selection treatment. n = 6 replicate populations per strain at each selection temperature; n = 6, 18, and 6 total replicates for the 1824, 1970s, and 1996 cohorts respectively.

Reciprocal transplant assay

To test for local adaptation, we carried out reciprocal transplants. There, relative growth responses – growth compared to a lineage grown and assayed at 22°C differed significantly among sediment age cohorts ($F_{2,135} = 6.01$, $p = 0.0032$), selection temperatures ($F_{2,135} = 16.51$, $p < 0.0001$), and assay temperatures ($F_{2,135} = 4.05$, $p = 0.0195$). The interaction between sediment age and selection temperature was also significant ($F_{4,135} = 2.56$, $p = 0.041$). In contrast, the interaction between selection and assay temperature was not significant ($F_{4,135} = 0.51$, $p = 0.7270$). Thus, although evolution altered overall growth performance, there was no statistical evidence for temperature-specific local adaptation in the reciprocal transplant assay.

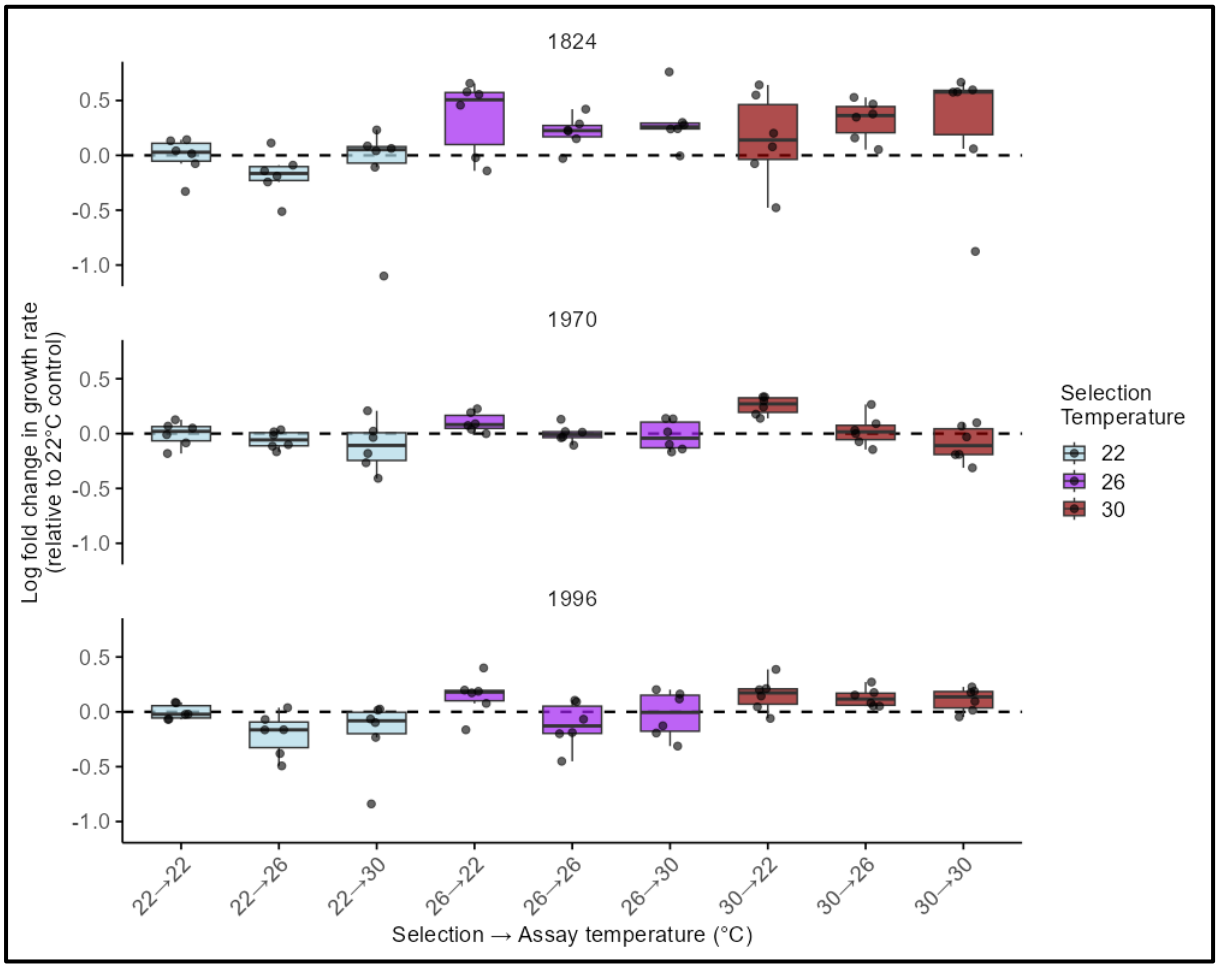

Fig. 3. Reciprocal transplant assay of thermal performance across sediment age cohorts. Log-transformed fold change in growth rate relative to the 22 °C selection–assay control for replicate lineages evolved at 22, 26, or 30 °C and assayed across all three temperatures. Boxplots represent biological replicate lineages; points indicate individual replicates. The dashed horizontal line denotes no change relative to control (log fold change = 0). Evolutionary history significantly influenced overall growth performance, but reaction norms remained largely parallel across assay environments, indicating limited evidence for temperature-specific local adaptation. n = 6 replicate populations per strain per selection * assay temperature combination; n = 6, 18, and 6 total replicates for the 1824, 1970s, and 1996 cohorts respectively.

Evolutionary change in carbon use efficiency under thermal selection

Carbon use efficiency (CUE) differed between ancestral and evolved populations (Time: $F_{1,135}$ = 11.94, p = 0.0007). Importantly evolutionary responses depended on both sediment age and selection temperature, as indicated by a significant three-way interaction (Age * Temperature * Time: $F_{4,135}$ = 3.0, p = 0.014). Post hoc contrasts (Tukey-adjusted) revealed significant evolutionary increases in CUE at elevated temperatures in the more recent sediment cohorts. In the 1996 cohort, CUE increased significantly following evolution at 26°C (ΔCUE = 0.210 ± 0.053 SE, p < 0.0001) and 30°C (ΔCUE = 0.111 ± 0.053 SE, p = 0.037). Similarly, the 1970 cohort exhibited a significant increase at 30°C (ΔCUE = 0.107 ± 0.030 SE, p = 0.001).

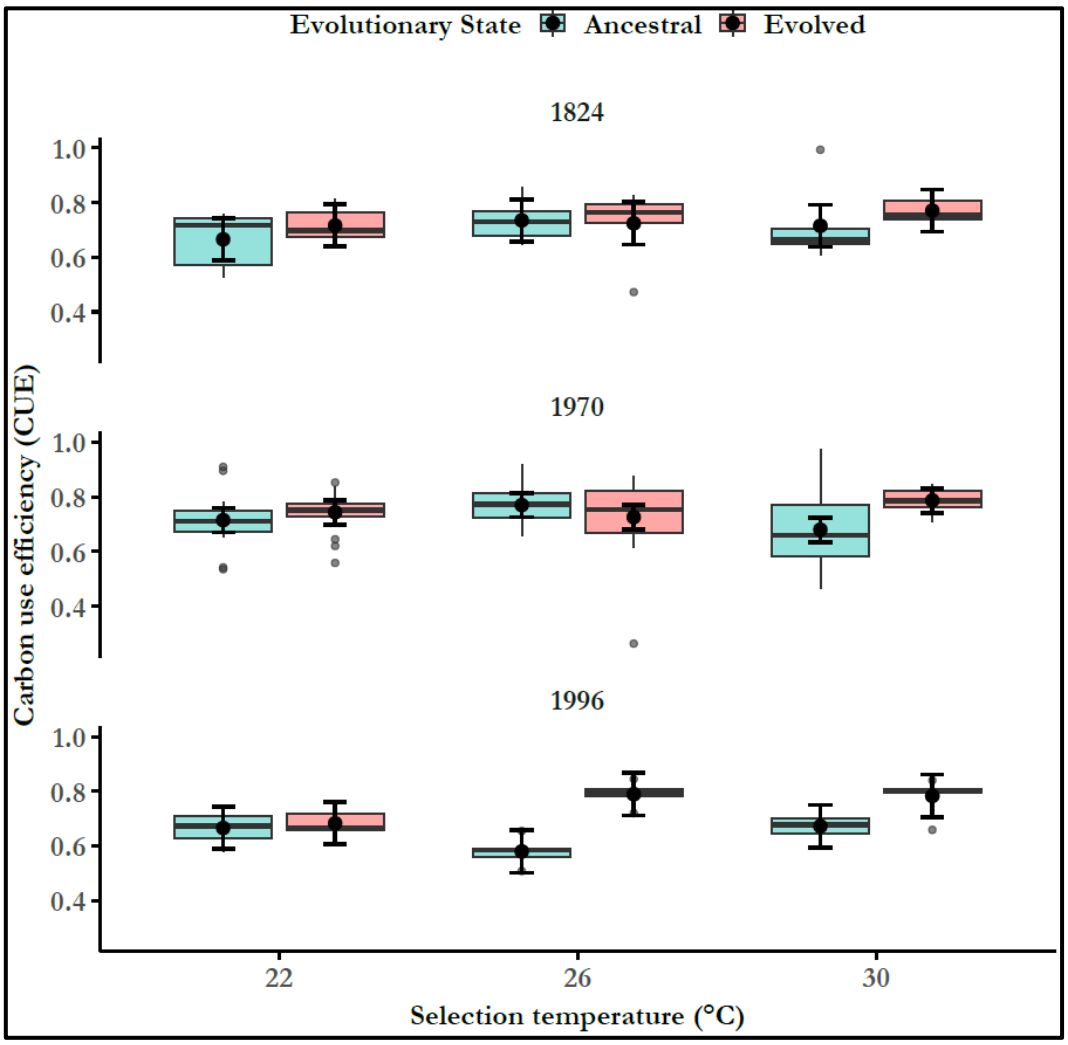

Fig. 4. Evolutionary shifts in carbon use efficiency (CUE) across thermal selection treatments and sediment age cohorts. Carbon use efficiency (CUE) of ancestral and evolved populations maintained at 22, 26, and 30 °C across sediment age cohorts (1824, 1970s, 1996). Boxplots represent biological replicate populations within each treatment, with colours denoting evolutionary state (ancestral = light blue, evolved = red). Black points denote estimated marginal means derived from linear mixed-effects models with replicate included as a random effect; error bars indicate 95% confidence intervals. Evolutionary responses differed among sediment age cohorts and temperature treatments, with significant increases in CUE observed at elevated temperatures in the 1970 and 1996 cohorts. n = 6 biological replicates per strain per treatment; n = 6, 18, and 6 total replicates for the 1824, 1970s, and 1996 cohorts respectively.

In contrast, no significant evolutionary changes were detected in the 1824 cohort across temperature treatments. Together, these findings indicate that warming-driven evolution modified carbon use efficiency primarily in more recently isolated lineages, whereas the oldest cohort exhibited limited evolutionary responsiveness in CUE.

Multivariate genomic divergence

Genomic composition of evolved populations differed strongly among sediment ages, with more modest evidence for an effect of selection temperature. Stacked mutation-category profiles showed consistent proportions of synonymous versus nonsynonymous SNPs within each temperature, but clear shifts across sediment ages (Fig. 5a). A PCoA on Bray-Curtis distances among SNP presence-absence profiles (38 samples, 266,836 variable SNPs) further revealed clear separation among ages classes, whereas temperature groups overlapped more extensively in ordination space (Fig. 5b). In a PERMANOVA on evolved samples only, sediment age explained 26.3% of the variation in multivariate SNP composition (Age: $R^2 = 0.263$, $F_{2,28} = 6.01$, $p = 0.001$), while selection temperature accounted for 8.6% (Age: $R^2 = 0.086$, $F_{2,28} = 1.97$, $p = 0.063$).

Complementary sPLS-DA on evolved-specific gene-product counts highlighted a restricted subset of loci (representing putative genomic targets associated with thermal selection, superimposed on a background of age-structured genomic divergence) with strong discriminatory loadings for selection temperature. The first two sPLS-DA components separated samples by temperature regime, and barplots of loading weights identified a small number of gene products associated with core cellular and metabolic processes, including DNA replication, translation, energy metabolism, and photosynthetic machinery, that contributed disproportionately to this separation (Fig. 5c,d).

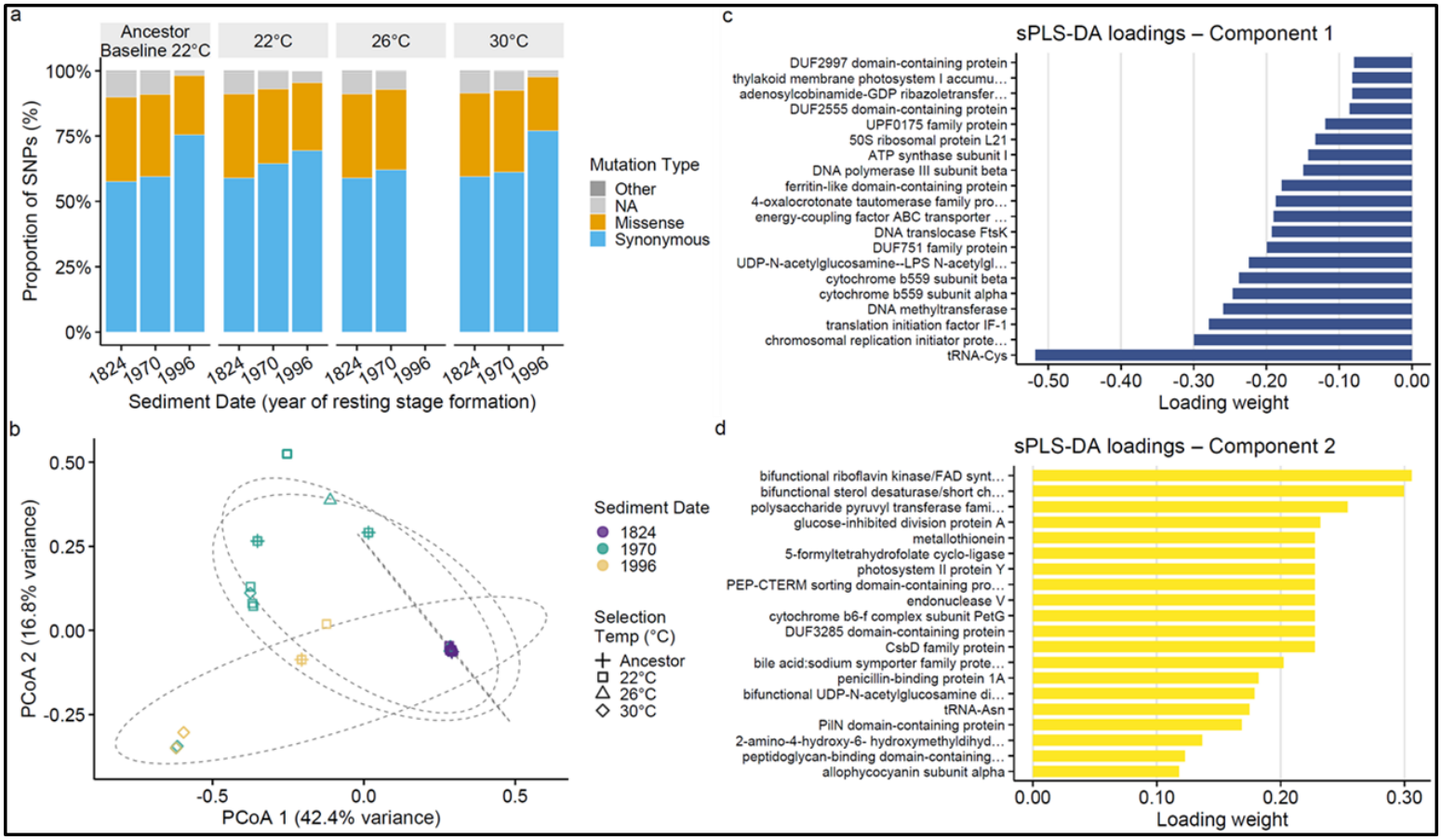

Fig. 5. Genomic variation and multivariate differentiation among evolved *Nodularia spumigena* lineages under long-term thermal selection. (a) Proportion of SNP effect types (synonymous, missense, NA, other) across selection temperatures and sediment ages. Mutation composition remained broadly consistent across treatments, with synonymous variants predominating. (b) Principal coordinates analysis (PCoA) of genome-wide SNP presence–absence (Bray-Curtis dissimilarity; 43 samples: five ancestral + 38 evolved). Colours indicate sediment date (purple = 1824, teal = 1970s, yellow = 1996); symbols indicate selection treatment (+ Ancestor, □ 22°C, △ 26°C, ◇ 30°C); dashed ellipses show 68% confidence regions per treatment. Sediment age explained significantly more genomic variation than selection temperature (PERMANOVA: Age $R^2 = 0.263$, $p = 0.001$; Treatment $R^2 = 0.086$, $p = 0.063$). (c–d) sPLS-DA loadings for discriminant components 1 and 2 based on evolved-specific gene product mutation counts (37 samples * 1,939 gene products), with selection temperature as the grouping variable. Bar direction indicates the sign and relative magnitude of each gene product's contribution. Functional annotations reflect loadings, not formal enrichment analysis.

Across evolved populations, novel mutation burden varied widely, with replicates carrying between 10 and 143,271 SNPs unique to evolved populations (absent in ancestral genomes). This heterogeneity is evident in the distribution of novel SNP counts across age * temperature combinations (Fig. 6a). Linear mixed-effects models on log-transformed counts (random intercept for nested biological replicate) showed that sediment age tended to influence total novel SNP counts, although individual age contrasts did not reach conventional significant thresholds (Fig. 6a). For log total novel SNPs, lineages from the 1970s and 1996 sediments had higher estimated burdens than the 1824 reference (Age 1970s: estimate 1.96 ± 1.08 SE, $p = 0.085$; Age 1996: 2.90 ± 1.56 SE, $p = 0.077$), indicating a trend toward greater mutation accumulation in more recent lineages. In contrast, selection temperature did not significantly affect total novel mutation counts (26 °C: 1.92 ± 1.18 SE, $p = 0.131$; 30 °C: -0.29 ± 0.98 SE, $p = 0.768$), in line with the overlapping boxplots across temperatures within each age class (Fig. 6a).

Patterns for novel missense mutations closely paralleled those for total novel SNPs. Missense counts spanned several orders of magnitude and showed similar age-structured variation in the boxplots (Fig. 6b). Mixed-effects models on log missense counts again suggested higher burdens in the 1970 and 1996 lineages than in 1824 (Age 1970: 1.88 ± 1.04 SE, $p = 0.084$; Age 1996: 2.60 ± 1.50 SE, $p = 0.099$), with non-significant temperature effects (26 °C: 1.87 ± 1.17 SE, $p = 0.135$; 30 °C: -0.45 ± 0.96 SE, $p = 0.652$).

Boxplots of dN/dS proxy across age * temperature combinations suggested clear differences among sediment ages but no systematic trend with increasing selection temperature (Fig. 6c). Mixed-effects models on the log-transformed dN/dS revealed a strong effect of sediment age but no detectable effect of selection temperature. Relative to the 1824 lineage, both the 1970s and 1996 lineages exhibited markedly lower dN/dS proxies (Age 1970: -0.97 ± 0.21 SE, $p = 0.001$; Age 1996: -1.31 ± 0.28 SE, $p = 0.001$), indicating a reduced accumulation of nonsynonymous relative to synonymous mutations in more recent sediments. In contrast, temperature effects were non-significant (26 °C: 0.06 ± 0.13 SE, $p = 0.663$; 30 °C: -0.14 ± 0.11 SE, $p = 0.229$), consistent with the overlapping temperature groups in Figure. 6c.

The proportion of novel SNPs that were missense variants (propmissense, logit-transformed) showed relative narrow variation across age * temperature combinations, with substantial overlap in boxplots within and among sediment ages (Fig. 6d). A mixed-effects model of logit-transformed missense proportion revealed no significant effects of sediment age or selection temperature (all fixed effects $p > 0.15$). Thus, while lineages differed in the total number of novel and missense

SNPs, the relative fraction of novel SNPs that were nonsynonymous versus synonymous remained broadly similar across historical backgrounds and thermal regimes (Fig. 6d).

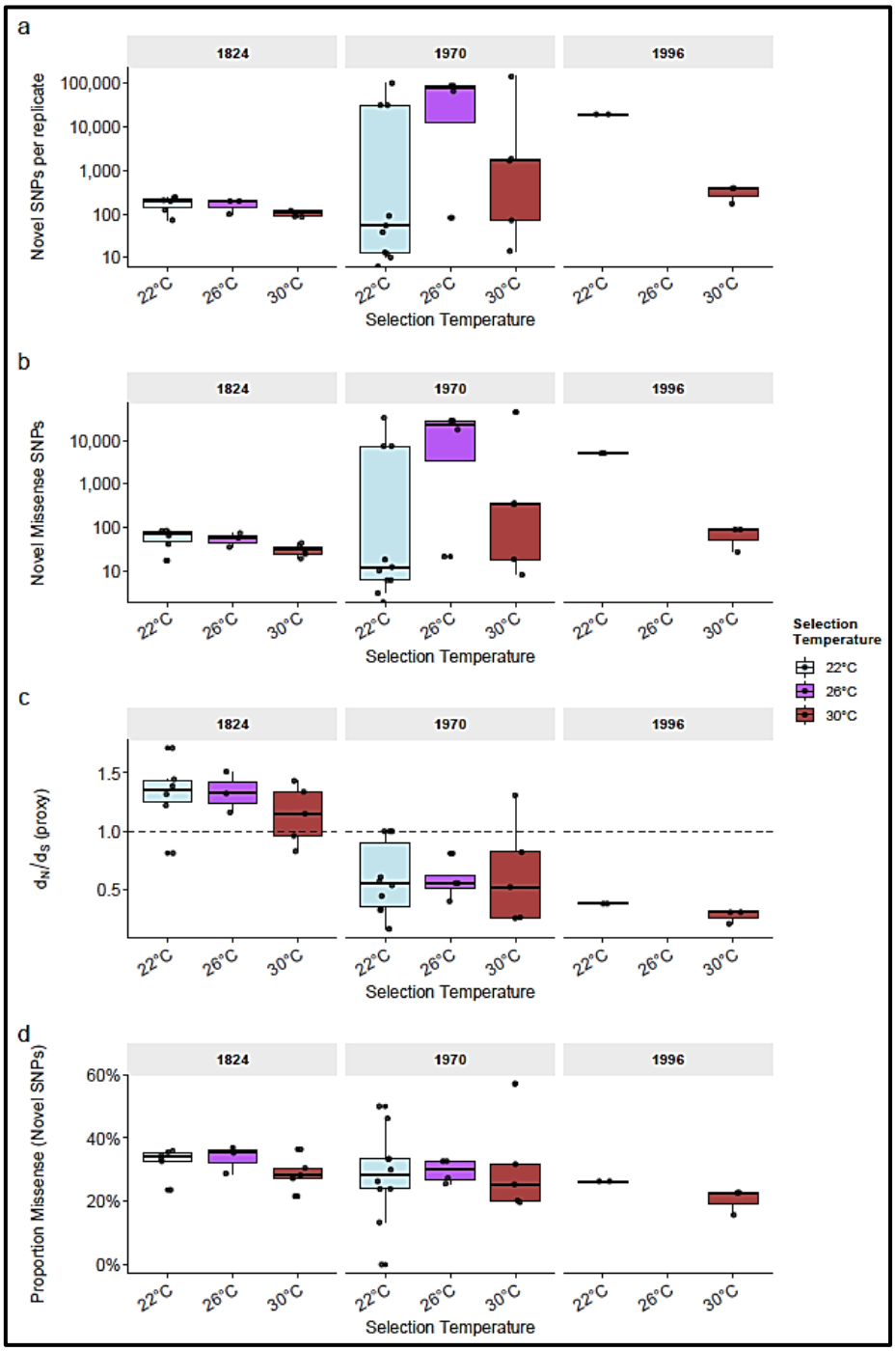

Fig. 6. Novel mutation burden and functional composition across sediment ages and selection temperatures in evolved *Nodularia spumigena* lineages. (a) Total SNPs unique to evolved populations (absent in ancestral genomes) (log_{10} scale). (b) Novel missense SNP counts per replicate (log_{10} scale). (c) Proxy dN/dS ratio (missense + 0.5) / (synonymous + 0.5) per replicate; dashed line indicates dN/dS = 1. (d) Proportion of novel SNPs classified as missense. In all panels, boxplots summarise biological replicates grouped by selection temperature (22°C, light blue; 26°C, purple; 30°C, dark red) within each sediment age facet (1824, 1970s, 1996). n = 6 replicate populations per strain per selection temperature, with the exception of the 1996 * 26°C treatment which is absent from genomic analyses due to technical failure during library preparation (total analysed: 38 evolved populations). Brackets indicate pairwise Wilcoxon test results (NS = not significant); primary inference is from linear mixed-effects models (see Results). One replicate with zero novel mutations is excluded from panels (a) and (b).

Discussion – Chapter 2.2

We exposed pre-industrial (1824), historical (1970s), and contemporary (1996) *Nodularia spumigena* lineages to ~100 generations of thermal selection at 22, 26, and 30°C. We then quantified evolutionary changes in thermal performance, carbon use efficiency, and genomic architecture. Three findings stand out and together define the central contribution of this study. First, all cohorts converged on similar post-selection thermal optima despite markedly different ancestral starting points, with the magnitude of shift differing substantially, with the 1970s and 1996 lineages shifting 5–6°C compared to negligible change in the pre-industrial lineage. Second, the capacity for carbon use efficiency evolution under warming is historically contingent. Only the more recently derived lineages could further adjust their CUE under experimental selection. Third, ~100 generations of thermal selection left the dominance of sediment age in the genomic landscape largely intact. We discuss each in turn before synthesising their combined implications for predicting *N. spumigena* responses to future Baltic Sea warming.

The convergence of T_{opt} values across cohorts following selection supports Hypothesis 1 in part: all *N. spumigena* cohorts shifted towards a similar post-selection T_{opt}, but the magnitude of shift differed substantially: the pre-industrial 1824 lineage, already near 30°C ancestrally, showed little further change, while the 1970s and 1996 lineages shifted upward by 5–6°C. Notably, lineages evolved at 22°C also showed substantial shifts in T_{opt}, raising the possibility that environmental stability, rather than directional warming *per se*, drives some of the observed TPC reorganisation. However, convergence in T_{opt} alone does not imply equivalent evolutionary potential across all performance dimensions: peak growth rate at T_{opt} (μ_{max},T_{opt}) differed substantially among cohorts and selection temperatures, indicating that thermal adaptation extends beyond niche repositioning to encompass the maximum performance achievable within that niche. T_{opt} is therefore a necessary but insufficient indicator of the full scope of evolutionary change in thermal performance. Together, these patterns confirm that *N. spumigena* lineages retain the capacity to shift their thermal optima within experimentally relevant timescales, consistent with rapid TPC evolution documented in other phytoplankton (Barton et al., 2023; Listmann et al., 2016; Padfield et al., 2016). Critically, however, this is not a uniform temperature shift. The pre-industrial lineage required no upward shift because it was already near the post-selection T_{opt} values reached by the other cohorts, while the 1970s and 1996 lineages, starting from ~25-27°C shifted the most. This convergence is itself an evolutionary signal: the 1970s and 1996 lineages retain the genetic variation necessary to reach a T_{opt} of ~30°C within ~100 generations, even though natural selection in the modern, more thermally variable Baltic Sea has maintained their optima at lower values (Chapter

2.1). The fact that all lineages converged on a similar post-selection T_{opt} despite spanning nearly two centuries of divergence, suggests that the molecular machinery underlying upward T_{opt} shifts, likely involving membrane composition, enzyme thermal stability, and photosystem regulation is broadly conserved in this species (Kontopoulos et al., 2020). Notably, this study examined an entirely different functional group from previous experimental evolution work on phytoplankton (e.g. diatoms; (Listmann et al., 2016), and the magnitude of the shift in the more recently derived lineages (~5-6°C) is larger than typical responses reported in microalgae, which may reflect the broad thermal range of our selection treatments (22–30°C), a span that exceeds the ~5–8°C differentials typically used in phytoplankton experimental evolution studies (Listmann et al., 2016; Padfield et al., 2016), and which may have provided sufficient selective pressure to reveal T_{opt} shifting capacity across all cohorts simultaneously.

Evidence for Hypothesis 2 that ancestral thermal strategy modulates evolutionary response was partial. The fold-change growth trajectory analysis showed that lineages evolved at 26°C tended toward reduced growth relative to their ancestral state, while those evolved at 30°C showed a non-significant positive trend. The 1970s cohort, whose ancestral T_{opt} most closely matched the 26°C selection temperature, showed the most pronounced reduction when evolved at 30°C, consistent with the prediction that greater thermal displacement from the ancestral fitness peak produces stronger directional responses. However, the age * temperature interaction did not reach significance at the model level, and the substantial among-lineage variance in the random effects underscores that individual genotype identity, rather than sediment-age cohort, is the dominant driver of individual evolutionary trajectories at this timescale.

The maximum growth rate at the thermal optimum ($\mu_{max,}$ T_{opt}) was not significantly altered by selection temperature in any sediment cohort, while the 1996 lineage exhibited higher $\mu_{max,}$ T_{opt} than the 1824 lineage regardless of selection treatment. This indicates that evolutionary responses in Chapter 2.2 primarily involved shifts in thermal sensitivity and thermal optima rather than changes in peak growth capacity, echoing the pattern identified in Chapter 2.1 where contemporary lineages maintained higher intrinsic growth performance. Such a separation of μ_{max} and T_{opt} responses is consistent with findings in other phytoplankton experimental evolution studies where the position and shape of the thermal performance curve evolve more readily than the overall maximal growth rate (Listmann et al., 2016; Padfield et al., 2016).

Activation energy (E_a) declined following selection at all three temperatures, including the lowest (22°C). Because this reduction occurred across all selection temperatures, it likely reflects a partial general response to controlled laboratory conditions rather than directional selection for reduced

thermal sensitivity analogous to domestication effects documented in long-term microbial evolution experiments (Barton et al., 2023; Kontopoulos et al., 2020). It is worth noting that elevated E_a of growth rate does not necessarily translate directly to elevated E_a of underlying metabolic rates, as the two can diverge when compensatory processes such as enzyme upregulation buffer metabolic flux against temperature change (Barton et al., 2020). Whether E_a reductions in our evolved lineages reflect genuine changes in the temperature sensitivity of metabolic machinery, or simply a relaxation of the steep sub-optimal performance curve that characterised the ancestral 1996 lineage under natural selection for thermally variable environments, remains to be resolved. Importantly, the loss of age-structured differences in E_a following evolution contrasts with the strong divergence in E_a documented in Chapter 2.1, suggesting that laboratory selection can rapidly homogenise the temperature sensitivity of growth across historically divergent lineages.

The absence of a significant selection * assay temperature interaction in the reciprocal transplant assay indicates that ~100 generations of constant thermal selection were insufficient to produce temperature-specific physiological specialisation (Hypothesis 3 not supported), though perhaps direct competition of evolved lineages with a preserved, non-evolved ancestor may have yielded a different picture. Reaction norms remained largely parallel across assay environments, meaning lineages evolved at a given temperature did not specifically outperform those evolved at other temperatures when assayed at their home temperature. This is consistent with findings from phytoplankton experimental evolution at comparable timescales (Listmann et al., 2016; Schaum et al., 2017) and with the theoretical expectation that local adaptation at the TPC level requires either longer selection durations or stronger selection differentials than those applied here (Kawecki & Ebert, 2004). The parallel reaction norms contrast with the specialist divergence reported over longer selection timescales in diatoms (Listmann et al., 2016; O'Donnell et al., 2018), and suggest that the ~100-generation timescale of this experiment is better suited to detecting shifts in overall performance level which we do observe via T_{opt} convergence than changes in temperature-specific performance specialisation. The absence of crossing reaction norms at this timescale is itself informative; longer-duration experiments or assays across a broader temperature range may yet reveal trade-offs. The similar magnitude of T_{opt} upward shift under 22°C as under 30°C selection is perhaps the most surprising finding of this study, and one that we cannot fully resolve from the present data. We tentatively suggest this reflects a combination of domestication-related relaxation of natural-environment constraints and de novo mutations arising during selection in the more recently derived lineages, but this interpretation requires direct testing.

One result warrants particular attention: the magnitude of T_{opt} shift in the 1970s and 1996 lineages was broadly similar whether lineages were selected at 22°C, 26°C, or 30°C (Table 2). This is unexpected because 22°C is sub-optimal for all lineages based on ancestral TPCs, and one would anticipate that stronger directional selection at supra-optimal temperatures (26°C and 30°C) would produce proportionally larger T_{opt} shifts. Several explanations are possible. First, laboratory domestication effects, whereby adaptation to controlled, resource-replete conditions rather than to temperature *per se*, may have driven part of the T_{opt} shift observed even under the 22°C treatment, analogous to domestication signals documented in long-term microbial evolution experiments (Barton et al., 2023; Kontopoulos et al., 2019). Second, the 1970s and 1996 lineages may reflect genetic differences that predispose rapid T_{opt} shifts regardless of selection temperature, with the specific thermal environment acting as a permissive rather than directional force. Third, if the effective number of generations was similar across treatments as our fixed-volume transfer protocol ensures, then comparable evolutionary time, rather than comparable thermal stress, may be the primary driver of T_{opt} displacement. Disentangling these possibilities would require fluctuating temperature selection regimes and extended selection durations.

The age-structured pattern in CUE evolution is one of the most ecologically meaningful results of this study. Both the 1970s and 1996 lineages showed significant increases in CUE at elevated selection temperatures: the 1996 cohort at both 26°C (ΔCUE = 0.21 ± 0.05) and 30°C (ΔCUE = 0.11 ± 0.05), and the 1970s cohort at 30°C (ΔCUE = 0.11 ± 0.03), whereas the pre-industrial 1824 lineage showed no significant evolutionary change in CUE at any temperature. This is consistent with the interpretation that thermal adaptation in phytoplankton can be achieved by reducing respiratory costs relative to photosynthetic carbon fixation, thereby increasing net carbon allocation to growth at higher temperatures (Barton et al., 2020; Padfield et al., 2016). The temperature-specificity of the CUE response, by which we mean that the magnitude of evolutionary CUE increase differed among selection temperatures. Rather than being uniform across all warming treatments, this was strongest at an intermediate warming level (26°C) but smaller and less consistent at other temperatures, suggesting that the relationship between thermal selection and carbon use efficiency is non-linear and may depend on the proximity of the selection temperature to the ancestral thermal optimum, though the precise mechanisms remain to be resolved. The absence of CUE evolution in the 1824 lineage despite comparable T_{opt} shifts suggests that the two traits respond to different selective pressures and are not tightly coupled in their evolution, echoing the broadly conserved CUE documented in Chapter 2.1, where temperature had no significant effect and all lineages maintained CUE above 0.5, despite a marginal age effect driven by lower baseline CUE in the 1996 lineage. More strikingly, the capacity for CUE evolution

under warming appears to be a derived trait: only the lineages that have already experienced a century of warming and metabolic remodelling in the modern Baltic Sea retain the ability to further adjust their carbon economy under experimental selection. Whether this age-structured difference in evolutionary lability reflects differences in de novo mutational input at metabolic loci, epigenetic flexibility (Chapter 2.3), or differences in the regulatory architecture of photosynthesis and respiration warrants direct investigation.

Multivariate genomic analysis confirmed that sediment age explained substantially more variation in evolved SNP profiles than selection temperature. This hierarchical structure with age as the dominant axis, and temperature as the secondary signal, is consistent with the view that the genomic background established over decades to centuries of natural selection in the Baltic Sea is not rapidly erased by a single episode of experimental evolution, and with the expectation that standing genetic variation accumulated over long timescales should contribute more to genomic differentiation than mutations acquired during short-term selection (Sjöqvist, 2022). The modest but directionally consistent contribution of selection temperature implies that thermal selection did leave a detectable genomic imprint, and that longer or more extreme selection experiments would likely yield stronger temperature-structured differentiation.

Complementary sPLS-DA identified a restricted set of gene products with disproportionate discriminatory power for selection temperature, superimposed on the broader age-structured divergence. Their discriminatory loading patterns suggest that temperature-driven selection acted on a small subset of loci associated with core cellular and metabolic functions, distinct from those driving age-structured divergence. While these loadings reflect correlational patterns rather than the output of formal enrichment tests, they are consistent with the hypothesis that the putative genomic targets of temperature-driven selection in *N. spumigena* overlap functionally with those identified in Chapter 2.1, where genomic divergence across sediment ages also implicated photosystem II and ATP-synthase-related genes.

The novel SNP burden analysis revealed a trend toward greater total and missense mutation accumulation in the 1970s and 1996 lineages compared to the 1824 lineage, although individual contrasts did not reach statistical significance. Selection temperature had no significant effect on total or missense novel SNP counts, indicating that the thermal selection regime applied here did not detectably elevate the mutation rate or the fraction of new mutations that were protein-altering, consistent with the relatively modest temperature differential between treatments (8°C). Importantly, the relative proportion of missense to synonymous novel SNPs was conserved across all age * temperature combinations, suggesting that functional constraints on protein-coding

sequences remained broadly similar regardless of sediment age or selection temperature (Tai et al., 2011).

The dN/dS proxy analysis revealed a striking age-structured pattern: both the 1970s and 1996 lineages exhibited markedly lower dN/dS ratios than the 1824 lineage, while selection temperature had no significant effect. A lower dN/dS reflects relatively higher accumulation of synonymous relative to nonsynonymous novel mutations, consistent with more effective purifying selection against deleterious amino acid changes (Tai et al., 2011). One possible interpretation is that the 1824 lineage, having the oldest genomic background and potentially a lower effective population size following long-term sediment dormancy, exhibits reduced efficiency of purifying selection, allowing a larger fraction of mildly deleterious nonsynonymous mutations to accumulate during experimental evolution. These patterns warrant cautious interpretation, as dN/dS proxies computed from short-timescale SNP data can be influenced by demographic history, mutation biases, and clonal population structure rather than reflecting selection alone (Mugal et al., 2014; Rocha et al., 2006)

These metabolic patterns are mirrored at the genomic level, as discussed below. Taken together, and connecting back to the findings of Chapter 2.1, a coherent picture emerges. The convergent patterns documented here are particularly striking given that Chapter 2.2 isolates a single, controlled selective factor, temperature, whereas the phenotypic divergence in Chapter 2.1 reflects the cumulative effects of two centuries of multi-factor environmental change in the Baltic Sea. Chapter 2.1 showed that natural evolutionary history has produced divergent ancestral phenotypes in Baltic Sea *N. spumigena*: the pre-industrial lineage is a broad, relatively slow-growing generalist with a high T_{opt}; contemporary lineages are steeper, faster-growing, with lower but more metabolically flexible optima. Chapter 2.2 shows that these divergent starting points do not translate into divergent endpoints. All cohorts converge on a similar post-selection T_{opt}, but they do reflect profoundly different magnitudes of adaptive effort: the 1970s and 1996 lineages shifted their T_{opt} by 5–6°C to reach this endpoint, while the pre-industrial 1824 lineage, already near 30°C ancestrally, required little further change (see also the unexpected parallel T_{opt} shifts under 22°C selection, discussed above). Divergent starting points do, however, translate into divergent capacity for carbon use efficiency evolution: only the more recently derived lineages can evolve CUE in response to warming. This asymmetry, conserved potential for some traits but contingent potential for others, adds an important nuance for predicting bloom dynamics under future Baltic Sea warming, although increasing environmental variability in the Baltic Sea suggests that experiments incorporating fluctuating conditions will be necessary to fully resolve these dynamics. The

conserved T_{opt} shifting capacity implies that future warming may elicit broadly similar adaptive thermal trajectories, but different peak growth, in *N. spumigena* regardless of the historical provenance of resident populations, while the additional CUE evolutionary capacity in contemporary lineages suggests that recent populations may be better positioned to capitalise on warming through improved metabolic efficiency, potentially reinforcing bloom formation under projected warming scenarios (Hense et al., 2013; Kniebusch et al., 2019). Comparisons with (Medwed et al., 2024), who documented an increase in photosynthetic T_{opt} from 15.3°C to 21.1°C between *N. spumigena* lineages dated to 1987 and 2020, raise the possibility that photosynthetic and growth-rate T_{opt} can diverge under the same environmental pressure, though a direct comparison between the two trait dimensions within the same lineages and time period would be needed to confirm this, a dimension that warrants direct integration with the TPC framework used here. Notably, the shift towards lower T_{opt} in contemporary lineages may be of ecological concern, as it increases the likelihood that ambient temperatures coincide with those that maximises short-term growth, potentially enhancing bloom formation relative to pre-industrial lineages.

The most important limitation of this study is shared with Chapter 2.1: only five lineages in total, meaning lineage-specific idiosyncrasies cannot be fully separated from sediment-age cohort patterns. The clonal structure of experimental populations, the constant rather than fluctuating temperature regime, the absence of competition and predation, and the relatively short selection duration relative to the centuries-scale timescales captured by the resurrection approach all limit direct extrapolation to natural settings (Collins, 2011; Litchman et al., 2012). The missing 1996 * 26°C genomic data point introduces an asymmetry in genomic comparisons that should be borne in mind when interpreting the PERMANOVA results. Future work should increase the number of resurrected lineages per sediment layer, extend selection duration, incorporate realistic temperature fluctuations, and combine experimental evolution with natural assemblages to test whether the adaptive potential demonstrated here is realised under ecologically realistic conditions (Litchman et al., 2012; Schaum et al., 2017).

Acknowledgements

We thank our laboratory technician Stefanie Schnell, Luisa Listmann, and the students Tabea Schneider, Nina Müller, Lydia Schramm, and Janice C. da Mata for their assistance during the experiments. We are grateful to Cynthia Medwed and the IOW-Leibniz Institute for Baltic Sea Research (Warnemünde) for resurrecting and providing the sediment core lineages used in this study. This research was supported by the Deutsche Forschungsgemeinschaft (DFG) grant (Project number – 450278268). ChatGPT (OpenAI, GPT-4) was used for language editing and grammar improvement, operated in a mode where user inputs were not used for model training, and all outputs were reviewed and validated by the authors.

Competing Interests

The authors declared no competing interests

Author Contributions

ES conceived the study. CM resurrected the lineages used for the study. ME and ES designed the experiments. ME conducted the experiments. ME produced and analysed the data and produced the figures and wrote the first and final draft of the manuscript. ES contributed to coding and code troubleshooting. ES contributed with analysis input. ES and SB contributed with manuscript revisions. All authors gave final approval for publication. Funding was acquired by ES.

Data Availability

The data supporting the findings of this study are available in the Supporting Information. R codes and processed data sets used for statistical analysis and figure generation are openly available on GitHub. *Nodularia spumigena* cultures are maintained in the laboratory at the Institute of Marine Ecosystem and Fisheries Science.

Chapter 2.3: Global DNA methylation correlates with thermal selection in Baltic Sea *Nodularia spumigena*

Michael Edetanlen[1]*, C.-Elisa Schaum[1]

*Corresponding author: michael.edetanlen@uni-hamburg.de

[1]Institute of Marine Ecosystem and Fisheries Science, University of Hamburg, Hamburg, Germany

[2]Leibniz-Institut for Baltic Sea Research Warnemünde, Rostock, Germany

Author ORCID IDs:

Michael Edetanlen: https://orcid.org/0009-0008-1852-006X

Elisa Schaum: https://orcid.org/0000-0001-6949-7367

Publication status and authorship statement

This study contains work prepared for publication in a peer-reviewed scientific journal.

Chapter 2.3, entitled "Global DNA methylation correlates with thermal selection in Baltic Sea *Nodularia spumigena*", is prepared for submission to Evolutionary Applications.

Michael Edetanlen is the first and corresponding author of the manuscript presented in the chapter. Elisa Schaum, Anke Kremp, and Inga Hense conceived the overarching research framework, and Elisa Schaum supervised the work. Elisa Schaum contributed to manuscript revisions. The co-author approved the final version of the manuscript.

Abstract

Environmental warming is altering the physiology and evolutionary trajectories of microorganisms. Cyanobacteria, which dominate many aquatic primary producer communities and frequently form harmful blooms, show strong physiological sensitivity to temperature. Epigenetic mechanisms such as DNA methylation have been proposed as potential regulators of rapid phenotypic adjustment in microbes, yet empirical evidence from long-term evolution experiments in diazotrophic cyanobacteria remains lacking. Here we quantified global DNA methylation (5-methylcytosine, 5-mC) in ancestral and evolved *Nodularia spumigena* lineages resurrected from Baltic Sea sediments dated to pre-industrial (ca. 1824), historical (1970s), and contemporary (ca. 1996) periods, following ~100 generations of thermal selection at 22, 26, and 30°C. Ancestral methylation levels differed markedly among sediment-age cohorts: the pre-industrial lineage exhibited the highest baseline methylation (mean 6.63%), while historical (2.71%) and contemporary (3.48%) lineages were substantially lower. Pre-industrial lineages exhibited substantially higher ancestral methylation levels and reduced methylation following evolution, whereas historical and contemporary lineages showed increases in methylation under thermal selection. Mean methylation co-varied positively with among-replicate variability in activation energy (E_a) and the growth rate parameter ln(c), but not with variability in T_{opt}. These results establish global DNA methylation as a dynamic, historically structured molecular correlate of thermal selection in *N. spumigena*, and suggest that epigenetic state may contribute to the regulation of metabolic flexibility rather than thermal niche position *per se*.

Keywords: DNA methylation; epigenetics; cyanobacteria; 5-methylcytosine; *Nodularia spumigena*; Baltic Sea; experimental evolution; phenotypic plasticity

Introduction – Chapter 2.3

Environmental changes can trigger phenotypic responses in microbial populations via both genetic and non-genetic mechanisms. Among the latter, epigenetic modifications such as heritable changes in gene expression that do not involve alterations to the underlying DNA sequence, have attracted increasing interest as potential contributors to rapid environmental responsiveness in microorganisms (Anton & Roberts, 2021). In prokaryotes, the best characterised epigenetic modification is DNA methylation, which in bacteria most commonly involves adenine (N6-methyladenine) and cytosine (5-methylcytosime, 5-mC) residues. While bacterial DNA methylation has historically been studied in the context of restriction-modification systems that protect against foreign DNA, emerging evidence suggests it also plays broader regulatory roles including transcriptional control, stress response, and cell cycle regulation (Anton & Roberts, 2021; Hu et al., 2018).

Particularly in cyanobacteria, genome-wide methylation profiling in *Synechocystis sp. PCC 6803* has shown that methylation patterns respond to environmental stress, with nutrient limitation and temperature change associated with systematic shifts in methylation state (Hu et al., 2018). Similarly, *Trichodesmium*, a diazotrophic cyanobacterium comparable in ecological role to *Nodularia spumigena,* showed dynamic long-term methylation changes that paralleled phenotypic adaptation under nutrient and CO_2 stress (Walworth et al., 2021). Despite these advances, it has not yet been directly investigated in bloom-forming cyanobacteria whether DNA methylation patterns differ systematically among lineages with distinct evolutionary histories, or whether sustained environmental selection can induce persistent, heritable epigenetic differences across generations in bloom-forming cyanobacteria.

This question is directly relevant to interpreting the results of Studies 2.1 and 2.2. In Chapter 2.1, we found that pre-industrial (1824) *N. spumigena* lineages had higher baseline thermal optima, shallower sub-optimal performance curves, and lower peak growth rates than contemporary lineages, a pattern inconsistent with the "hotter is broader and better" prediction and more consistent with adaptation to increased thermal variability over two centuries. In Chapter 2.2, we found that T_{opt} converged to similar values, albeit from very different starting points, across cohorts following experimental evolution, but that evolution of carbon use efficiency to higher values was restricted to the more recently derived lineages. A remaining open question is whether these phenotypic differences between historical and contemporary lineages are accompanied by systematic differences in epigenetic state, and whether thermal selection induces consistent methylation changes that co-vary with observed phenotypic shifts.

We address this in this study, by quantifying global 5-mC methylation in ancestral (T_{start}) and evolved (T_{end}) populations of the same five *N. spumigena* lineages used in Studies 2.1 and 2.2. We test three hypotheses. First, that baseline methylation levels differ among sediment-age cohorts, reflecting divergent epigenetic architectures accumulated over two centuries of environmental change (H1). Second, that sustained thermal selection induces changes in global methylation, and that the direction and magnitude of these changes depend on the historical origin of the lineage (H2). Third, that variation in global methylation co-varies with variability in thermal performance traits, linking epigenetic state to phenotypic diversification without implying causality (H3).

Materials and Methods – Chapter 2.3

Sample selection and DNA extraction

A subset of ancestral (T_{start}) and evolved (T_{end}) populations from Chapter 2.2 was selected for global DNA methylation analyses. In total, 105 samples were analysed spanning three sediment ages (1824, 1970s, 1996), two evolutionary states (ancestral and evolved), and three selection temperatures (22, 26, and 30°C for evolved lineages; 22°C only for ancestral lineages, reflecting baseline condition prior to experimental evolution). Ancestral samples comprised n = 15 observations across sediment ages (n = 3 for 1824, n = 9 for 1970s, n = 3 for 1996); evolved samples comprised n = 90 observations (n = 7,6,6 at 22, 26 and 30°C respectively), 1970s (n = 18,18,17), and 1996 (n = 6,6,6), with minor imbalance due to replicate exclusions). DNA was extracted following the CTAB protocol described in Chapter 2.1. DNA quality and concentration were assessed using a Qubit 3 fluorometer (Thermo Fisher Scientific, Waltham, MA, USA); samples with insufficient yield were re-extracted as necessary.

Global DNA methylation quantification

Global DNA methylation levels were quantified using the MethylFlash™ Methylated DNA Quantification Kit (Fluorometric; EpigenTek Group Inc., Farmingdale, NY, USA), which targets 5-methylcytosine (5-mC). The assay was performed according to the manufacturer's instructions (EpigenTek, 2022). Briefly, extracted genomic DNA was bound to assay wells, washed, and incubated with capture and detection reagents specific to 5-mC. Fluorescence signals were measured using a SpectraMax® iD3 microplate reader (Molecular Devices LLC, San Jose, CA, USA) and quantified by comparison to a manufacturer-provided standard curve and expressed both as absolute methylated DNA quantity (ng) and as a percentage of total DNA input (%). Because absolute methylation signal depends on the quantity of DNA loaded which varied among samples, percentage methylation (% 5-mC) was used as the primary response variable for all statistical analyses. Water blanks confirmed negligible background signal.

Statistical Analysis

All statistical analyses were conducted in R v.4.5.1 (R Core Team, 2025). Percentage methylation values were converted to proportions relative to the amount of DNA in the sample and logit-transformed to meet assumptions of normality and homoscedasticity. Linear mixed-effects models were fitted using *lme4* (Wahl et al., 2014), with sediment-age, selection temperature (as continuous numeric predictor), evolutionary state (ancestral vs. evolved), and all two-way interactions as fixed effects in the global model. Replicate identity was included as a random intercept to account for

non-independence among samples from the same biological replicate. Model significance was assessed using Type III analysis of variance with Satterthwaite's approximation for degrees of freedom (*lmerTest*; (Kuznetsova et al., 2017). Estimated marginal means were calculated using emmeans (Lenth & Piaskowski, 2017) with Tukey adjustment for multiple comparisons. Model fit was assessed using *DHARMa* residual diagnostics (Hartig, 2016) and marginal R^2 following (Nakagawa & Schielzeth, 2013).

Log_2 fold-change in percentage methylation of evolved populations relative to age-specific ancestral means at 22°C was computed per sediment age * selection temperature combination as:

$$log_2(FC) = log_2\left(\frac{mean\,\%\,methylation_{evolved}}{mean\,\%\,methylation_{ancestral}}\right)$$

To assess associations between epigenetic state and phenotypic variability, coefficient of variation (CV) among biological replicates was computed for T_{opt}, E_a, and ln(c), from Chapter 2.2 TPC parameters. Mean percentage methylation per sediment-age cohort (pooled across all evolved populations) was used as a predictor, and associations were visualised using linear regression across the three sediment-age data points.

Results – Chapter 2.3

Ancestral methylation differs strongly among sediment-age cohorts

Ancestral (T_{start}) lineages assayed at 22°C showed markedly different baseline methylation levels across sediment ages (Fig. 1, left panel). The pre-industrial (1824) lineage had the highest ancestral methylation (mean ± SD: 6.63 ± 1.08%), approximately 2.4-fold higher than the historical 1970s lineage (2.71 ± 0.59%) and 1.9-fold higher than the contemporary 1996 lineage (3.48 ± 0.54%).

Evolutionary state and its interaction with sediment age drive methylation change

Following ~100 generations of experimental evolution, global methylation diverged from ancestral states in an age-dependent direction (Fig. 1, right panel; Fig. 2). The mixed-effects model revealed a significant main effect of evolutionary state (evolutionary state (ancestral vs. evolved): $F_{1,96}$ = 5.45, p = 0.022) and a strong age * evolutionary state interaction ($F_{2,96}$ = 15.94, p < 0.001), indicating that the direction of epigenetic change following selection depended on the historical origin of the lineage. Sediment age alone ($F_{2,96}$ = 2.16, p = 0.120) and selection temperature alone ($F_{1,96}$ = 2.72, p = 0.102) did not reach significance as main effects, though temperature showed a positive directional trend. The model explained 45.3% of variance in logit-transformed methylation (marginal R^2 = 0.453).

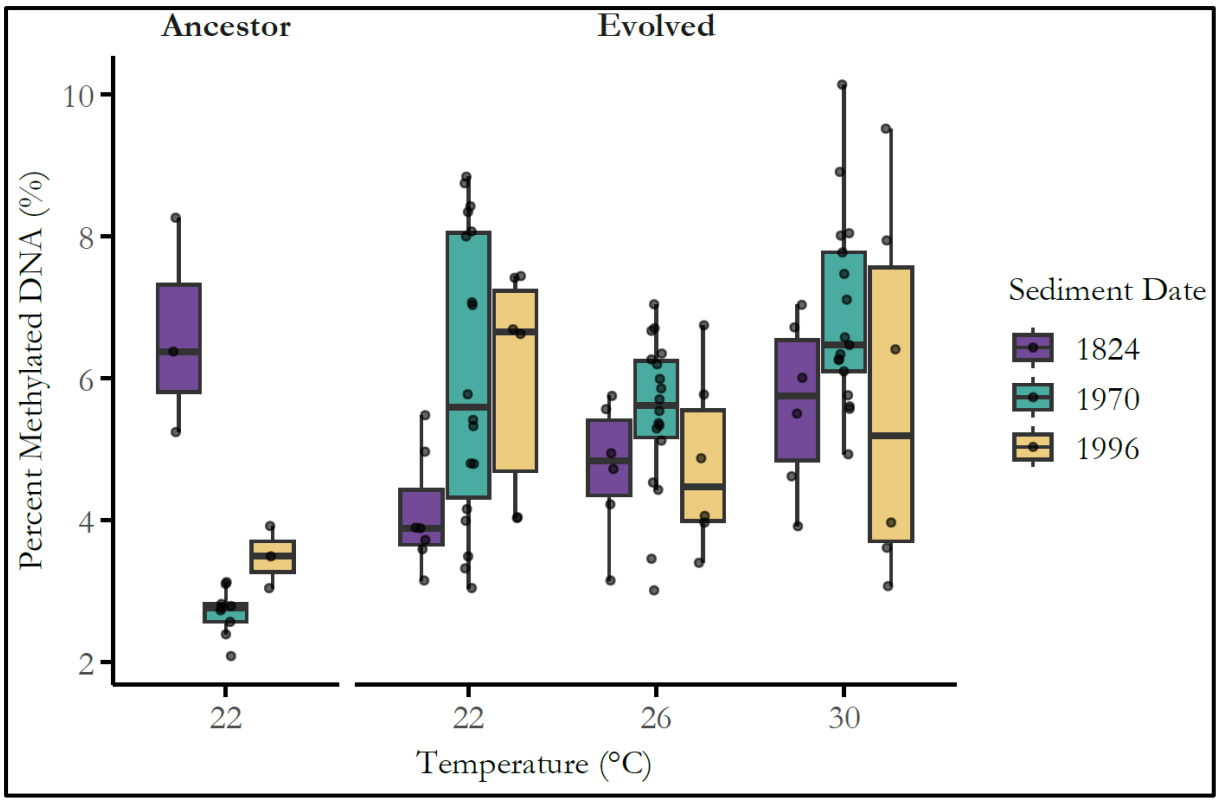

Fig. 1. Global DNA methylation (% 5-mC) in ancestral and evolved *Nodularia spumigena* lineages across sediment ages and selection temperatures. Boxplots show the distribution of percent methylated DNA for lineages originating from sediments dated to 1824 (purple), 1970s (teal), and 1996 (yellow). Left panel: ancestral (T_{start}) lineages assayed at 22°C only, reflecting baseline epigenetic states prior to experimental evolution (n = 3, 9, and 3 biological replicates for 1824, 1970s, and 1996 respectively). Right panel: evolved (T_{end}) lineages following ~100 generations of selection at 22, 26, and 30°C (n = 19, 53, and 18 biological observations for 1824, 1970s, and 1996 respectively across all temperatures). Points represent individual biological replicates; boxes indicate interquartile ranges with median values. The pre-industrial 1824 lineage had the highest ancestral methylation but reduced it following evolution; the historical and contemporary lineages had lower ancestral methylation but increased it under selection.

The $\log_2$ fold-change analysis clarifies the direction of these effects (Fig. 2). The pre-industrial 1824 lineage consistently reduced its methylation relative to its ancestral state across all three selection temperatures ($\log_2$FC: −0.69 at 22°C, −0.49 at 26°C, −0.24 at 30°C), with the largest reduction at the lowest selection temperature. In contrast, the historical 1970s lineage showed the largest increases in methylation across all temperatures ($\log_2$FC: +1.16 at 22°C, +1.02 at 26°C, +1.35 at 30°C), and the contemporary 1996 lineage also increased substantially ($\log_2$FC: +0.80 at 22°C, +0.46 at 26°C, +0.72 at 30°C). Post hoc pairwise contrasts confirmed that the 1970s and 1996 lineages differed significantly from the 1824 lineage in their age * evolutionary state response ($p < 0.001$ and $p < 0.001$ respectively).

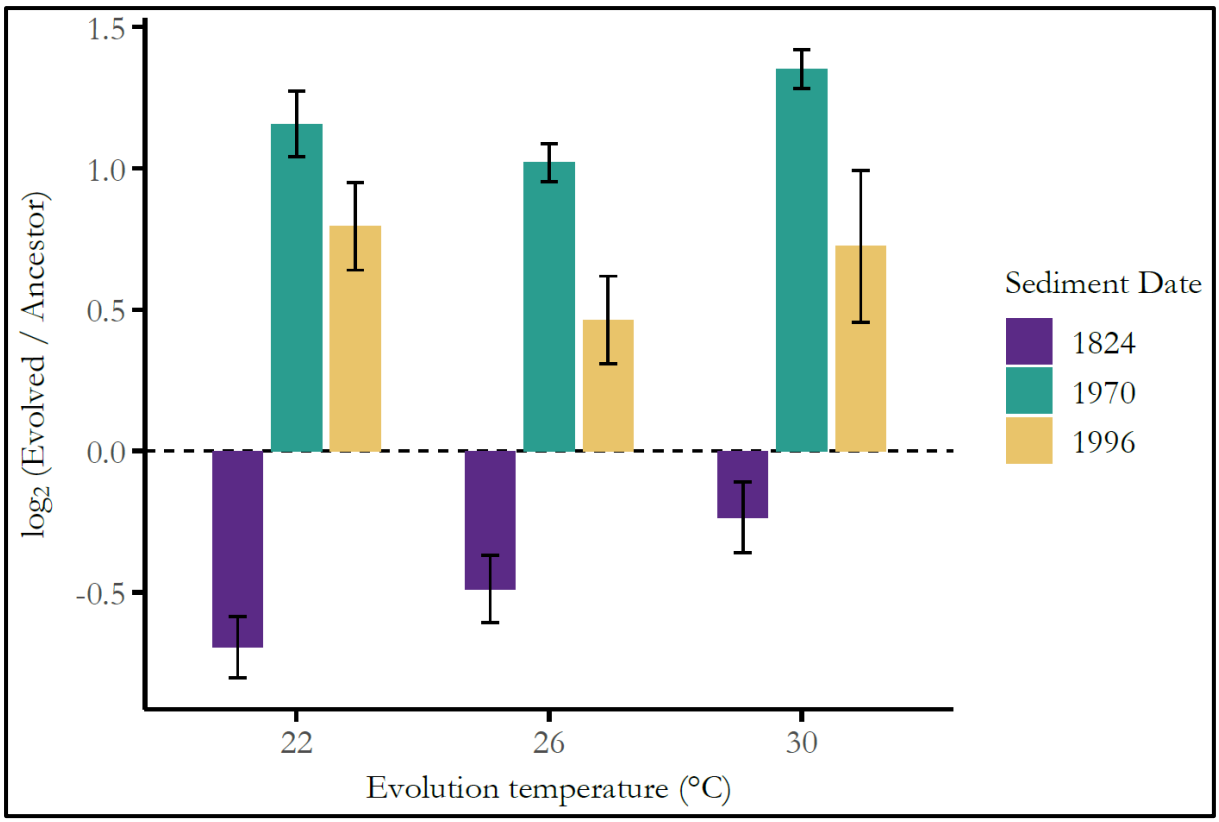

Fig. 2. Evolutionary change in global DNA methylation relative to age-specific ancestral baselines. Log_2 fold change in percentage methylated DNA of evolved *N. spumigena* lineages compared to their sediment-age-specific ancestral means at 22°C, shown across three selection temperatures (22, 26, and 30°C). Bars represent mean log_2(evolved / ancestor) values for lineages from sediment ages 1824 (purple), 1970s (teal), and 1996 (yellow). Error bars indicate ± 1 SE across biological replicates. The dashed horizontal line denotes no change relative to the ancestral baseline. The pre-industrial 1824 lineage consistently reduced methylation below its ancestral state (all log_2FC negative), while the 1970s and 1996 lineages increased methylation following selection (all log_2FC positive). n = 6–7 evolved replicates per sediment age per temperature (1824: n = 6–7; 1970s: n = 17–18; 1996: n = 6).

Methylation co-varies with variability in metabolic but not thermal optimum traits

Evolutionary change in global DNA methylation (log_2FC relative to age-specific ancestral baselines) co-varied significantly with evolutionary change in two of the three TPC parameters examined (Fig. 3). The change in baseline growth rate proxy (Δ ln(c)) showed a strong negative relationship with log_2FC methylation (slope = −0.155 ± 0.033 SE; R^2 = 0.759; $F_{1,7}$ = 22.03, p = 0.002). Lineages that increased their methylation following selection, the 1970s and 1996 cohorts, consistently reduced ln(c) relative to their ancestral state, while the pre-industrial 1824 lineage, which reduced its methylation, maintained or increased ln(c) (Fig. 3b). The change in thermal optimum (Δ T_{opt}) showed a strong positive relationship with log_2FC methylation (slope = 3.831 ± 0.960 SE; R^2 = 0.695; $F_{1,7}$ = 15.92, p = 0.005). Lineages that increased methylation showed the largest upward shifts in T_{opt}, consistent with the response of T_{opt} under warming (Fig. 3c). In contrast, the change in activation (Δ E_a) showed no significant relationship with methylation change (slope = −0.131 ± 0.118 SE; R^2 = 0.150; $F_{1,7}$ = 1.23, p = 0.304; Fig. 3a).

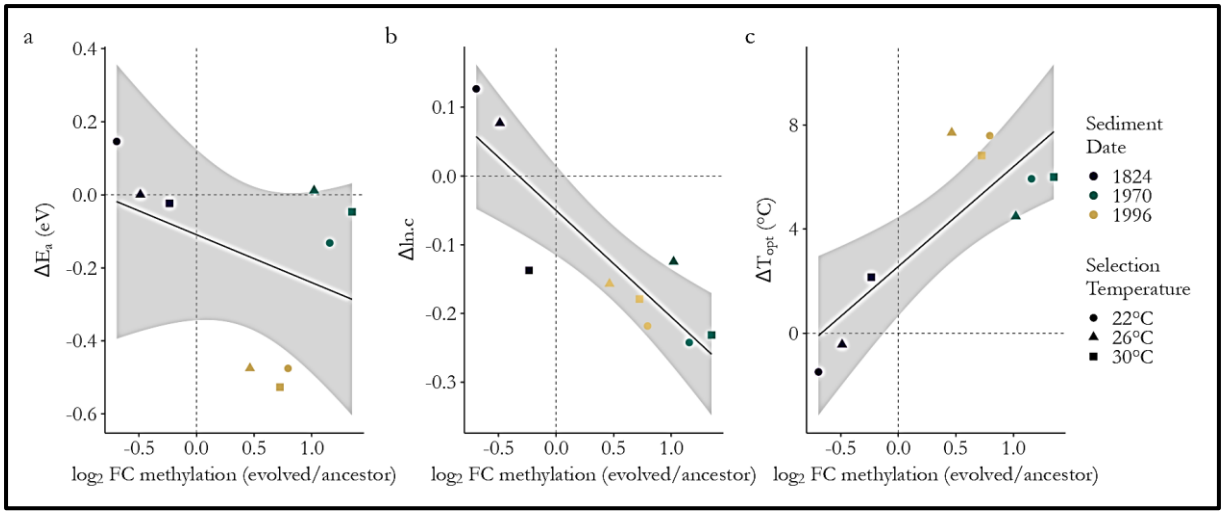

Fig. 3. Co-variation between evolutionary change in global DNA methylation and evolutionary change in thermal performance curve (TPC) parameters across sediment age * selection temperature combinations. Each point represents one Age * selection temperature combination (n = 9; three sediment ages * three selection temperatures), with colour indicating sediment age (1824: purple; 1970s: teal; 1996: yellow) and shape indicating selection temperature (circle: 22°C; triangle: 26°C; square: 30°C). The x-axis shows $\log_2$ fold change in percentage methylated DNA of evolved populations relative to age-specific ancestral baselines at 22°C (negative values indicate methylation reduction; positive values indicate methylation increase). The y-axis shows the change in each TPC parameter (evolved mean minus ancestral mean per sediment age): (a) activation energy Δ Ea (eV), (b) baseline growth rate proxy Δ ln(c), and (c) thermal optimum Δ Topt (°C). Solid lines show ordinary least-squares regression fits across all nine data points; shaded regions indicate 95% confidence intervals. Δ ln(c) declined significantly with increasing methylation (R^2 = 0.759, p = 0.002), and Δ Topt increased significantly with increasing methylation (R^2 = 0.695, p = 0.005), while Δ Ea showed no significant relationship (R^2 = 0.150, p = 0.304). TPC parameters are derived from biorep-level Sharpe-Schoolfield fits from Chapter 2.2 (n = 6 replicates per Age * selection temperature combination).

Discussion – Chapter 2.3

Global DNA methylation in *N. spumigena* is both historically structured and evolutionarily responsive to thermal selection, but the direction of change following ~100 generations of evolution is opposite in the pre-industrial lineage compared to the historical and contemporary lineages. Rather than a uniform warming-driven increase, the data reveal a divergence: the pre-industrial 1824 lineage, which began with the highest ancestral methylation (~6.6%), reduced its methylation across all selection temperatures following evolution, while the 1970s and 1996 lineages, which began with substantially lower baseline methylation (~2.7% and ~3.5%, respectively), increased theirs, particularly at elevated temperatures. This divergence directly addresses and corrects the initial interpretation of these data, and is consistent with the broader pattern of historical contingency in adaptive responses documented across Studies 2.1 and 2.2.

The markedly higher ancestral methylation in the pre-industrial 1824 lineage relative to historical and contemporary lineages is itself a biologically meaningful result. It suggests that the two centuries of environmental change separating pre-industrial from contemporary Baltic Sea conditions have been accompanied not only by shifts in TPC shape and growth rate (Chapter 2.1), and other phenotypes, but also by systematic changes in global epigenetic state. Whether this reflects differential selection pressure on methylation-based regulatory systems, changes in the activity of DNA methyltransferases or demethylases, or demographic effects on clonal methylation maintenance is not resolvable from global assay data alone. However, the pattern is consistent with findings in *Synechocystis* (Hu et al., 2018) and *Trichodesmium* (Walworth et al., 2021), where environmental history leaves persistent signatures in methylation architecture. The concept that prior environmental exposure shapes baseline epigenetic regulatory capacity, effectively encoding a form of cellular memory, has been termed epigenetic priming (Herdean et al., 2025), and the pre-industrial lineage's high-methylation ancestral state may reflect adaptation to the more thermally stable pre-industrial Baltic Sea, where tighter transcriptional control under a predictable environment may have been advantageous.

The reduction in methylation following evolution in the 1824 lineage, and the increase in the 1970s and 1996 lineages, suggests that laboratory thermal selection drives lineages toward an intermediate methylation state, regardless of their starting point. This convergence in epigenetic state parallels the convergence in T_{opt} documented in Chapter 2.2, reinforcing the idea that experimental evolution under constant temperature tends to homogenise trait values that were divergent under natural selection in the heterogeneous Baltic Sea environment. The 1970s lineage showed the largest absolute increase in methylation and the highest post-selection values at 30°C (~6.9%),

consistent with its already-documented capacity for CUE evolution under warming in Chapter 2.2, with both results pointing to greater metabolic and epigenetic lability in this cohort.

The analysis of evolutionary change (Δ, computed as evolved mean minus ancestral mean per sediment-age cohort for TPC parameters; $\log_2$ fold-change of evolved relative to ancestral percentage 5-mC for methylation) linking evolutionary methylation change to evolutionary TPC parameter change revealed a clear and interpretable pattern. Lineages that increased their methylation following selection, the 1970s and 1996 cohorts, showed the largest upward shifts in T_{opt} and the largest reductions in ln(c), while the pre-industrial 1824 lineage, which reduced its methylation, showed smaller T_{opt} shifts and maintained baseline-growth capacity (Fig. 3b,c). The significant positive relationship between $\log_2$FC methylation and ΔT_{opt} suggests that epigenetic remodelling co-varies with thermal niche repositioning, while the significant negative relationship with Δln(c) indicates a trade-off between epigenetic upregulation and baseline metabolic output. Activation energy change (ΔE_a) showed no significant relationship with methylation change, suggesting that the sensitivity of the sub-optimal performance curve to temperature is not the primary phenotypic axis associated with epigenetic remodelling in this system. Taken together, these associations are consistent with a model in which methylation-associated regulatory changes preferentially affect the thermal niche position and metabolic scaling of growth, rather than the fundamental thermodynamic sensitivity of enzyme kinetics. This interpretation aligns with findings in *Dunaliella salina* (Leung et al., 2022) and *Desmodesmus armatus* (Herdean et al., 2025), where epigenetic variation was linked to phenotypic shifts in environmentally responsive traits rather than to the core biochemical parameters of metabolism. Extrapolating these patterns to a warmer and more environmentally unpredictable future, the trade-off we observe where epigenetic upregulation accompanies T_{opt} repositioning at the cost of baseline growth, suggests that this mechanism may become increasingly constrained as warming intensifies and as organisms face concurrent stressors beyond temperature alone. Whether cyanobacteria can sustain or reverse epigenetic changes under multi-stressor conditions remains untested, but is indirectly relevant. (Brennan et al., 2025) found that in the marine copepod, *Acartia tonsa* evolved across 25 generations under warming, ocean acidification, and their combination, epigenetic and genetic changes contributed to resilience through complementary but spatially non-overlapping mechanisms where epigenetic divergence concentrated in stress-response genes and transposable element regulation, while genetic divergence dominated other genomic regions. Whether an analogous division of labour operates in bloom-forming cyanobacteria under multi-stressor conditions represents a compelling and entirely open question.

Several important limitations apply to this study. First, the MethylFlash assay quantifies global 5-mC content and provides no information on which loci or regulatory regions are methylated. The patterns we observe, particularly the reduction in methylation in the 1824 lineage, could reflect changes at many different genomic contexts, and whether any specific gene or pathway is differentially regulated cannot be determined without locus-specific methods such as bisulfite sequencing or ChIP-seq. Bisulfite sequencing in particular, by enabling base-resolution mapping of 5-mC across the genome would identify which regulatory regions are differentially methylated and provide the mechanistic resolution that global assays cannot. Second, the association between methylation and TPC parameter variability is based on nine data points (three sediment ages * three selection temperatures) and is therefore illustrative rather than statistically inferential; additional lineages would be required to test this relationship properly. Third, because ancestral samples were assayed only at 22°C, we cannot determine whether the observed evolutionary changes in methylation reflect directed responses to the selection temperature or more general effects of prolonged laboratory culture. Fourth, the singular fit of the random effects in the mixed model indicates that replicate-level variance was negligible, indicating that biological replicates within each condition were highly similar to each other. Future work should combine global methylation assays with whole-transcriptome sequencing and locus-specific methylation profiling to resolve which regulatory pathways are affected, and should extend the approach to a larger number of resurrected lineages to properly test whether the patterns documented here are reproducible across the full genetic diversity of Baltic Sea *N. spumigena*.

Acknowledgements

We thank our laboratory technician Stefanie Schnell, Luisa Listmann, and the student Moritz Aehle for their assistance during the experiments. We are grateful to Cynthia Medwed and the IOW-Leibniz Institute for Baltic Sea Research (Warnemünde) for resurrecting and providing the sediment core lineages used in this study. This research was supported by the Deutsche Forschungsgemeinschaft (DFG) grant (Project number – 450278268). ChatGPT (OpenAI, GPT-4) was used for language editing and grammar improvement, operated in a mode where user inputs were not used for model training, and all outputs were reviewed and validated by the authors.

Competing Interests

The authors declared no competing interests

Author Contributions

ES conceived the study. CM resurrected the lineages used for the study. ME and ES designed the experiments. ME and Molly Showers conducted the experiments. ME produced and analysed the data and produced the figures and wrote the first and final draft of the manuscript. ES contributed to coding and code troubleshooting. ES contributed with analysis input. ES contributed with manuscript revisions. The co-author gave final approval for publication. Funding was acquired by ES.

Data Availability

The data supporting the findings of this study are available in the Supporting Information. R codes and processed data sets used for statistical analysis and figure generation are openly available on GitHub. *Nodularia spumigena* cultures are maintained in the laboratory at the Institute of Marine Ecosystem and Fisheries Science.

Chapter Three: Summary and conclusions

Overview: what this dissertation set out to do, and what it found

This dissertation investigated how *Nodularia spumigena*, a bloom-forming diazotrophic cyanobacterium central to Baltic Sea biogeochemistry, has evolved in response to two centuries of environmental change, and how rapidly it can continue to evolve under sustained experimental warming. The overarching question: how, and how fast, does this organism evolve in response to warming demanded an approach that no single method could provide alone. By integrating resurrection ecology (Chapter 2.1), experimental evolution (Chapter 2.2), and global epigenomic profiling (Chapter 2.3), and by grounding all three in the same five lineages spanning pre-industrial (ca. 1824) to contemporary (ca. 1996) Baltic Sea sediments, this work provides a multi-timescale, multi-level answer.

The short answer to how fast is: remarkably fast. Within ~100 generations of experimental selection, the thermal optimum for growth (T_{opt}) shifted upward by 5–6 °C in the 1970s and 1996 lineages, a magnitude larger than most microalgal responses reported in the literature (Listmann et al., 2016; O'Donnell et al., 2018; Padfield et al., 2016), and achieved across a lineage that dates its ancestry to pre-industrial times and one that was isolated less than three decades ago. But how evolution occurs is the more nuanced and scientifically richer answer: not all traits evolve equally, not all lineages respond identically, and the capacity for evolutionary change is itself shaped by prior evolutionary history. These are the central contributions of this dissertation.

Timescales, studies and key contributions

The three studies of this dissertation address evolutionary responses to warming across three interlocking timescales. Table 3.1 provides an overview of the temporal scales, approaches, principal findings, and knowledge gaps addressed by each study.

Tab. 3.1. Overview of the three studies, their temporal scales, and principal findings.

Study	**Approach**	Timescale	Principal findings
Chapter 2.1: Resurrection ecology	TPC, CUE, allelopathy, organic C, genomics in 5 lineages (1824–1996)	~200 years (natural evolution)	Evolution inconsistent with "hotter is broader and better"; lower T_{opt} but higher bloom-season growth rates in contemporary lineages; reduced allelopathy; CUE broadly conserved; age-structured genomic divergence
Chapter 2.2: Experimental evolution	TPC, CUE, genomics; ~100 gen. at 22, 26, 30 °C	~100 gen. (~31 weeks, experimental)	All lineages reach similar post selection T_{opt}; magnitude of shift historically contingent; CUE evolution historically contingent (recent lineages only); no temperature-specific trade-offs at this timescale; genomic divergence dominated by sediment age
Chapter 2.3: Epigenomics	Global 5-mC methylation in ancestral and evolved populations	~200 years (natural) + ~100 generations (experimental)	Methylation historically structured; direction of evolutionary change opposite in pre-industrial vs. recent lineages; methylation change co-varies with T_{opt} shift and metabolic scaling (ln(c)), not with E_a

The direction of past evolution does not follow the "hotter is broader and better" prediction

Chapter 2.1 tested a straightforward prediction: that two centuries of warming and environmental change in the Baltic Sea would have left a signature consistent with the "hotter is broader and better" hypothesis, contemporary lineages with higher T_{opt}, broader thermal breadth, and higher peak growth rates than pre-industrial ones (Knies et al., 2009). The data inverted this prediction

systematically. The pre-industrial 1824 lineage had the highest T_{opt} (30.1 °C), the shallowest sub-optimal curve, and the lowest peak growth rates. The contemporary 1996 lineage had the lowest T_{opt} (24.2 °C), the steepest sub-optimal curve, and the highest peak growth rates.

The key to interpreting this pattern is not T_{opt} in isolation but the crossing of the curves near 30 °C. Below that threshold, contemporary lineages grow faster; above it, the pre-industrial lineage outperforms all others. Baltic Sea summer temperatures in the basins where these lineages were collected now routinely fall in the 18–26 °C range (Kniebusch et al., 2019). Contemporary lineages are therefore not "better adapted to warming" in a global sense, rather they are better matched to the temperatures they actually experience. This is adaptation to increased thermal variability, not to directional warming alone (Angilletta Jr., 2009; Schaum et al., 2022). The Baltic Sea over the past two centuries has not simply become warmer; it has become more variable, more stratified, and more eutrophied (Meier et al., 2022), and these compound environmental changes appear to have selected for a fundamentally different TPC shape: steeper sub-optimal slopes that deliver high growth rates across the prevailing summer temperature range, at the cost of high-temperature performance.

This interpretation is reinforced by the findings of Hinners et al. (2017), who studied dinoflagellates revived from ~100-year-old Baltic Sea sediments and found shifts consistent with adaptation to historical environmental change in that taxon. Our results extend the temporal window to 200 years and reveal that a bloom-forming cyanobacterium has undergone a qualitatively different evolutionary trajectory from co-occurring protists in the same sea, a reminder that even within the same environment, taxon-specific evolutionary responses can diverge substantially. The functional signals in the genomic data are consistent with this interpretation: photosystem II and hydrogenase genes dominated the genomic discriminant loadings of pre-industrial lineages, while ATP synthase subunits, stress-response genes, and recombinases dominated in contemporary lineages, reflecting a shift from optimisation of photosynthetic performance under stable conditions toward enhanced energy metabolism and genome maintenance under fluctuating stress.

The allelopathic results add an ecologically important third dimension to this picture. Pre-industrial lineages exerted substantially stronger inhibitory effects on co-occurring picophytoplankton (*Ostreococcus tauri*), particularly at 30 °C, while contemporary lineages showed reduced inhibition and, at 22 °C, modest facilitation in indirect co-culture. Both spike and ThinCert treatments produced nearly identical results, implicating soluble exudates rather than cell-contact effects. This temporal shift in allelopathic capacity likely reflects an evolutionary trade-off: as contemporary

lineages have reallocated metabolic resources toward growth and thermal performance, investment in secondary metabolite production has declined. A complementary shift toward broader organic carbon substrate use at elevated temperatures in contemporary lineages reinforces this picture of metabolic opportunism replacing competitive exclusion as the dominant ecological strategy. Together, these multi-trait patterns suggest that two centuries of Baltic Sea change have selected for lineages that are faster-growing, metabolically more flexible, and less ecologically dominant through chemical competition, a combination that may favour co-existence with other phytoplankton groups in modern blooms (Munkes et al., 2021) while simultaneously sustaining or increasing bloom biomass through intrinsically higher growth rates.

Evolutionary potential is conserved for thermal niche repositioning but historically contingent for metabolic efficiency

Chapter 2.2 asked whether the divergent ancestral strategies documented in Chapter 2.1 constrain or enable further evolutionary change. The central finding is a clear dissociation between two dimensions of evolutionary potential, and it is this dissociation, more than any individual result that constitutes the principal scientific contribution of this dissertation.

Thermal niche repositioning is ancestrally conserved. Under ~100 generations of experimental selection at 22, 26, and 30 °C, T_{opt} converged across all three sediment-age cohorts to values near 30 °C. The 1970s lineages shifted from 26.8 °C to 29.1–30.4 °C; the 1996 lineages shifted from 24.2 °C to 30.7–31.5 °C; the pre-industrial 1824 lineage, whose ancestral T_{opt} was already ~30 °C, showed minimal further change. This convergence directly supports Objective 2, Hypothesis 1 — the capacity for T_{opt} elevation under warming is broadly intact across two centuries of divergence. The molecular machinery underlying this capacity: membrane remodelling, enzyme thermal stability, photosystem regulation (Kontopoulos et al., 2020), appears to be conserved across lineages whose genomic profiles are otherwise substantially divergent (PERMANOVA on evolved SNP profiles: Age $R^2 = 0.263$, $p = 0.001$). For bloom-management and ecosystem modelling purposes, this finding implies that future Baltic Sea warming may elicit broadly similar adaptive thermal trajectories in *N. spumigena* regardless of the historical provenance of resident populations, a somewhat reassuring result for predictive models, though one that must be tempered by the limited number of lineages examined.

Carbon economy evolution is historically contingent. CUE evolved significantly under warming in the 1970s and 1996 lineages, particularly at 26 °C and 30 °C but showed no detectable evolutionary change in the pre-industrial 1824 lineage at any temperature. This asymmetry is interpretable in light of Chapter 2.1: the 1996 lineage had the lowest ancestral CUE (0.64 ± 0.06)

among the three age groups, providing more room for improvement, while the pre-industrial lineage with its broader, shallower TPC and higher T_{opt} may lack the standing genetic variation at metabolic loci relevant to CUE optimisation under the temperatures tested here. The capacity for CUE evolution thus appears to be a derived trait that has emerged over the past century of warming and metabolic remodelling in the modern Baltic Sea, and is not shared equally across the evolutionary time series. More recently derived lineages may therefore be better positioned to capitalise on future warming through improved metabolic efficiency, potentially reinforcing bloom formation under projected warming scenarios (Hense et al., 2013).

The absence of crossing reaction norms in the reciprocal transplant assay (Hypothesis 3 not supported) means that ~100 generations were insufficient to produce temperature-specific physiological specialisation. This is consistent with experimental evolution in other phytoplankton at comparable timescales (Listmann et al., 2016; Schaum et al., 2017) and does not undermine the evidence for adaptation: T_{opt} convergence is real and substantial. Rather, it indicates that the form of adaptation achieved here operated on overall performance level, a general upward shift rather than on the relative advantage at specific temperatures. Whether specialist trade-offs emerge at longer selection durations, or under fluctuating rather than constant temperature regimes, remains an important open question.

Epigenetic state is historically structured and mechanistically coherent with phenotypic evolution

Chapter 2.3 reveals that the phenotypic divergence documented in Studies 2.1 and 2.2 is accompanied by systematic differences in global DNA methylation that are themselves historically structured and evolutionarily responsive. The pre-industrial 1824 lineage entered the experiment with ~2.4-fold higher baseline 5-mC methylation (~6.6%) than the contemporary lineage (~3.5%), providing direct evidence that two centuries of Baltic Sea environmental change have left a persistent signature not only in phenotype and genotype but in the epigenome. This supports Objective 3, Hypothesis 1 and Hypothesis 2.

The direction of methylation change following ~100 generations of selection was opposite in the 1824 lineage (decreased across all temperatures) versus the 1970s and 1996 lineages (increased, particularly at elevated temperatures), producing convergence in global methylation state analogous to the convergence in T_{opt} observed in Chapter 2.2. This parallel convergence at both phenotypic and epigenomic levels under identical laboratory conditions reinforces the interpretation that constant-temperature experimental evolution homogenises trait dimensions that were divergent under the heterogeneous natural selection of the Baltic Sea environment.

The co-variation between methylation change and T_{opt} change ($R^2 = 0.695$, $p = 0.005$) and between methylation change and $\Delta\ln(c)$ ($R^2 = 0.759$, $p = 0.002$), Hypothesis 3 supported, is consistent with a model in which epigenetic remodelling modulates the regulatory landscape of genes involved in thermal niche positioning and baseline metabolic scaling, without directly affecting the fundamental thermodynamic sensitivity of enzyme kinetics (no significant relationship with ΔE_a). This pattern aligns with findings in *Desmodesmus armatus* (Herdean et al., 2025) and *Dunaliella salina* (Leung et al., 2022), where epigenetic variation was associated with phenotypic shifts in environmentally responsive traits rather than core metabolic biochemistry. The trade-off implied by the negative methylation: $\Delta\ln(c)$ relationship and epigenetic upregulation that enables T_{opt} repositioning at the cost of baseline metabolic output raises the possibility that epigenetic flexibility is a limited regulatory resource, and that its depletion under sustained or multi-stressor warming could constrain further adaptation.

Whether the methylation changes documented here are heritable across generations, a prerequisite for epigenetic contributions to long-term adaptation rather than reversible acclimation, cannot be resolved from global assay data and remains the critical unresolved question for Chapter 2.3. Combining the MethylFlash global quantification with bisulfite sequencing on the same samples would be the natural next step, and is achievable within the existing experimental framework.

How this dissertation addresses the knowledge gaps identified in Chapter One

Section 1.8 of this dissertation identified five knowledge gaps that limit our ability to predict *N. spumigena* responses to warming. The three studies collectively address all five, to varying degrees of resolution.

Gap 1.8.1 – Absence of historical baselines for cyanobacterial thermal adaptation. Chapter 2.1 directly fills this gap for *N. spumigena* by providing the first multi-century phenotypic baseline from the Baltic Sea, extending the temporal window of Medwed et al. (2024), who compared lineages from 1987 and 2020, back to 1824. The pre-industrial lineage establishes what *N. spumigena* thermal performance looked like before industrialisation, and demonstrates that contemporary performance is the product of evolutionary change, not simply inherent species traits. This gap is substantially addressed.

Gap 1.8.2 – Insufficient quantification of lineage-level thermal variation. Chapter 2.1 characterised five lineages across three sediment-age cohorts with replicated TPCs, CUE assays, and biotic interaction experiments, revealing that intraspecific variation is both large (5.8 °C difference in T_{opt} between 1824 and 1996 lineages) and ecologically meaningful (crossing growth

rates near 30 °C). The three 1970s lineages from two different Baltic Sea basins further demonstrate that within-cohort variation is substantial. This gap is partially addressed — a larger number of lineages per sediment layer would be needed to fully characterise intraspecific variation.

Gap 1.8.3 – Unknown evolutionary potential under sustained warming. Chapter 2.2 directly addresses this gap, demonstrating that *N. spumigena* can shift T_{opt} by 5–6 °C within ~100 generations, that this capacity is broadly conserved across two centuries of divergence, and that CUE evolution under warming is possible but historically contingent. The gap is substantially addressed for thermal and metabolic traits, though the absence of trade-offs at ~100 generations leaves open whether evolutionary constraints emerge at longer selection durations.

Gap 1.8.4 – Limited mechanistic understanding linking traits to molecular change. Chapter 2.3 provides the first empirical evidence in this species that global DNA methylation is historically structured and co-varies with evolutionary shifts in thermal performance and metabolic capacity. The mechanistic link remains correlational and locus-specific methylation data are required to identify the specific regulatory targets. However, the direction, magnitude, and phenotypic coherence of the epigenetic patterns documented here substantially advance understanding beyond a purely phenotypic or genomic picture. This gap is partially addressed.

Gap 1.8.5 – Missing integration of ecological and evolutionary processes. The combination of resurrection ecology and experimental evolution across the same lineages, incorporating growth, carbon metabolism, biotic interactions, genomics, and epigenomics, provides the most direct integration of ecological and evolutionary perspectives attempted for *N. spumigena* to date. The allelopathy results in particular link evolutionary change in *N. spumigena* to consequences for co-occurring phytoplankton, connecting the evolutionary trajectory of the bloom-former to community-level dynamics. The gap is addressed at the conceptual level; quantitative integration with field bloom observations or ecosystem models would be the natural extension.

Synthesis: a multi-timescale framework for *N. spumigena* responses to warming

N. spumigena responses to warming can be understood across three interlocking timescales that together describe a coherent evolutionary trajectory.

On the multi-century scale (Chapter 2.1), natural selection in the modern Baltic Sea has produced contemporary lineages that differ from their pre-industrial counterparts in virtually every functional dimension measured: lower T_{opt} but higher growth rates at prevailing summer temperatures; steeper sub-optimal TPC slopes; marginally lower ancestral CUE but greater evolutionary CUE headroom; broader organic carbon substrate use at elevated temperatures;

reduced allelopathic competitiveness. This is not adaptation to a simply warmer world but rather an adaptation to a more variable, more eutrophied, and ecologically more complex world, in which high bloom-season growth performance and metabolic flexibility appear to be at a premium.

On the experimental timescale of ~100 generations (Chapter 2.2), *N. spumigena* demonstrates that it can evolve rapidly in response to warming. All lineages converge on a similar post-selection T_{opt} regardless of their two-century divergence history, though the magnitude of shift required differs substantially across cohorts. But the capacity for CUE evolution optimising the ratio of photosynthetic carbon retained versus lost to respiration is restricted to lineages with more recent evolutionary histories, suggesting that the metabolic evolutionary potential of this organism is not fixed but has itself evolved over the past century. This asymmetry, conserved potential for thermal niche repositioning, contingent potential for metabolic efficiency evolution, is the most important synthetic finding of this dissertation.

On the molecular scale (Chapter 2.3), epigenetic state mirrors both the historical divergence and the experimental convergence documented at the phenotypic level. Pre-industrial lineages carry high baseline methylation that declines under experimental evolution; contemporary lineages carry lower baseline methylation that increases under warming selection. These opposite trajectories converge on an intermediate epigenetic state, and their co-variation with T_{opt} and ln(c) change suggests that DNA methylation represents a dynamically regulated molecular layer that accompanies, and may modulate thermal adaptation, operating principally on thermal niche positioning and metabolic scaling rather than on the fundamental kinetics of enzyme thermal sensitivity.

Taken together, these three timescales tell a story in which *N. spumigena* is neither evolutionarily static nor infinitely malleable. It has already evolved substantially in response to Baltic Sea change; it retains the capacity to evolve further and rapidly under continued warming; but the specific traits through which that evolution is expressed depend on the prior evolutionary history of the lineage, and the epigenetic architecture may set the regulatory limits within which rapid phenotypic adjustment is possible. Whether these conclusions generalise to other cyanobacteria populations across the Baltic Sea, or to bloom-forming cyanobacteria in other warming aquatic systems, remains to be tested but the multi-method, multi-timescale framework demonstrated here provides a template for such investigations.

Limitations and caveats

Several limitations apply across all three studies and must be considered collectively. The most fundamental is the small number of lineages (n = 5 total: one pre-industrial, three historical, one contemporary) from two Baltic Sea locations. This severely constrains statistical power for detecting age-structured effects and means that lineage-specific idiosyncrasies - the 1996 lineage is represented by a single individual, as is the 1824 lineage, cannot be fully disentangled from sediment-age cohort patterns. All conclusions about temporal evolutionary trends should be interpreted as directional signals from a small temporal sample rather than as species-level inferences.

Location and sediment depth are partially confounded with age in the current design (EGB Deep = 1824; EGB and GOF Mid = 1970s; GOF Shallow = 1996), meaning that geographic and environmental differences between sampling sites cannot be fully excluded as alternative explanations for observed phenotypic divergence. Co-varying changes in salinity, nutrient loading, light regime, and biotic community composition across the past two centuries in the Baltic Sea mean that the trait shifts documented in Chapter 2.1 cannot be attributed exclusively to temperature-driven selection, even under common-garden conditions (Hinners et al., 2017).

The experimental evolution design used constant rather than fluctuating temperature, excluded competition, predation, and nutrient fluctuations, and was conducted at a single salinity. Natural Baltic Sea populations experience all of these simultaneously, and the adaptive responses documented here may be modified, attenuated, or reversed under greater ecological complexity (Collins, 2011; Litchman et al., 2012). The ~100-generation timescale, while sufficient to detect T_{opt} convergence, may be too short to reveal trade-offs or specialist divergence that could emerge over longer selection durations. The missing 1996 * 26 °C genomic data point introduces a structural asymmetry in the evolved genomic comparisons.

The global methylation assay in Chapter 2.3 provides no information on which loci are differentially methylated, cannot distinguish heritable from reversible methylation changes, and is based on ancestral samples measured only at 22 °C. The nine-point regression linking methylation change to TPC parameter change is illustrative, not inferential, and additional lineages would be required to test the relationship formally.

Conclusions and future directions

This dissertation provides the most temporally comprehensive assessment to date of thermal evolutionary responses in *Nodularia spumigena*, spanning pre-industrial baselines to short-term

experimental evolution and integrating phenotypic, genomic, and epigenomic perspectives across the same five lineages. Four conclusions stand out.

First, past evolution in *N. spumigena* has not followed the "hotter is broader and better" trajectory predicted under directional warming, but instead reflects multi-trait adaptation to increased thermal variability, with lower T_{opt}, steeper sub-optimal TPC slopes, higher bloom-season growth rates, and reduced allelopathic capacity relative to pre-industrial lineages.

Second, all lineages can achieve similar post-selection T_{opt} values under experimental warming, though the magnitude of shift required reflects their divergent evolutionary histories, demonstrating that *N. spumigena* retains substantial evolutionary potential for thermal adaptation regardless of historical provenance.

Third, the capacity for metabolic efficiency (CUE) evolution under warming is historically contingent, restricted to lineages with more recent evolutionary histories, suggesting that the evolutionary potential itself has evolved, with contemporary lineages better positioned to capitalise on future warming through improved carbon economy.

Fourth, global DNA methylation is historically structured and epigenomically responsive to thermal selection in ways that co-vary coherently with phenotypic evolution, establishing epigenetic state as a biologically meaningful layer of the organism's thermal response system.

Looking forward, expanding the number of resurrected lineages per sediment layer, ideally spanning the full sediment archive of 27 lineages isolated by Cynthia Medwed, would be the single most impactful improvement. Incorporating realistic thermal fluctuations and multi-stressor designs (warming * eutrophication; warming * salinity change) into experimental evolution would test whether the adaptive potential demonstrated here is maintained under ecologically realistic conditions. Applying locus-specific epigenetic profiling (bisulfite sequencing) to identify the regulatory targets of the methylation changes documented in Chapter 2.3 would provide the mechanistic resolution that the MethylFlash global assay cannot offer. And connecting the trait-level and genomic findings presented here to field-based observations of *N. spumigena* bloom phenology, community composition, and toxin production in the warming Baltic Sea would ultimately determine whether the adaptive capacity demonstrated in the laboratory is realised, and whether it matters in the ecology of a changing sea.

Chapter Four: Supplementary information

Supplementary Information – Chapter 2.1

Table S1. Fluorescence-to-cell-count calibration for the five *Nodularia spumigena* lineages used in this study. Chlorophyll a fluorescence (Chla RFU; excitation 432 nm, emission 676 nm) was measured alongside direct cell counts obtained by FlowCam imaging across all assay temperatures (15–36°C) and three biological replicates per lineage per temperature. Slope and R^2 are from linear regression of cell count (Cells mL^{-1}) on Chla RFU across all observations for each lineage.

Lineage ID	Date	Basin	Depth	Age group	n	Chla RFU range	Cells mL^{-1} range	Slope	R^2
6-MUC-46-2.1	1824	EGB	Deep	Pre-industrial	30	19,501 – 237,447	5,146 – 370,015	−0.12	0.005
6-MUC-17-2	1970	EGB	Mid	Historical (1970s)	30	1,964 – 1,108,946	10,003 – 126,385	−0.01	0.015
12-MUC-10-6	1970	GOF	Mid	Historical (1970s)	27	542 – 27,403	7,625 – 124,007	2.10	0.216
12-MUC-10-5	1970	GOF	Mid	Historical (1970s)	30	3,751 – 212,696	24,857 – 2,211,726	7.50	0.580
12-MUC-5-30	1996	GOF	Shallow	Contemporary	33	8,555 – 185,436	11,665 – 1,479,230	6.77	0.615

Note on R^2 values: Low R^2 for EGB lineages (6-MUC-46-2.1 and 6-MUC-17-2) reflects high within-strain variability in chlorophyll content per cell across the broad temperature range tested (15–36°C), not measurement error *per se*. Chlorophyll-to-cell ratios are temperature-dependent and vary with growth state, meaning that a single linear conversion factor cannot capture fluorescence–abundance relationships across the full thermal gradient. Fluorescence was therefore used as a relative growth proxy within temperature treatments (i.e., to calculate growth rates from time-series fluorescence at a fixed temperature), rather than as an absolute cell-density estimator across temperatures. This approach is standard practice in phytoplankton thermal performance experiments.

38°C: Growth rate was zero for all lineages and replicates at 38°C. This temperature was included in Sharpe-Schoolfield model fitting to constrain the upper thermal limit (CT_{max}) and was not included in the calibration dataset above.

Abbreviations: EGB = Eastern Gotland Basin; GOF = Gulf of Finland; RFU = relative fluorescence units; n = number of paired fluorescence–cell count observations.

Table S2. Biological replication structure for the thermal performance curve (TPC) experiment in Chapter 2.1. Values indicate the number of independent biological replicates per lineage per assay temperature. Each replicate was initiated from an independent sub-culture of the lineage stock and pre-acclimated for ≥8 days (≥3 generations) prior to measurement.

Lineage ID	Date	Basin	Age group	15	18	20	22	24	26	28	30	32	34	36	38	Total
6-MUC-46-2.1	1824	EGB	Pre-industrial (1824)	3	3	3	3	3	3	3	3	3	3	3	3	36
6-MUC-17-2	1970	EGB	Historical (1970s)	3	3	3	3	3	3	3	3	3	3	3	3	36
12-MUC-10-6	1970	GOF	Historical (1970s)	3	3	3	3	3	3	3	3	3	3	3	3	36
12-MUC-10-5	1970	GOF	Historical (1970s)	3	3	3	3	3	3	3	3	3	3	3	3	36
12-MUC-5-30	1996	GOF	Contemporary (1996)	3	3	3	3	3	3	3	3	3	3	3	3	36

Age-group totals per temperature: Pre-industrial (1824): n = 3 (1 lineage × 3 replicates); Historical (1970s): n = 9 (3 lineages × 3 replicates); Contemporary (1996): n = 3 (1 lineage × 3 replicates).

38°C: Growth rate was zero for all lineages and replicates. This temperature point was retained in Sharpe-Schoolfield model fitting to constrain CT_{max}; growth rates were set to 0 d^{-1} prior to model fitting.

Abbreviations: EGB = Eastern Gotland Basin; GOF = Gulf of Finland.

Table S3. Model selection and pairwise comparisons for Sharpe-Schoolfield thermal performance curve parameters across sediment age cohorts. Part A: likelihood ratio tests (LRT) comparing models with sediment age as a fixed effect against intercept-only models (*nlme*, method = ML; random intercept: 1 | Biorep). Part B: pairwise contrasts from estimated marginal means (emmeans; Tukey adjustment). Part C: estimated marginal means per sediment age cohort (method = REML). Analyses conducted in R (*nlme*, *emmeans* packages).

Part A. Likelihood ratio tests (sediment age as fixed effect)

Parameter	χ^2	df	p-value	Post-hoc comparison (Tukey-adjusted)
T_{opt} (°C)	5.42	2	0.066	1824 vs 1996: ΔT_{opt} = 5.8°C, p = 0.046; other contrasts n.s.
E_a (eV)	7.14	2	0.028	1996 > 1824 (p = 0.045); 1996 > 1970s (p = 0.034); 1824 vs 1970s: n.s. (p = 0.888)
E_h (eV)	2.58	2	0.275	n.s.

Part B. Pairwise contrasts (Tukey-adjusted p-values)

Parameter	Contrast	Estimate	SE	df	t-ratio	p (Tukey)
T_{opt} (°C)	1824 − 1970s	3.25	2.10	10	1.551	0.310
	1824 − 1996	5.85	2.56	10	2.279	0.106
	1970s − 1996	2.60	2.10	10	1.240	0.458
E_a (eV)	1824 − 1970s	-0.055	0.118	10	-0.467	0.888
	1824 − 1996	-0.407	0.145	10	-2.807	0.045
	1970s − 1996	-0.352	0.118	10	-2.970	0.034

Part C. Estimated marginal means per sediment age cohort

Parameter	Sediment age	Emmean	SE	Lower 95% CI	Upper 95% CI	df
T_{opt} (°C)	1824	30.1	1.81	22.3	37.9	2
	1970s	26.8	1.05	22.3	31.3	2
	1996	24.2	1.81	16.4	32.0	2
E_a (eV)	1824	0.254	0.102	-0.187	0.695	2
	1970s	0.310	0.059	0.055	0.564	2
	1996	0.661	0.102	0.220	1.102	2

Abbreviations: χ^2 = likelihood ratio test statistic; df = degrees of freedom; SE = standard error; CI = confidence interval; n.s. = not significant. Containment method used for denominator degrees of freedom. T_{opt} (°C) and E_a (eV) are the parameters with significant age effects. Eh (eV) did not differ significantly across sediment ages ($p = 0.275$) and is not included in pairwise tests.

Table S4. Model selection and fixed-effect estimates for the linear mixed-effects model of *Ostreococcus tauri* fold-change growth rate in response to Nodularia spumigena exposure. Response variable: fold-change in *O. tauri* growth rate relative to monoculture controls (fold-change = 1: no effect; < 1: inhibition; > 1: facilitation). Models compared by AICc (*MuMIn* dredge function). The best-supported model (ΔAICc = 0, weight = 0.580) included sediment age (StrainAge), temperature, and their interaction as fixed effects, with biological replicate as a random intercept. Treatment (Spike vs ThinCert) was retained in the final fitted model (Part C) for design completeness despite non-significance ($p = 0.289$). All models included random intercept: ~1 | Biorep. Selection used ML; final estimates used REML (*nlme package, R*).

Part A. Model selection (top models, ΔAICc < 10; all models included random intercept ~1|Biorep)

Rank	Fixed effects	df	logLik	AICc	ΔAICc	Weight
1	StrainAge + Temp + StrainAge * Temp	11	45.1	-63.8	0.00	0.580
2	StrainAge + Treatment + Temp + StrainAge * Temp	12	45.8	-62.2	1.58	0.264
3	StrainAge + Treatment + Temp + StrainAge * Temp + StrainAge:Treatment	14	48.1	-60.9	2.91	0.136
4	StrainAge + Treatment + Temp + StrainAge * Temp + Treatment:Temp	14	45.9	-56.4	7.40	0.014
5	StrainAge + Treatment + Temp + StrainAge * Temp + StrainAge:Treatment + Treatment:Temp	16	48.3	-54.6	9.16	0.006

Part B. Type I ANOVA - selected model (StrainAge + Treatment + Temp + StrainAge * Temp)

Term	numDF	denDF	F-value	p-value
(Intercept)	1	59	2879	< 0.001
StrainAge	2	59	14	< 0.001
Treatment	1	59	1	0.289
Temperature	2	59	16	< 0.001
StrainAge * Temp	4	59	11	< 0.001

Part C. Fixed-effect estimates from selected model (REML; reference: 1824, Spike treatment, 22°C)

Part C. Fixed-effect estimates from selected model (REML; reference: 1824, Spike treatment, 22°C)

Term	Estimate	CI lower	CI upper	SE	df	t-value	p-value
Intercept (1824, Spike, 22°C)	0.945	0.842	1.048	0.052	59	18.307	< 0.001
StrainAge: 1970s	0.031	-0.107	0.169	0.069	59	0.454	0.652
StrainAge: 1996	0.034	-0.104	0.172	0.069	59	0.490	0.626
Treatment: ThinCert	0.035	-0.030	0.100	0.033	59	1.070	0.289
Temperature: 26°C	0.020	-0.118	0.158	0.069	59	0.290	0.773
Temperature: 30°C	-0.505	-0.643	-0.367	0.069	59	-7.333	< 0.001
StrainAge 1970s * Temp 26°C	-0.025	-0.220	0.170	0.097	59	-0.257	0.798
StrainAge 1996 * Temp 26°C	-0.029	-0.224	0.166	0.097	59	-0.295	0.769
StrainAge 1970s * Temp 30°C	0.426	0.231	0.621	0.097	59	4.377	< 0.001
StrainAge 1996 * Temp 30°C	0.509	0.314	0.704	0.097	59	5.224	< 0.001

Significant effects (bold p-values): Temperature at 30°C reduced *O. tauri* growth across all sediment ages relative to 22°C. The StrainAge * Temp interaction revealed that at 30°C, contemporary lineages (1970s and 1996) showed significantly less inhibition than pre-industrial (1824) lineages. Treatment type (Spike vs indirect co-culture in ThinCert inserts) did not significantly affect *O. tauri* growth ($F_{1,59} = 1$, $p = 0.289$).

Model selection note: The best model by AICc (rank 1) excluded Treatment; the second-best model (ΔAICc = 1.58) included Treatment but received only 26% of model weight. Treatment was retained in the final model (Part C) because it was an explicit design factor. Conclusions are unchanged regardless of Treatment inclusion.

Abbreviations: AICc = Akaike Information Criterion corrected for small sample size; CI = 95% confidence interval; df = degrees of freedom; numDF/denDF = numerator/denominator degrees of freedom; SE = standard error; n = 4 biological replicates per lineage per treatment per temperature.

Supplementary Information – Chapter 2.2

Figure S1

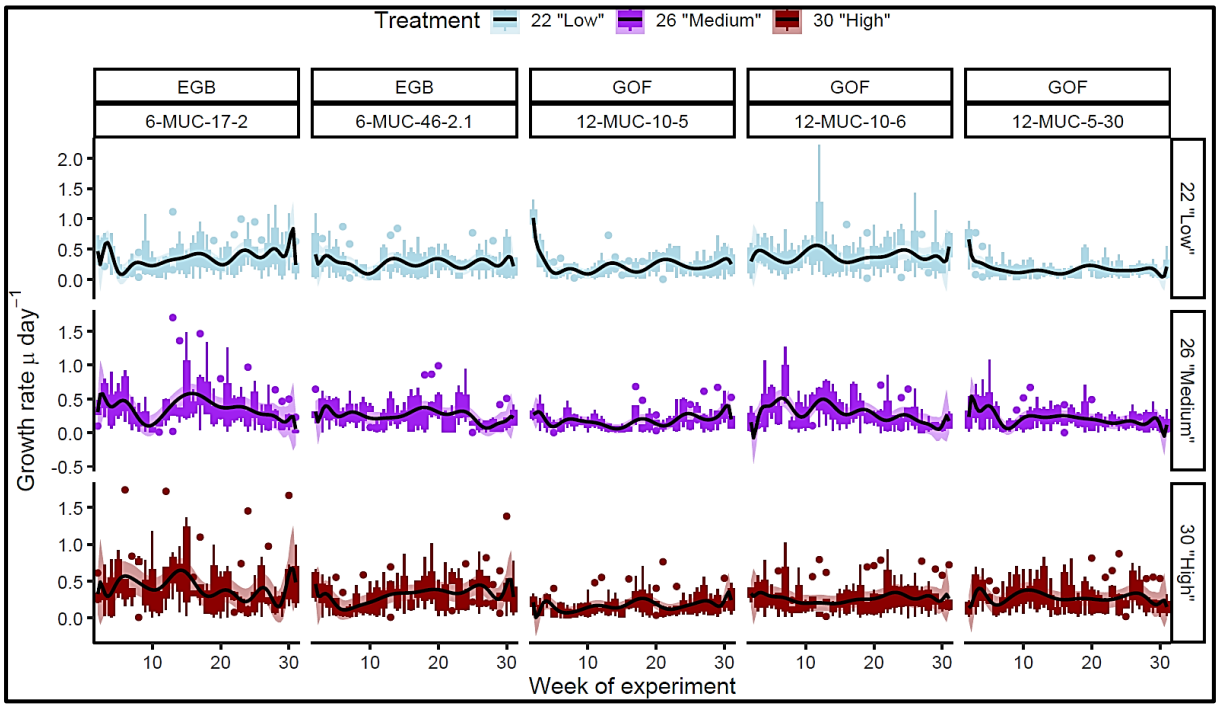

Fig. S1. Growth rate trajectories of *Nodularia spumigena* lineages across 31 weeks of experimental evolution under three thermal selection treatments. Boxplots show the distribution of growth rates (μ, day^{-1}) measured weekly from chlorophyll *a* fluorescence (excitation 432 nm, emission 676 nm) across six biological replicates per lineage per treatment. Panels are faceted by selection temperature (rows: 22°C "Low", light blue; 26°C "Medium", purple; 30°C "High", dark red) and by sampling location and strain identity (columns: EGB = Eastern Gotland Basin; GOF = Gulf of Finland). Black lines show polynomial smooth fits (degree 15) to characterise overall trajectory trends. Individual data points (outliers) are shown as filled circles. x-axis tick marks shown at intervals of 10 weeks.

Table S5. Model selection and fixed-effect estimates for linear mixed-effects models of thermal performance curve (TPC) parameters in Chapter 2.2 experimental evolution. Sharpe-Schoolfield parameters (E_a, T_{opt}, $\mu(T_{opt})$) were fitted per biological replicate using *nlsLoop* (R). Mixed-effects models included sediment age (Age: 1824, 1970s, 1996) and selection temperature (Sel_T: Anc, 22, 26, 30°C) with unique biological lineages (Age * Biorep) as random intercepts (*nlme*). Models fitted by ML for comparison (Part A), refitted by REML for inference (Parts B-C). Reference category: 1824, Ancestral (Anc). Interaction term retained for E_a and T_{opt} (LRT $p < 0.001$); additive model selected for $\mu(T_{opt})$ (LRT $p = 0.18$). Significant p-values in bold.

Part A. Likelihood ratio test (LRT): interaction vs additive model (ML estimation)

Trait	Model	df	AIC	BIC	logLik	LRT statistic	p-value	Selected
E_a (eV)	Age * Sel_T (interaction)	14	-43.1	-13.1	35.5			
	Age + Sel_T (additive)	8	-30.1	-13.0	23.1	25.0	< 0.001	Interaction
T_{opt} (°C)	Age * Sel_T (interaction)	14	292	322	-132			
	Age + Sel_T (additive)	8	305	323	-145	25.7	< 0.001	Interaction
$\mu(T_{opt})$ (day^{-1})	Age * Sel_T (interaction)	14	-59.9	-29.9	44.0			
	Age + Sel_T (additive)	8	-63.0	-45.9	39.5	8.91	0.179	Additive

Part B. Type I ANOVA of final models (REML estimation)

Trait	Term	numDF	denDF	F-value	p-value
E_a (eV)	(Intercept)	1	36	182.2	< 0.001
	Age	2	15	1.4	0.284
	Selection temp	3	36	3.4	0.027
	Age * Sel_T	6	36	4.6	0.001
T_{opt} (°C)	(Intercept)	1	36	8098	< 0.001
	Age	2	15	1.0	0.339
	Selection temp	3	36	12.0	< 0.001
	Age * Sel_T	6	36	5.0	0.001

Trait	Term	numDF	denDF	F-value	p-value
μ(Topt) (day⁻¹)	(Intercept)	1	42	1796	< 0.001
	Age	2	15	14.0	< 0.001
	Selection temp	3	42	5.0	0.004

Part C. Fixed-effect coefficient estimates from final models (REML; 95% CI)

Trait	Term	Estimate	CI lower	CI upper	SE	df	t-value	p-value
Ea (eV)	Intercept (ref: 1824, Anc)	0.223	0.044	0.403	0.088	36	2.531	0.016
	Age: 1970s	0.085	-0.181	0.351	0.125	15	0.683	0.505
	Age: 1996	0.550	0.283	0.816	0.125	15	4.401	< 0.001
	Sel_T: 22°C	0.174	-0.038	0.386	0.104	36	1.664	0.105
	Sel_T: 26°C	0.028	-0.184	0.240	0.104	36	0.269	0.789
	Sel_T: 30°C	0.006	-0.206	0.217	0.104	36	0.054	0.957
	Age 1970s * Sel_T 22°C	-0.308	-0.608	-0.009	0.148	36	-2.088	0.044
	Age 1996 * Sel_T 22°C	-0.654	-0.953	-0.354	0.148	36	-4.426	< 0.001
	Age 1970s * Sel_T 26°C	-0.019	-0.319	0.280	0.148	36	-0.130	0.897
	Age 1996 * Sel_T 26°C	-0.507	-0.807	-0.208	0.148	36	-3.436	0.002
	Age 1970s * Sel_T 30°C	-0.055	-0.355	0.245	0.148	36	-0.373	0.712
	Age 1996 * Sel_T 30°C	-0.537	-0.836	-0.237	0.148	36	-3.635	0.001
Topt (°C)	Intercept (ref: 1824, Anc)	30.68	28.13	33.23	1.260	36	24.382	< 0.001
	Age: 1970s	-6.198	-9.991	-2.400	1.780	15	-3.483	0.003

Trait	Term	Estimate	CI lower	CI upper	SE	df	t-value	p-value
	Age: 1996	-6.786	-10.579	-2.993	1.780	15	-3.813	0.002
	Sel_T: 22°C	-1.890	-4.846	1.066	1.460	36	-1.297	0.203
	Sel_T: 26°C	-0.839	-3.796	2.118	1.460	36	-0.576	0.568
	Sel_T: 30°C	1.812	-1.144	4.768	1.460	36	1.243	0.222
	Age 1970s * Sel_T 22°C	7.928	3.747	12.109	2.060	36	3.845	< 0.001
	Age 1996 * Sel_T 22°C	9.576	5.395	13.757	2.060	36	4.645	< 0.001
	Age 1970s * Sel_T 26°C	5.435	1.254	9.616	2.060	36	2.636	0.012
	Age 1996 * Sel_T 26°C	8.643	4.462	12.824	2.060	36	4.193	< 0.001
	Age 1970s * Sel_T 30°C	4.294	0.113	8.475	2.060	36	2.083	0.044
	Age 1996 * Sel_T 30°C	5.111	0.930	9.292	2.060	36	2.479	0.018
μ(Topt) (day^{-1})	Intercept (ref: 1824)	0.650	0.547	0.754	0.051	42	12.660	< 0.001
	Age: 1970s	0.066	-0.023	0.156	0.042	15	1.580	0.135
	Age: 1996	0.216	0.127	0.306	0.042	15	5.160	< 0.001
	Sel_T: 22°C	-0.065	-0.177	0.047	0.056	42	-1.180	0.246
	Sel_T: 26°C	0.079	-0.033	0.191	0.056	42	1.420	0.162
	Sel_T: 30°C	-0.080	-0.192	0.032	0.056	42	-1.450	0.155

Abbreviations: E_a = activation energy below T_{opt} (eV); T_{opt} = optimum temperature for growth (°C); $\mu(T_{opt})$ = maximum growth rate at T_{opt} (day^{-1}); Sel_T = selection temperature; CI = 95% confidence interval; SE = standard error; df = degrees of freedom; LRT = likelihood ratio test; AIC = Akaike Information Criterion; BIC = Bayesian Information Criterion.

Sample sizes: E_a model n = 51 observations across 18 unique biological lineages; T_{opt} model n = 51; $\mu(T_{opt})$ model n = 57. Ancestral lineages included as Sel_T = "Anc" level to enable mixed-model comparison with evolved populations.

Table S6. PERMANOVA and linear mixed-effects model outputs for genomic burden metrics in Chapter 2.2 evolved *Nodularia spumigena* lineages. Part A: PERMANOVA on Bray-Curtis dissimilarities of genome-wide SNP presence-absence profiles (38 samples * 266,836 variable SNP positions; evolved populations only, n = 33 after QC; additive marginal tests, 999 permutations, *vegan::adonis2*). Part B: Additive linear mixed-effects models for four genomic burden metrics in evolved populations (n = 37; one replicate with zero novel mutations excluded). Response variables log- or logit-transformed as specified. Random intercept: ~1|Biorep_nested (Strain * Biorep). Reference category: Age = 1824, Selection temperature = 22°C. Interaction model not fitted owing to incomplete factorial structure (1996 * 26°C absent). Significant p-values in bold.

Part A. PERMANOVA – multivariate SNP composition (evolved populations, n = 33)

Term	Df	Sum Of Sqs	R^2	F	Pr(>F)
Age (sediment date)	2	2.44	0.263	6.01	0.001
Treatment (selection temp.)	2	0.80	0.086	1.97	0.063
Residual	28	5.70	0.613		
Total	32	9.30	1.000		

Part B. Fixed-effect estimates – genomic burden LME models (evolved populations, n = 37)

Response variable	Term	Estimate	CI lower	CI upper	SE	df	t-value	p-value
log(Total novel SNPs)	Intercept(ref: 1824, 22°C)	4.632	2.624	6.640	0.963	20	4.811	< 0.001
	Age: 1970s	1.956	-0.298	4.210	1.081	20	1.810	0.085
	Age: 1996	2.903	-0.343	6.150	1.556	20	1.866	0.077
	Sel_T: 26°C	1.917	-0.656	4.490	1.181	12	1.623	0.131

Response variable	Term	Estimate	CI lower	CI upper	SE	df	t-value	p-value
	Sel_T: 30°C	-0.294	-2.419	1.830	0.975	12	-0.301	0.768
log(Novel missense SNPs + 1)	Intercept (ref: 1824, 22°C)	3.550	1.616	5.484	0.927	20	3.828	0.001
	Age: 1970s	1.883	-0.278	4.044	1.036	20	1.818	0.084
	Age: 1996	2.599	-0.531	5.729	1.501	20	1.732	0.099
	Sel_T: 26°C	1.872	-0.672	4.416	1.168	12	1.603	0.135
	Sel_T: 30°C	-0.446	-2.545	1.653	0.964	12	-0.462	0.652
logit(Proportion missense)	Intercept (ref: 1824, 22°C)	-0.726	-1.060	-0.392	0.160	20	-4.535	< 0.001
	Age: 1970s	-0.147	-0.537	0.243	0.187	20	-0.786	0.441
	Age: 1996	-0.379	-0.911	0.153	0.255	20	-1.485	0.153
	Sel_T: 26°C	-0.021	-0.318	0.276	0.136	12	-0.154	0.880
	Sel_T: 30°C	-0.175	-0.425	0.075	0.115	12	-1.528	0.152
log(dN/dS proxy)	Intercept (ref: 1824, 22°C)	0.240	-0.123	0.603	0.174	20	1.380	0.183
	Age: 1970s	-0.971	-1.399	-0.542	0.205	20	-4.727	< 0.001
	Age: 1996	-1.305	-1.883	-0.728	0.277	20	-4.717	< 0.001
	Sel_T: 26°C	0.057	-0.220	0.333	0.127	12	0.447	0.663
	Sel_T: 30°C	-0.137	-0.371	0.098	0.108	12	-1.268	0.229

Observed ranges: Total novel SNPs per replicate: 10 – 143,271; dN/dS proxy: 0.166 – 1.713. Novel SNPs = evolved-specific mutations absent from the matched ancestral genome. dN/dS proxy = (missense + 0.5) / (synonymous + 0.5).

Abbreviations: SNP = single nucleotide polymorphism; PERMANOVA = permutational multivariate ANOVA; R^2 = proportion of variance explained; CI = 95% confidence interval; SE = standard error; df = degrees of freedom; logit = log(p / (1 − p)).

PERMANOVA note: Five evolved samples present in the LME dataset (n = 38) could not be matched to pa_wide presence-absence rows and were excluded from PERMANOVA (n = 33), owing to Sample_ID formatting differences introduced during matrix construction. LME models use the full n = 37 dataset and are the primary inferential tool.

References

Angilletta, M. J. (2006). Estimating and comparing thermal performance curves. *Journal of Thermal Biology*, *31*(7), 541–545. https://doi.org/10.1016/j.jtherbio.2006.06.002

Angilletta, M. J. (2009). Thermal Sensitivity. In M. J. Angilletta Jr. (Ed.), *Thermal Adaptation* (pp. 35–87). Oxford University Press. https://doi.org/10.1093/acprof:oso/9780198570875.003.0003

Angilletta Jr., M. J. (Ed.). (2009). *Thermal Adaptation*. Oxford University Press. https://doi.org/10.1093/acprof:oso/9780198570875.001.1

Anton, B. P., & Roberts, R. J. (2021). Beyond Restriction Modification: Epigenomic Roles of DNA Methylation in Prokaryotes. *Annual Review of Microbiology*, *75*, 129–149. https://doi.org/10.1146/annurev-micro-040521-035040

Baker, K. G., Robinson, C. M., Radford, D. T., McInnes, A. S., Evenhuis, C., & Doblin, M. A. (2016). Thermal Performance Curves of Functional Traits Aid Understanding of Thermally Induced Changes in Diatom-Mediated Biogeochemical Fluxes. *Frontiers in Marine Science*, *3*. https://doi.org/10.3389/fmars.2016.00044

Barton, S., Jenkins, J., Buckling, A [Angus], Schaum, E., Smirnoff, N [Nicholas], Raven, J. A., & Yvon-Durocher, G [Gabriel] (2020). Evolutionary temperature compensation of carbon fixation in marine phytoplankton. *Ecology Letters*, *23*(4), 722–733. https://doi.org/10.1111/ele.13469

Barton, S., Jenkins, J., Buckling, A [Angus], Schaum, E., Smirnoff, N [Nicholas], & Yvon-Durocher, G [Gabriel]. (2018). *Universal metabolic constraints on the thermal tolerance of marine phytoplankton*. https://doi.org/10.1101/358002

Barton, S., Padfield, D., Masterson, A., Buckling, A [Angus], Smirnoff, N [Nicholas], & Yvon-Durocher, G [Gabriel] (2023). Comparative experimental evolution reveals species-specific idiosyncrasies in marine phytoplankton adaptation to warming. *Global Change Biology*, *29*(18), 5261–5275. https://doi.org/10.1111/gcb.16827

Bernhardt, J. R., Sunday, J. M., Thompson, P. L., & O'Connor, M. I. (2018). Nonlinear averaging of thermal experience predicts population growth rates in a thermally variable environment. *Proceedings. Biological Sciences*, *285*(1886). https://doi.org/10.1098/rspb.2018.1076

Botero, C. A., Weissing, F. J., Wright, J., & Rubenstein, D. R. (2015). Evolutionary tipping points in the capacity to adapt to environmental change. *Proceedings of the National Academy of Sciences of the United States of America*, *112*(1), 184–189. https://doi.org/10.1073/pnas.1408589111

Brennan, R. S., deMayo, J. A., Finiguerra, M., Baumann, H., Dam, H. G., & Pespeni, M. H. (2025). Complementary genetic and epigenetic changes facilitate rapid adaptation to multiple global change stressors. *Proceedings of the National Academy of Sciences of the United States of America*, *122*(29), e2422782122. https://doi.org/10.1073/pnas.2422782122

Brown, J. H., Gillooly, J. F., Allen, A. P., van Savage, M., & West, G. B. (2004). TOWARD A METABOLIC THEORY OF ECOLOGY. *Ecology*, *85*(7), 1771–1789. https://doi.org/10.1890/03-9000

Buckley, L. B., & Kingsolver, J. G [Joel G.] (2021). Evolution of Thermal Sensitivity in Changing and Variable Climates. *Annual Review of Ecology, Evolution, and Systematics*, *52*(1), 563–586. https://doi.org/10.1146/annurev-ecolsys-011521-102856

Bullerjahn, G. S., & Post, A. F. (2014). Physiology and molecular biology of aquatic cyanobacteria. *Frontiers in Microbiology*, *5*, 359. https://doi.org/10.3389/fmicb.2014.00359

Burga, A., & Lehner, B. (2012). Beyond genotype to phenotype: Why the phenotype of an individual cannot always be predicted from their genome sequence and the environment that they experience. *The FEBS Journal*, *279*(20), 3765–3775. https://doi.org/10.1111/j.1742-4658.2012.08810.x

Carpenter, E. J., & Romans, K. (1991). Major role of the cyanobacterium trichodesmium in nutrient cycling in the north atlantic ocean. *Science (New York, N.Y.)*, *254*(5036), 1356–1358. https://doi.org/10.1126/science.254.5036.1356

Cegłowska, M., Toruńska-Sitarz, A., Kowalewska, G., & Mazur-Marzec, H. (2018). Specific Chemical and Genetic Markers Revealed a Thousands-Year Presence of Toxic Nodularia spumigena in the Baltic Sea. *Marine Drugs*, *16*(4). https://doi.org/10.3390/md16040116

Cheng, L., Xu, X., Wang, M., & Wang, D.-Z. (2024). Rapid Adaption but Genetic Diversity Loss of a Globally Distributed Diatom in the Warmer Ocean. *Global Change Biology*, *30*(12), e17602. https://doi.org/10.1111/gcb.17602

Collins, S. (2011). Competition limits adaptation and productivity in a photosynthetic alga at elevated CO2. *Proceedings. Biological Sciences*, *278*(1703), 247–255. https://doi.org/with

Collins, S., Rost, B., & Rynearson, T. A. (2014). Evolutionary potential of marine phytoplankton under ocean acidification. *Evolutionary Applications*, *7*(1), 140–155. https://doi.org/10.1111/eva.12120

Collins, S., & Schaum, E. (2021). Growth strategies of a model picoplankter depend on social milieu and pCO2. *Proceedings. Biological Sciences*, *288*(1955), 20211154. https://doi.org/10.1098/rspb.2021.1154

Del Giorgio, P. A., & Cole, J. J. (1998). BACTERIAL GROWTH EFFICIENCY IN NATURAL AQUATIC SYSTEMS. *Annual Review of Ecology and Systematics*, *29*(1), 503–541. https://doi.org/10.1146/ANNUREV.ECOLSYS.29.1.503

Doyle, J. J., & Doyle, J. L. (1987). A rapid DNA isolation procedure for small quantities of fresh leaf tissue. *PHYTOCHEMICAL BULLETIN*. https://worldveg.tind.io/record/33886/

Draghi, J. A., & Whitlock, M. C. (2012). Phenotypic plasticity facilitates mutational variance, genetic variance, and evolvability along the major axis of environmental variation. *Evolution; International Journal of Organic Evolution*, *66*(9), 2891–2902. https://doi.org/10.1111/j.1558-5646.2012.01649.x

Elken, J., Lehmann, A [Andreas], & Myrberg, K. (2015). Recent Change—Marine Circulation and Stratification. In T. B. A. Team II (Ed.), *Regional Climate Studies. Second Assessment of Climate Change for the Baltic Sea Basin* (pp. 131–144). Springer International Publishing. https://doi.org/10.1007/978-3-319-16006-1_7

Ellegaard, M., & Ribeiro, S. (2018). The long-term persistence of phytoplankton resting stages in aquatic 'seed banks'. *Biological Reviews of the Cambridge Philosophical Society*, *93*(1), 166–183. https://doi.org/10.1111/brv.12338

Feistel, R., Nausch, G., & Wasmund, N. (2008). *State and Evolution of the Baltic Sea, 1952-2005: A Detailed 50-Year Survey of Meteorology and Climate, Physics, Chemistry, Biology, and Marine Environment*. John Wiley & Sons.

Fistarol, G. O., Legrand, C [C.], & Granéli, E. (2005). Allelopathic effect on a nutrient-limited phytoplankton species. *Aquatic Microbial Ecology*, *41*, 153–161. https://doi.org/10.3354/ame041153

García-Carreras, B., Sal, S., Padfield, D., Kontopoulos, D.-G., Bestion, E., Schaum, E., Yvon-Durocher, G [Gabriel], & Pawar, S [Samrāt] (2018). Role of carbon allocation efficiency in the temperature dependence of autotroph growth rates. *Proceedings of the National Academy of Sciences of the United States of America*, *115*(31), E7361-E7368. https://doi.org/10.1073/pnas.1800222115

Ghalambor, C. K., McKAY, J. K., Carroll, S. P., & Reznick, D. N. (2007). Adaptive versus non-adaptive phenotypic plasticity and the potential for contemporary adaptation in new environments. *Functional Ecology*, *21*(3), 394–407. https://doi.org/10.1111/j.1365-2435.2007.01283.x

Gienapp, P., Teplitsky, C., Alho, J. S., Mills, J. A., & Merilä, J. (2008). Climate change and evolution: Disentangling environmental and genetic responses. *Molecular Ecology*, *17*(1), 167–178. https://doi.org/10.1111/j.1365-294X.2007.03413.x

Gill, R. L., Collins, S., Argyle, P. A., Larsson, M. E., Fleck, R., & Doblin, M. A. (2022). Predictability of thermal fluctuations influences functional traits of a cosmopolitan marine diatom. *Proceedings. Biological Sciences*, *289*(1973), 20212581. https://doi.org/10.1098/rspb.2021.2581

Gomulkiewicz, R., & Holt, R. D. (1995). When DOES EVOLUTION BY NATURAL SELECTION PREVENT EXTINCTION? *Evolution; International Journal of Organic Evolution*, *49*(1), 201–207. https://doi.org/10.1111/j.1558-5646.1995.tb05971.x

Gross, J., Avrani, S., Katz, S., & Hershberg, R. (2020). *Culture volume influences the dynamics of adaptation under long-term stationary phase*. https://doi.org/10.1101/2020.08.13.249599

Hallegraeff, G. M., & Bolch, C. J. (1992). Transport of diatom and dinoflagellate resting spores in ships' ballast water: implications for plankton biogeography and aquaculture. *Journal of Plankton Research*, *14*(8), 1067–1084. https://doi.org/10.1093/PLANKT/14.8.1067

Hartig, F. (2016). *CRAN: Contributed Packages*. https://doi.org/10.32614/CRAN.package.DHARMa

Hense, I., Meier, H. E. M., & Sonntag, S. (2013). Projected climate change impact on Baltic Sea cyanobacteria. *Climatic Change*, *119*(2), 391–406. https://doi.org/10.1007/s10584-013-0702-y

Herdean, A., Bedoya, M., Kim, M., Poddar, N., Hoch, L., & Ralph, P. J. (2025). Phenotypic plasticity can be modulated by epigenetic means via DNA methylation in the microalgae Desmodesmus armatus. *Algal Research*, *90*, 104206. https://doi.org/10.1016/j.algal.2025.104206

Hinners, J., Kremp, A., & Hense, I. (2017). Evolution in temperature-dependent phytoplankton traits revealed from a sediment archive: Do reaction norms tell the whole story? *Proceedings. Biological Sciences*, *284*(1864). https://doi.org/10.1098/rspb.2017.1888

Hobbs, J. K., Jiao, W., Easter, A. D., Parker, E. J., Schipper, L. A., & Arcus, V. L. (2013). Change in heat capacity for enzyme catalysis determines temperature dependence of enzyme catalyzed rates. *ACS Chemical Biology*, *8*(11), 2388–2393. https://doi.org/10.1021/cb4005029

Hu, L., Xiao, P., Jiang, Y., Dong, M., Chen, Z., Li, H., Hu, Z., Lei, A., & Wang, J. (2018). Transgenerational Epigenetic Inheritance Under Environmental Stress by Genome-Wide DNA Methylation Profiling in Cyanobacterium. *Frontiers in Microbiology*, *9*, 1479. https://doi.org/10.3389/fmicb.2018.01479

Huey, R. B [R. B.], & Kingsolver, J. G [J. G.] (1989). Evolution of thermal sensitivity of ectotherm performance. *Trends in Ecology & Evolution*, *4*(5), 131–135. https://doi.org/10.1016/0169-5347(89)90211-5

Huey, R. B [Raymond B.], & Kingsolver, J. G [Joel G.] (1993). Evolution of Resistance to High Temperature in Ectotherms. *The American Naturalist*, *142*, S21-S46. https://doi.org/10.1086/285521

Kawecki, T. J., & Ebert, D. (2004). Conceptual issues in local adaptation. *Ecology Letters*, *7*(12), 1225–1241. https://doi.org/10.1111/J.1461-0248.2004.00684.X

Kerfoot, W. C., & Weider, L. J. (2004). Experimental paleoecology (resurrection ecology): Chasing Van Valen's Red Queen hypothesis. *Limnology and Oceanography*, *49*(4part2), 1300–1316. https://doi.org/10.4319/lo.2004.49.4_part_2.1300

Kingsolver, J. G [Joel G.] (2009). The well-temperatured biologist. (American Society of Naturalists Presidential Address). *The American Naturalist*, *174*(6), 755–768. https://doi.org/10.1086/648310

Kniebusch, M., Meier, H. M., Neumann, T., & Börgel, F. (2019). Temperature Variability of the Baltic Sea Since 1850 and Attribution to Atmospheric Forcing Variables. *Journal of Geophysical Research: Oceans*, *124*(6), 4168–4187. https://doi.org/10.1029/2018JC013948

Knies, J. L., Kingsolver, J. G [Joel G.], & Burch, C. L. (2009). Hotter is better and broader: Thermal sensitivity of fitness in a population of bacteriophages. *The American Naturalist*, *173*(4), 419–430. https://doi.org/10.1086/597224

Kontopoulos, D.-G., Smith, T. P., Barraclough, T. G., & Pawar, S [Samraat]. (2019). *Adaptive evolution shapes the present-day distribution of the thermal sensitivity of population growth rate.* https://doi.org/10.1101/712885

Kontopoulos, D.-G., Smith, T. P., Barraclough, T. G., & Pawar, S [Samraat] (2020). Adaptive evolution shapes the present-day distribution of the thermal sensitivity of population growth rate. *PLoS Biology*, *18*(10), e3000894. https://doi.org/10.1371/journal.pbio.3000894

Kremp, A., Hinners, J., Klais, R., Leppänen, A.-P., & Kallio, A. (2018). Patterns of vertical cyst distribution and survival in 100-year-old sediment archives of three spring dinoflagellate species from the Northern Baltic Sea. *European Journal of Phycology*, *53*(2), 135–145. https://doi.org/10.1080/09670262.2017.1386330

Kuznetsova, A., Brockhoff, P. B., & Christensen, R. H. B. (2017). lmerTest Package: Tests in Linear Mixed Effects Models. *Journal of Statistical Software*, *82*(13). https://doi.org/10.18637/JSS.V082.I13

Leão, P. N., Engene, N., Antunes, A., Gerwick, W. H., & Vasconcelos, V. (2012). The chemical ecology of cyanobacteria. *Natural Product Reports*, *29*(3), 372–391. https://doi.org/10.1039/c2np00075j

Lehmann, A [A.], Getzlaff, K., & Harlaß, J. (2011). Detailed assessment of climate variability in the Baltic Sea area for the period 1958 to 2009. *Climate Research*, *46*(2), 185–196. https://doi.org/10.3354/CR00876

Lehtimaki, J., Moisander, P., Sivonen, K [K.], & Kononen, K. (1997). Growth, nitrogen fixation, and nodularin production by two baltic sea cyanobacteria. *Applied and Environmental Microbiology*, *63*(5), 1647–1656. https://doi.org/10.1128/aem.63.5.1647-1656.1997

Lenth, R. V., & Piaskowski, J. (2017). *CRAN: Contributed Packages*. https://doi.org/10.32614/CRAN.package.emmeans

Leung, C., Grulois, D., & Chevin, L.-M. (2022). Plasticity across levels: Relating epigenomic, transcriptomic, and phenotypic responses to osmotic stress in a halotolerant microalga. *Molecular Ecology*, *31*(18), 4672–4687. https://doi.org/10.1111/mec.16542

Listmann, L., Kerl, F., Martens, N., & Schaum, E. (2021). Differences in Carbon Acquisition Could Explain Adaptive Responses in a Baltic Sea Pico-Phytoplankton. *Frontiers in Marine Science*, *8*, Article 740763. https://doi.org/10.3389/fmars.2021.740763

Listmann, L., LeRoch, M., Schlüter, L., Thomas, M. K [Mridul K.], & Reusch, T. B. H. (2016). Swift thermal reaction norm evolution in a key marine phytoplankton species. *Evolutionary Applications*, *9*(9), 1156–1164. https://doi.org/10.1111/eva.12362

Litchman, E [E.], Edwards, K. F., Klausmeier, C. A [C. A.], & Thomas, M. K [M. K.] (2012). Phytoplankton niches, traits and eco-evolutionary responses to global environmental change. *Marine Ecology Progress Series*, *470*, 235–248. https://doi.org/10.3354/MEPS09912

M. Kahru, U. Horstmann, & O. Rud (1994). Satellite Detection of Increased Cyanobacteria Blooms in the Baltic Sea: Natural Fluctuation or Ecosystem Change?, *23*(8), 469–472. https://doi.org/10.2307/4314262

MacKenzie, B. R., & Schiedek, D. (2007). Daily ocean monitoring since the 1860s shows record warming of northern European seas. *Global Change Biology*, *13*(7), 1335–1347. https://doi.org/10.1111/j.1365-2486.2007.01360.x

Mäkelä, J., Kandavalli, V., & Ribeiro, A. S. (2017). Rate-limiting steps in transcription dictate sensitivity to variability in cellular components. *Scientific Reports*, *7*(1), 10588. https://doi.org/10.1038/s41598-017-11257-2

Manzoni, S., Čapek, P., Porada, P., Thurner, M., Winterdahl, M., Beer, C., Brüchert, V., Frouz, J., Herrmann, A. M., Lindahl, B. D., Lyon, S. W., Šantrůčková, H., Vico, G., & Way, D.

(2018). Reviews and syntheses: Carbon use efficiency from organisms to ecosystems – definitions, theories, and empirical evidence. *Biogeosciences*, *15*(19), 5929–5949. https://doi.org/10.5194/BG-15-5929-2018

Martens, N., Ehlert, E., Putri, W., Sibbertsen, M., & Schaum, E. (2024). Organic compounds drive growth in phytoplankton taxa from different functional groups. *Proceedings. Biological Sciences*, *291*(2016), 20232713. https://doi.org/10.1098/rspb.2023.2713

Mazur-Marzec, H., Bertos-Fortis, M., Toruńska-Sitarz, A., Fidor, A., & Legrand, C [Catherine] (2016). Chemical and Genetic Diversity of Nodularia spumigena from the Baltic Sea. *Marine Drugs*, *14*(11). https://doi.org/10.3390/md14110209

McGregor, G. B., Stewart, I., Sendall, B. C., Sadler, R., Reardon, K., Carter, S., Wruck, D., & Wickramasinghe, W. (2012). First report of a toxic Nodularia spumigena (Nostocales/ Cyanobacteria) bloom in sub-tropical Australia. I. Phycological and public health investigations. *International Journal of Environmental Research and Public Health*, *9*(7), 2396–2411. https://doi.org/10.3390/ijerph9072396

McQUOID, M. R., Godhe, A., & NORDBERG, K. (2002). Viability of phytoplankton resting stages in the sediments of a coastal Swedish fjord. *European Journal of Phycology*, *37*(2), 191–201. https://doi.org/10.1017/S0967026202003670

Medwed, C., Karsten, U., Romahn, J., Kaiser, J., Dellwig, O., Arz, H., & Kremp, A. (2024). Archives of cyanobacterial traits: Insights from resurrected Nodularia spumigena from Baltic Sea sediments reveal a shift in temperature optima. *ISME Communications*, *4*(1), ycae140. https://doi.org/10.1093/ismeco/ycae140

Meier, H. E. M., Kniebusch, M., Dieterich, C., Gröger, M., Zorita, E., Elmgren, R., Myrberg, K., Ahola, M. P., Bartosova, A., Bonsdorff, E., Börgel, F., Capell, R., Carlén, I., Carlund, T., Carstensen, J., Christensen, O. B., Dierschke, V., Frauen, C., Frederiksen, M., . . . Zhang, W. (2022). Climate change in the Baltic Sea region: a summary. *Earth System Dynamics*, *13*(1), 457–593. https://doi.org/10.5194/esd-13-457-2022

Michaletz, S. T., & Garen, J. C. (2024). Hotter is not (always) better: Embracing unimodal scaling of biological rates with temperature. *Ecology Letters*, *27*(2), e14381. https://doi.org/10.1111/ele.14381

Monchamp, M.-E., Walser, J.-C., Pomati, F., & Spaak, P. (2016). Sedimentary DNA Reveals Cyanobacterial Community Diversity over 200 Years in Two Perialpine Lakes. *Applied and Environmental Microbiology*, *82*(21), 6472–6482. https://doi.org/10.1128/AEM.02174-16

Mugal, C. F., Wolf, J. B. W., & Kaj, I. (2014). Why time matters: Codon evolution and the temporal dynamics of dN/dS. *Molecular Biology and Evolution*, *31*(1), 212–231. https://doi.org/10.1093/molbev/mst192

Munkes, B., Löptien, U., & Dietze, H. (2021). Cyanobacteria blooms in the Baltic Sea: a review of models and facts. *Biogeosciences*, *18*(7), 2347–2378. https://doi.org/10.5194/bg-18-2347-2021

Nakagawa, S., & Schielzeth, H. (2013). A general and simple method for obtaining R2 from generalized linear mixed-effects models. *Methods in Ecology and Evolution*, *4*(2), 133–142. https://doi.org/10.1111/j.2041-210x.2012.00261.x

Nalley, J. O., O'Donnell, D. R., & Litchman, E [Elena] (2018). Temperature effects on growth rates and fatty acid content in freshwater algae and cyanobacteria. *Algal Research*, *35*, 500–507. https://doi.org/10.1016/j.algal.2018.09.018

Neumann, T., Eilola, K., Gustafsson, B., Müller-Karulis, B., Kuznetsov, I., Meier, H. E. M., & Savchuk, O. P. (2012). Extremes of temperature, oxygen and blooms in the Baltic sea in a changing climate. *Ambio*, *41*(6), 574–585. https://doi.org/10.1007/s13280-012-0321-2

O'Donnell, D. R., Hamman, C. R., Johnson, E. C., Kremer, C. T., Klausmeier, C. A [Christopher A.], & Litchman, E [Elena] (2018). Rapid thermal adaptation in a marine diatom reveals constraints and trade-offs. *Global Change Biology*, *24*(10), 4554–4565. https://doi.org/10.1111/gcb.14360

Oksanen, J., Simpson, G. L., Blanchet, F. G., Kindt, R., Legendre, P., Minchin, P. R., O'Hara, R. B., Solymos, P., Stevens, M. H. H., Szoecs, E., Wagner, H., Barbour, M., Bedward, M., Bolker, B., Borcard, D., Borman, T., Carvalho, G., Chirico, M., Caceres, M. de, . . . Weedon, J. (2001). *CRAN: Contributed Packages*. https://doi.org/10.32614/CRAN.package.vegan

Padfield, D., O'Sullivan, H., & Pawar, S [Samraat] (2021). rTPC and nls.multstart : A new pipeline to fit thermal performance curves in r. *Methods in Ecology and Evolution*, *12*(6), 1138–1143. https://doi.org/10.1111/2041-210X.13585

Padfield, D., Yvon-Durocher, G [Genevieve], Buckling, A [Angus], Jennings, S., & Yvon-Durocher, G [Gabriel] (2016). Rapid evolution of metabolic traits explains thermal adaptation in phytoplankton. *Ecology Letters*, *19*(2), 133–142. https://doi.org/10.1111/ele.12545

Petzoldt, T. (2016). *CRAN: Contributed Packages*. https://doi.org/10.32614/CRAN.package.growthrates

Pörtner, H. O., Bennett, A. F., Bozinovic, F., Clarke, A., Lardies, M. A., Lucassen, M., Pelster, B., Schiemer, F., & Stillman, J. H. (2006). Trade-offs in thermal adaptation: The need for a molecular to ecological integration. *Physiological and Biochemical Zoology : PBZ*, *79*(2), 295–313. https://doi.org/10.1086/499986

R Core Team. (2025, October 20). *R: The R Project for Statistical Computing*. https://www.r-project.org/

Raven, J. A., & Geider, R. J. (1988). Temperature and algal growth. *New Phytologist*, *110*(4), 441–461. https://doi.org/10.1111/j.1469-8137.1988.tb00282.x

Rescan, M., Leurs, N., Grulois, D., & Chevin, L.-M. (2022). Experimental evolution of environmental tolerance, acclimation, and physiological plasticity in a randomly fluctuating environment. *Evolution Letters*, *6*(6), 522–536. https://doi.org/10.1002/evl3.306

Rocha, E. P. C., Smith, J. M., Hurst, L. D., Holden, M. T. G., Cooper, J. E., Smith, N. H., & Feil, E. J. (2006). Comparisons of dN/dS are time dependent for closely related bacterial genomes. *Journal of Theoretical Biology*, *239*(2), 226–235. https://doi.org/10.1016/J.JTBI.2005.08.037

Rohart, F., Gautier, B., Singh, A., & Lê Cao, K.-A. (2017). Mixomics: An R package for 'omics feature selection and multiple data integration. *PLoS Computational Biology*, *13*(11), e1005752. https://doi.org/10.1371/journal.pcbi.1005752

Sanyal, A., Larsson, J., van Wirdum, F., Andrén, T., Moros, M., Lönn, M., & Andrén, E. (2022). Not dead yet: Diatom resting spores can survive in nature for several millennia. *American Journal of Botany*, *109*(1), 67–82. https://doi.org/10.1002/ajb2.1780

Savage, C., Leavitt, P. R., & Elmgren, R. (2010). Effects of land use, urbanization, and climate variability on coastal eutrophication in the Baltic Sea. *Limnology and Oceanography*, *55*(3), 1033–1046. https://doi.org/10.4319/lo.2010.55.3.1033

Schaum, E., Barton, S., Bestion, E., Buckling, A [Angus], Garcia-Carreras, B., Lopez, P., Lowe, C., Pawar, S [Samraat], Smirnoff, N [Nicholas], Trimmer, M., & Yvon-Durocher, G [Gabriel] (2017). Adaptation of phytoplankton to a decade of experimental warming linked to increased photosynthesis. *Nature Ecology & Evolution*, *1*(4), 94. https://doi.org/10.1038/s41559-017-0094

Schaum, E., Buckling, A [A.], Smirnoff, N [N.], Studholme, D. J., & Yvon-Durocher, G [G.] (2018). Environmental fluctuations accelerate molecular evolution of thermal tolerance in a marine diatom. *Nature Communications*, *9*(1), 1719. https://doi.org/10.1038/s41467-018-03906-5

Schaum, E., Buckling, A [A.], Smirnoff, N [N.], & Yvon-Durocher, G [G.] (2022). Evolution of thermal tolerance and phenotypic plasticity under rapid and slow temperature fluctuations. *Proceedings. Biological Sciences*, *289*(1980), 20220834. https://doi.org/10.1098/rspb.2022.0834

Schaum, E., & Collins, S. (2014). Plasticity predicts evolution in a marine alga. *Proceedings. Biological Sciences*, *281*(1793). https://doi.org/10.1098/rspb.2014.1486

Schaum, E., Ffrench-Constant, R., Lowe, C., Ólafsson, J. S., Padfield, D., & Yvon-Durocher, G [Gabriel] (2018). Temperature-driven selection on metabolic traits increases the strength of an algal-grazer interaction in naturally warmed streams. *Global Change Biology*, *24*(4), 1793–1803. https://doi.org/10.1111/gcb.14033

Schaum, E., Rost, B., & Collins, S. (2016). Environmental stability affects phenotypic evolution in a globally distributed marine picoplankton. *The ISME Journal*, *10*(1), 75–84. https://doi.org/10.1038/ismej.2015.102

Schlüter, L., Lohbeck, K. T., Gröger, J. P., Riebesell, U., & Reusch, T. B. H. (2016). Long-term dynamics of adaptive evolution in a globally important phytoplankton species to ocean acidification. *Science Advances*, *2*(7), e1501660. https://doi.org/10.1126/sciadv.1501660

Schmidt, A., Romahn, J., Andrén, E., Kremp, A., Kaiser, J., Arz, H. W., Dellwig, O., Bálint, M., & Epp, L. S. (2024). Decoding the Baltic Sea's past and present: A simple molecular index for ecosystem assessment. *Ecological Indicators*, *166*, 112494. https://doi.org/10.1016/j.ecolind.2024.112494

Schoolfield, R. M., Sharpe, P. J., & Magnuson, C. E. (1981). Non-linear regression of biological temperature-dependent rate models based on absolute reaction-rate theory. *Journal of Theoretical Biology*, *88*(4), 719–731. https://doi.org/10.1016/0022-5193(81)90246-0

Sharpe, P. J., & DeMichele, D. W. (1977). Reaction kinetics of poikilotherm development. *Journal of Theoretical Biology*, *64*(4), 649–670. https://doi.org/10.1016/0022-5193(77)90265-X

Singh, S. P., Rastogi, R. P., Häder, D.-P., & Sinha, R. P. (2011). An improved method for genomic DNA extraction from cyanobacteria. *World Journal of Microbiology and Biotechnology*, *27*(5), 1225–1230. https://doi.org/10.1007/s11274-010-0571-8

Sivonen, K [K.], Kononen, K., Carmichael, W. W., Dahlem, A. M., Rinehart, K. L., Kiviranta, J., & Niemela, S. I. (1989). Occurrence of the hepatotoxic cyanobacterium Nodularia spumigena in the Baltic Sea and structure of the toxin. *Applied and Environmental Microbiology*, *55*(8), 1990–1995. https://doi.org/10.1128/aem.55.8.1990-1995.1989

Sjöqvist, C. (2022). Evolution of Phytoplankton as Estimated from Genetic Diversity. *Journal of Marine Science and Engineering*, *10*(4), 456. https://doi.org/10.3390/jmse10040456

Śliwińska-Wilczewska, S., Felpeto, A. B., Możdżeń, K., Vasconcelos, V., & Latała, A. (2019). Physiological Effects on Coexisting Microalgae of the Allelochemicals Produced by the Bloom-Forming Cyanobacteria Synechococcus sp. And Nodularia Spumigena. *Toxins*, *11*(12). https://doi.org/10.3390/toxins11120712

Stigebrandt, A., & Andersson, A. (2020). The Eutrophication of the Baltic Sea has been Boosted and Perpetuated by a Major Internal Phosphorus Source. *Frontiers in Marine Science*, *7*, Article 572994. https://doi.org/10.3389/fmars.2020.572994

Striebel, M., Schabhüttl, S., Hodapp, D., Hingsamer, P., & Hillebrand, H. (2016). Phytoplankton responses to temperature increases are constrained by abiotic conditions and community composition. *Oecologia*, *182*(3), 815–827. https://doi.org/10.1007/s00442-016-3693-3

Suikkanen, S., Fistarol, G. O., & Granéli, E. (2005). Effects of cyanobacterial allelochemicals on a natural plankton community. *Marine Ecology Progress Series*, *287*, 1–9. https://doi.org/10.3354/meps287001

Tai, V., Poon, A. F. Y., Paulsen, I. T., & Palenik, B. (2011). Selection in coastal Synechococcus (cyanobacteria) populations evaluated from environmental metagenomes. *PLOS ONE*, *6*(9), e24249. https://doi.org/10.1371/journal.pone.0024249

Teikari, J. (2018). Toxic and bloom-forming Baltic Sea cyanobacteria under changing environmental conditions. https://helda.helsinki.fi/handle/10138/234267

Travisano, M., Maeda, M., Fuji, F., & Kudo, T. (2018). Rapid adaptation to near extinction in microbial experimental evolution. *Journal of Bioeconomics*, *20*(1), 141–152. https://doi.org/10.1007/S10818-017-9257-8

Vahtera, E., Conley, D. J., Gustafsson, B. G., Kuosa, H., Pitkänen, H., Savchuk, O. P., Tamminen, T., Viitasalo, M., Voss, M., Wasmund, N., & Wulff, F. (2007). Internal Ecosystem Feedbacks Enhance Nitrogen-fixing Cyanobacteria Blooms and Complicate Management in the Baltic Sea. *AMBIO: A Journal of the Human Environment*, *36*(2), 186–194. https://doi.org/10.1579/0044-7447(2007)36[186:IEFENC]2.0.CO;2

Voss, B., Bolhuis, H., Fewer, D. P., Kopf, M., Möke, F., Haas, F., El-Shehawy, R., Hayes, P., Bergman, B., Sivonen, K [Kaarina], Dittmann, E., Scanlan, D. J., Hagemann, M., Stal, L. J., & Hess, W. R. (2013). Insights into the physiology and ecology of the brackish-water-adapted Cyanobacterium Nodularia spumigena CCY9414 based on a genome-transcriptome analysis. *PLOS ONE*, *8*(3), e60224. https://doi.org/10.1371/journal.pone.0060224

Wahl, S., Fenske, N., Zeilinger, S., Suhre, K., Gieger, C., Waldenberger, M., Grallert, H., & Schmid, M. (2014). On the potential of models for location and scale for genome-wide

DNA methylation data. *BMC Bioinformatics*, *15*, 232. https://doi.org/10.1186/1471-2105-15-232

Walworth, N. G., Lee, M. D., Dolzhenko, E., Fu, F.-X., Smith, A. D., Webb, E. A., & Hutchins, D. A. (2021). Long-Term m5C Methylome Dynamics Parallel Phenotypic Adaptation in the Cyanobacterium Trichodesmium. *Molecular Biology and Evolution*, *38*(3), 927–939. https://doi.org/10.1093/molbev/msaa256

Wickham, H. (2016). *ggplot2*. Springer International Publishing. https://doi.org/10.1007/978-3-319-24277-4

Worden, A. Z., Follows, M. J., Giovannoni, S. J., Wilken, S., Zimmerman, A. E., & Keeling, P. J. (2015). Environmental science. Rethinking the marine carbon cycle: Factoring in the multifarious lifestyles of microbes. *Science*, *347*(6223), 1257594. https://doi.org/10.1126/science.1257594

Statutory Declaration | Eidesstattliche Versicherung

Eidesstattliche Versicherung:

Hiermit versichere ich an Eides statt, die vorliegende Dissertationsschrift selbst verfasst und keine anderen als die angegebenen Hilfsmittel und Quellen benutzt zu haben.

Sofern im Zuge der Erstellung der vorliegenden Dissertationsschrift generative Künstliche Intelligenz (gKI) basierte elektronische Hilfsmittel verwendet wurden, versichere ich, dass meine eigene Leistung im Vordergrund stand und dass eine vollständige Dokumentation aller verwendeten Hilfsmittel gemäß der Guten wissenschaftlichen Praxis vorliegt. Ich trage die Verantwortung für eventuell durch die gKI generierte fehlerhafte oder verzerrte Inhalte, fehlerhafte Referenzen, Verstöße gegen das Datenschutz- und Urheberrecht oder Plagiate.

Affidavit:

I hereby declare and affirm that this doctoral dissertation is my own work and that I have not used any aids and sources other than those indicated.

If electronic resources based on generative artificial intelligence (gAI) were used in the course of writing this dissertation, I confirm that my own work was the main and value-adding contribution and that complete documentation of all resources used is available in accordance with good scientific practice. I am responsible for any erroneous or distorted content, incorrect references, violations of data protection and copyright law or plagiarism that may have been generated by the gAI.

Hamburg, den, 20.03.2026

Unterschrift